

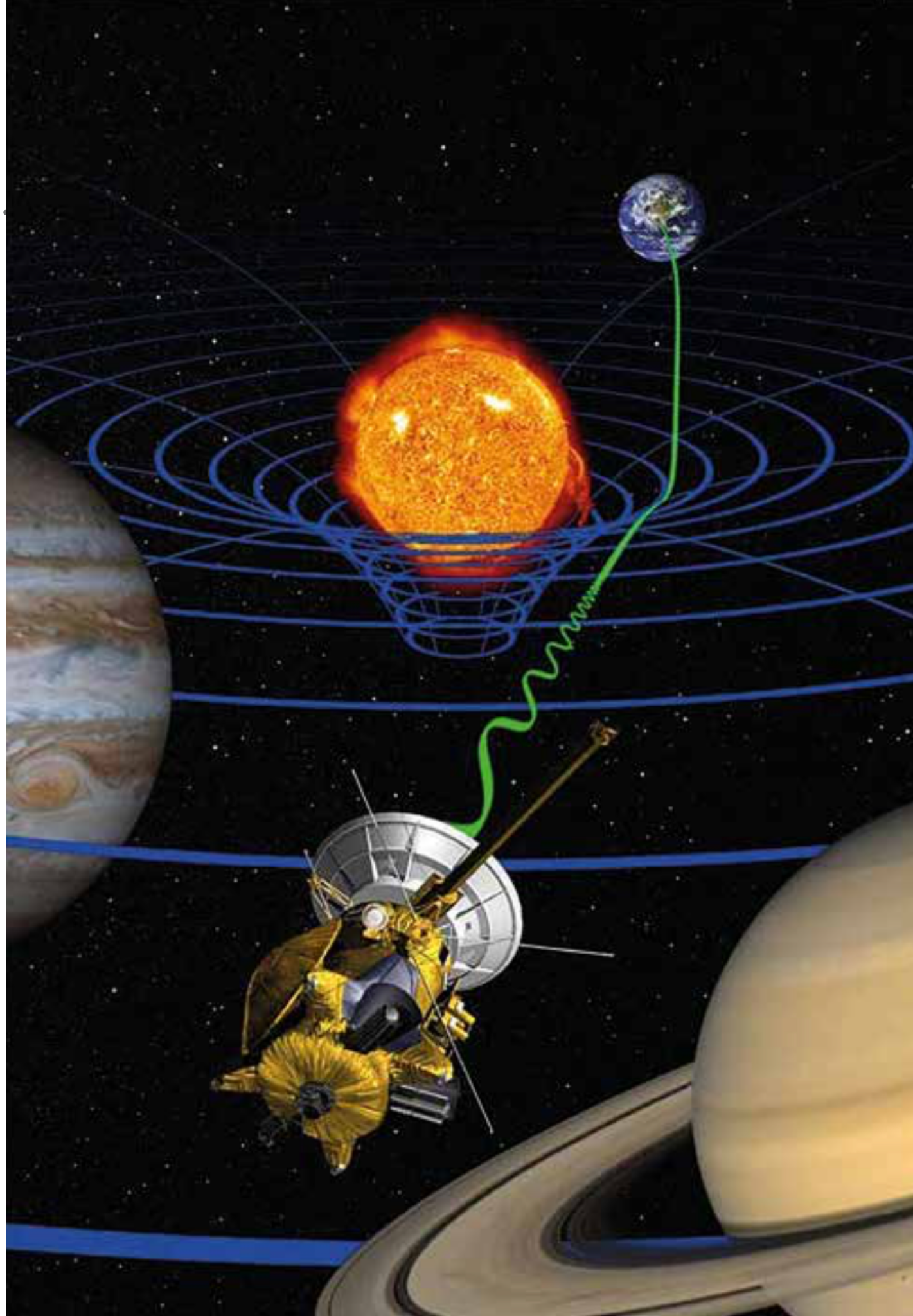
GRAVITATIONAL LENSING

7 - THE LENS MAP II

R. Benton Metcalf
2022-2023

SHAPIRO DELAY AS A TEST OF GR

- Send a radio signal towards another planet (Mercury, Venus, Mars) behind the sun
- Measure time needed to the signal to come back after being reflected
- Measurement done in 2003 with the Cassini spacecraft
- Delay is few ~ 100 microseconds
- GR confirmed at the level of 0.002%



TOY LENS POTENTIALS

POINT MASS

LENSING POTENTIAL

$$\psi(\vec{\theta}) = C \ln |\vec{\theta}|$$

**SINGULAR
ISOTHERMAL SPHERE**

SIS

$$\psi(\vec{\theta}) = C |\vec{\theta}|$$

**SINGULAR
ISOTHERMAL ELLIPSOID**

SIE

$$\psi(\vec{\theta}) = C \sqrt{\frac{\theta_1^2}{(1-\epsilon)} + \theta_2^2(1-\epsilon)}$$

**PSEUDO
ISOTHERMAL ELLIPSOID**

PSIE

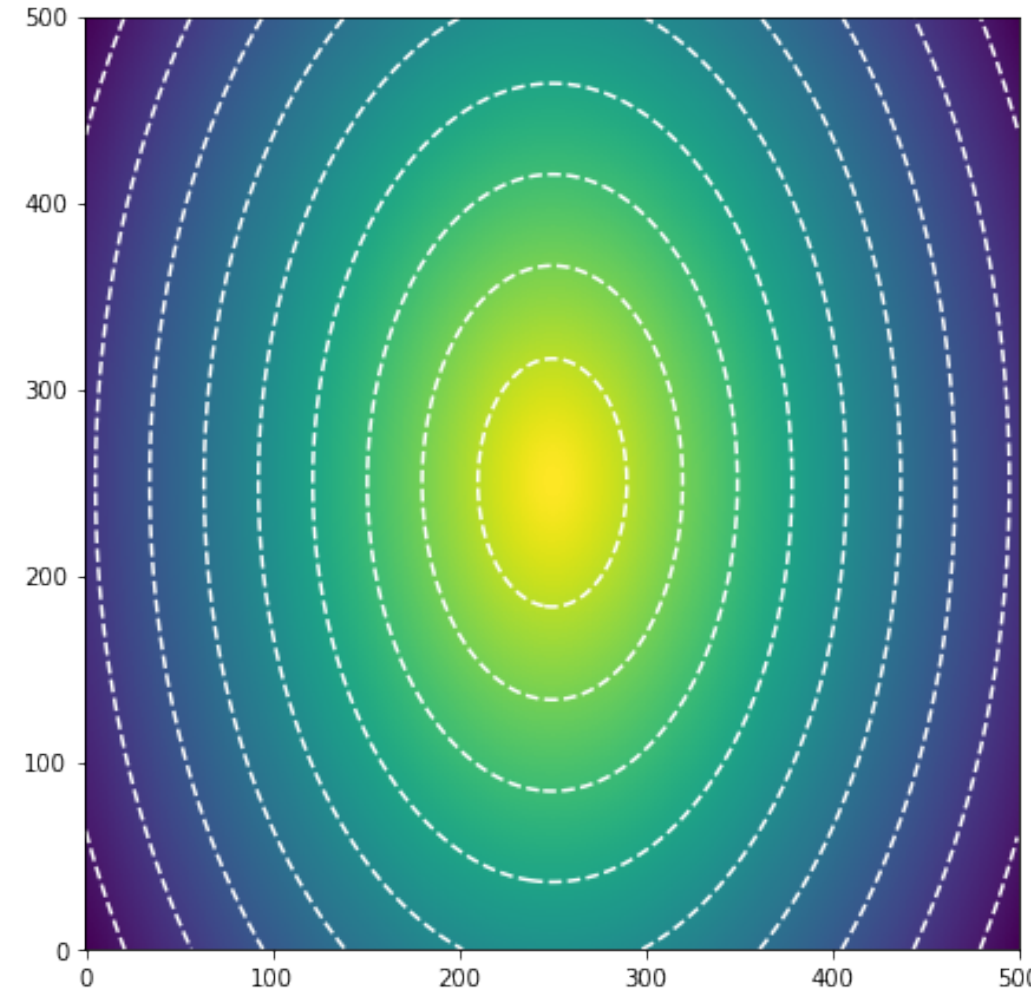
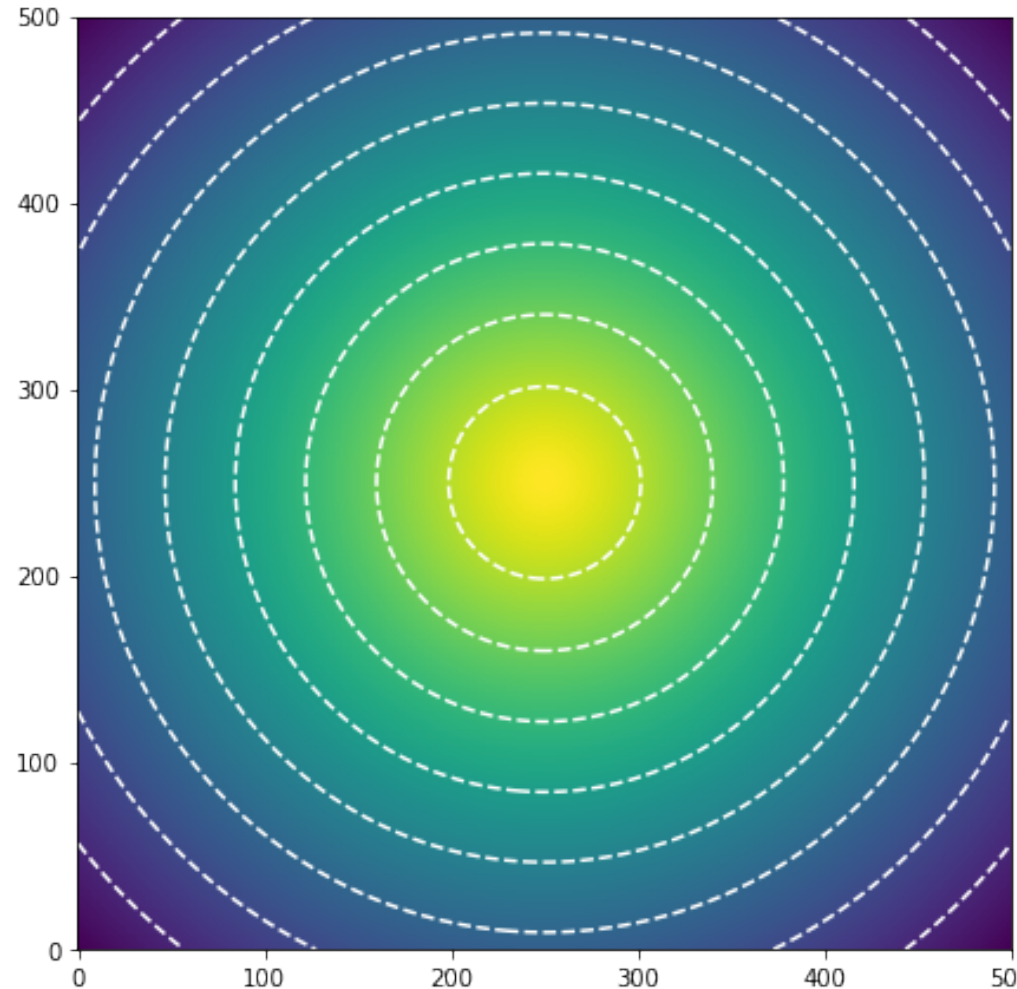
$$\psi(\vec{\theta}) = C \sqrt{\frac{\theta_1^2}{(1-\epsilon)} + \theta_2^2(1-\epsilon) + \theta_c^2}$$

INTRODUCING ELLIPTICITY

SINGULAR ISOTHERMAL ELLIPSOID

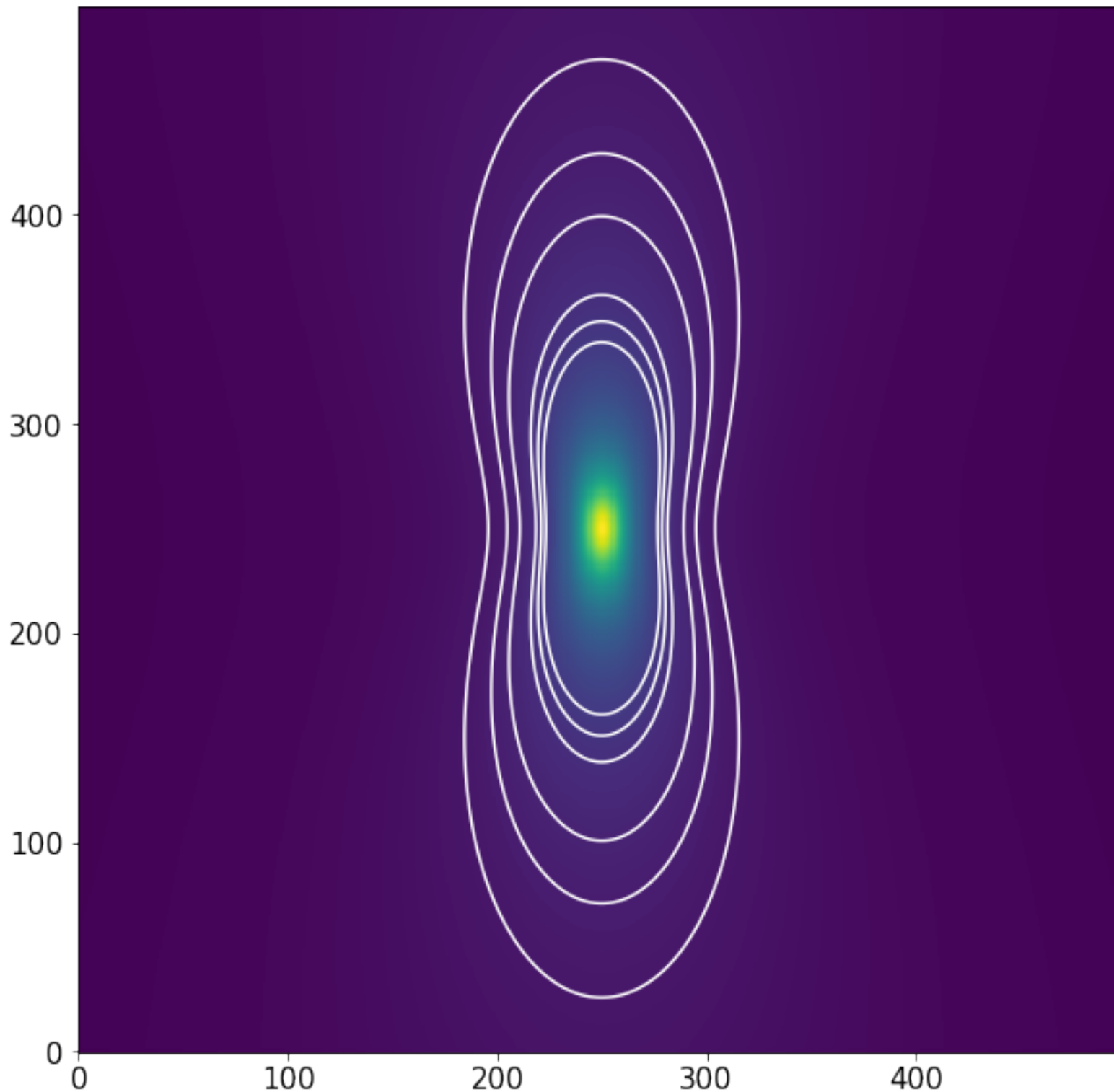
$$|\theta| \rightarrow \sqrt{\frac{\theta_1^2}{1-\epsilon} + \theta_2^2(1-\epsilon)}$$

This makes the potential constant over ellipses rather than on circles.



CAUTION: PSEUDO ELLIPTICAL LENSES

The surface density is not always so realistic for these simple potentials.



TYPES OF IMAGES

There are three types of images:

eigenvalues

$$a_1 = 1 - \kappa - \gamma$$

$$a_2 = 1 - \kappa + \gamma$$

magnification

Type I

$$\begin{aligned} a_1 &> 0 \\ a_2 &> 0 \end{aligned}$$

$$\mu = \frac{1}{|A|} > 0$$

Minimum of the time-delay,

Type II

One of the eigenvalues is negative and one positive.

$$\mu = \frac{1}{|A|} < 0$$

Saddle point of the time delay.

Type III

$$\begin{aligned} a_1 &< 0 \\ a_2 &< 0 \end{aligned}$$

$$\mu = \frac{1}{|A|} > 0$$

Maximum of time-delay.

TYPES OF IMAGES

There are three types of images: eigenvalues

$$a_1 = 1 - \kappa - \gamma$$

$$a_2 = 1 - \kappa + \gamma$$

Theorem : Type I images have a magnification equal to or larger than 1.

Theorem :

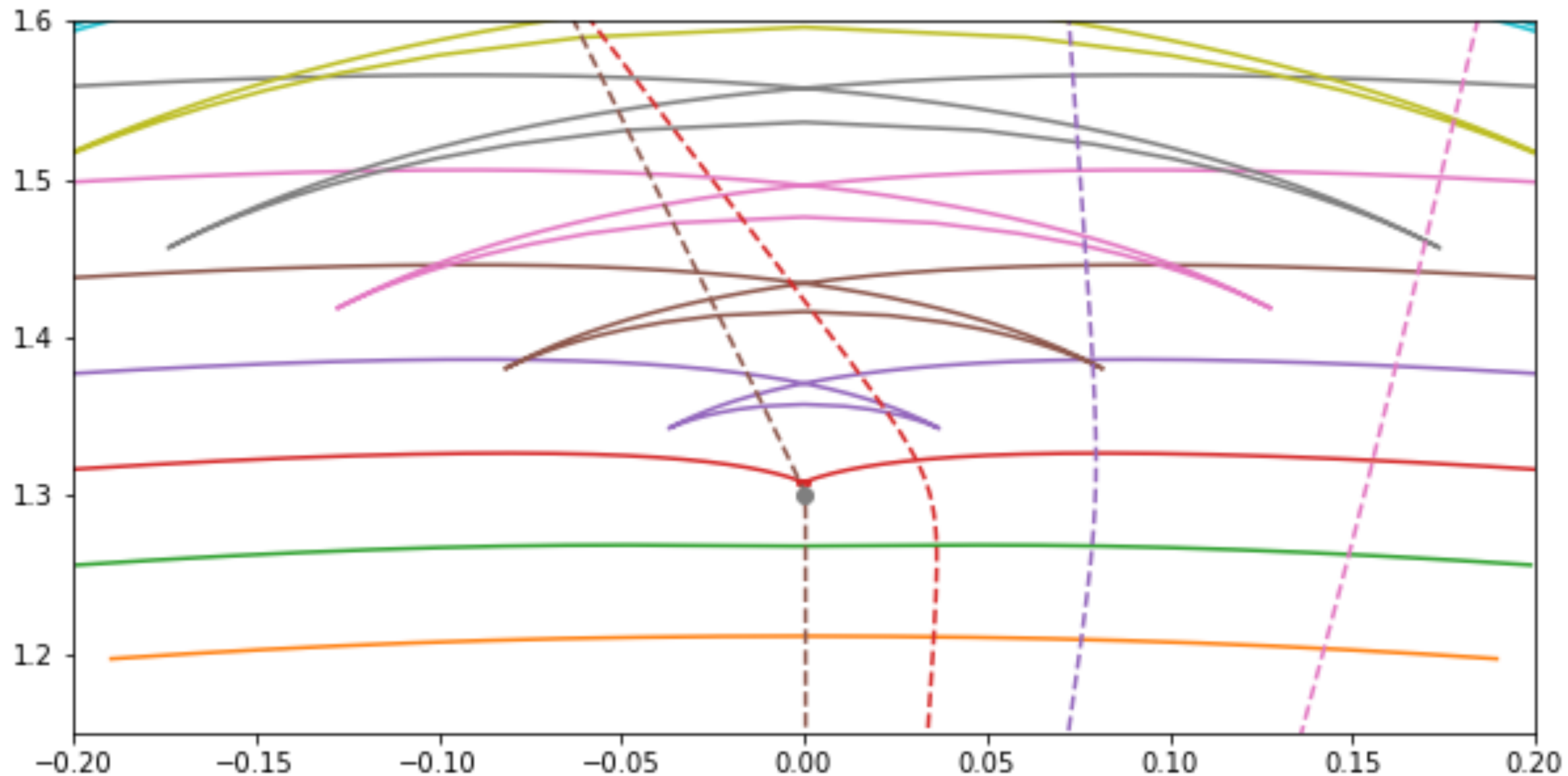
a) $n_I \geq 1$ - There is at least one ordinary image.

b) $n_I + n_{III} = n_{II} + 1$

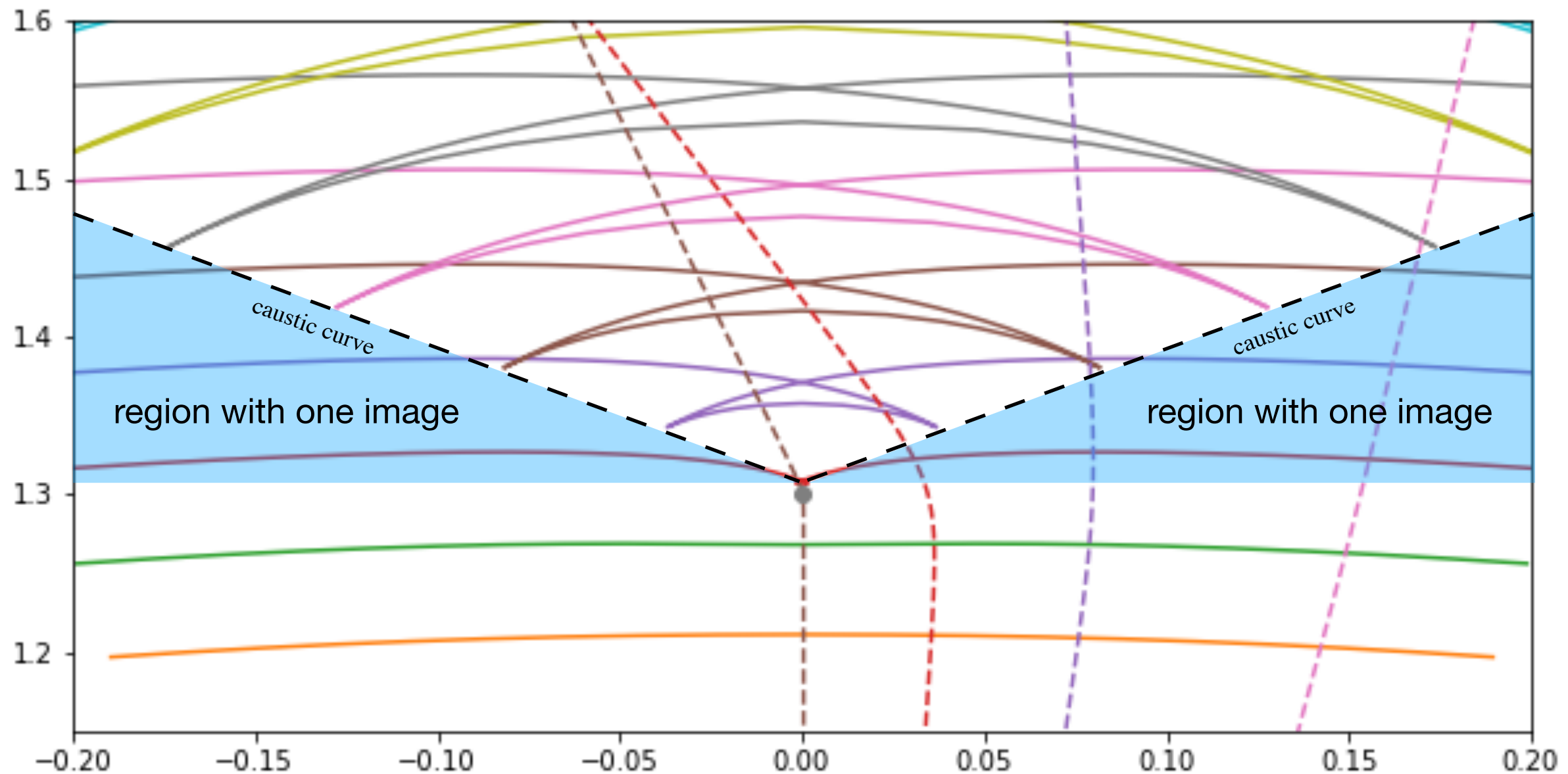
c) $n = n_I + n_{II} + n_{III}$ is odd - The total number of images is odd.

Theorem : Image with the shortest time-delay will be type I.

WAVEFRONTS



WAVEFRONTS

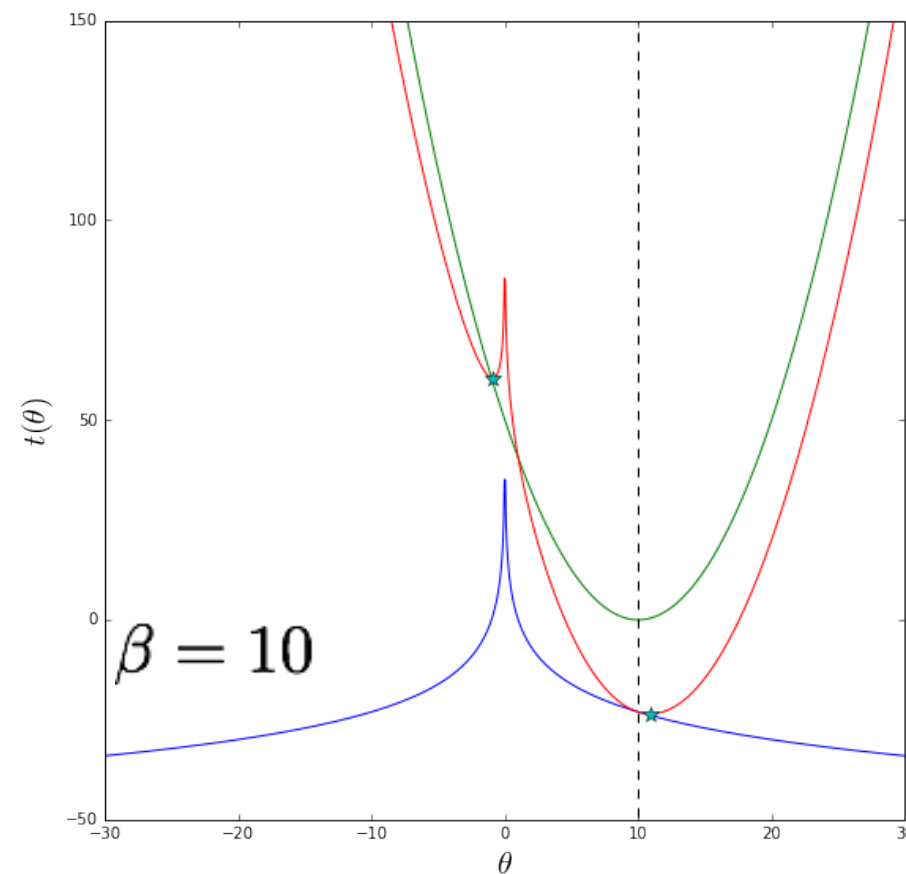
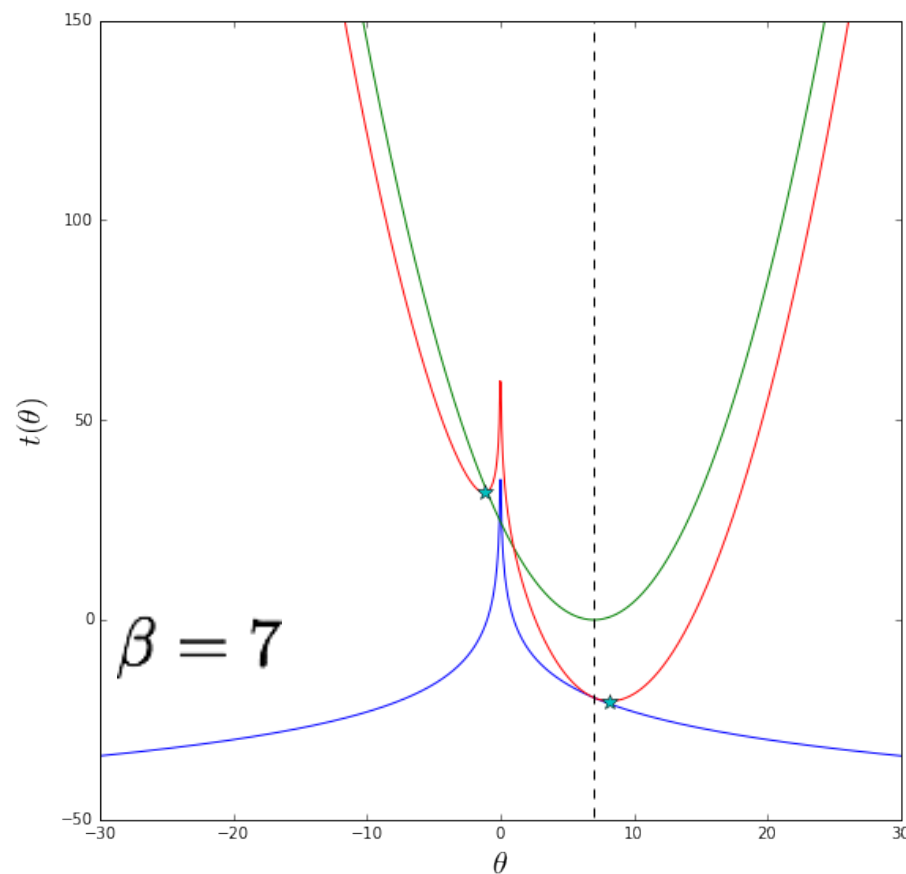
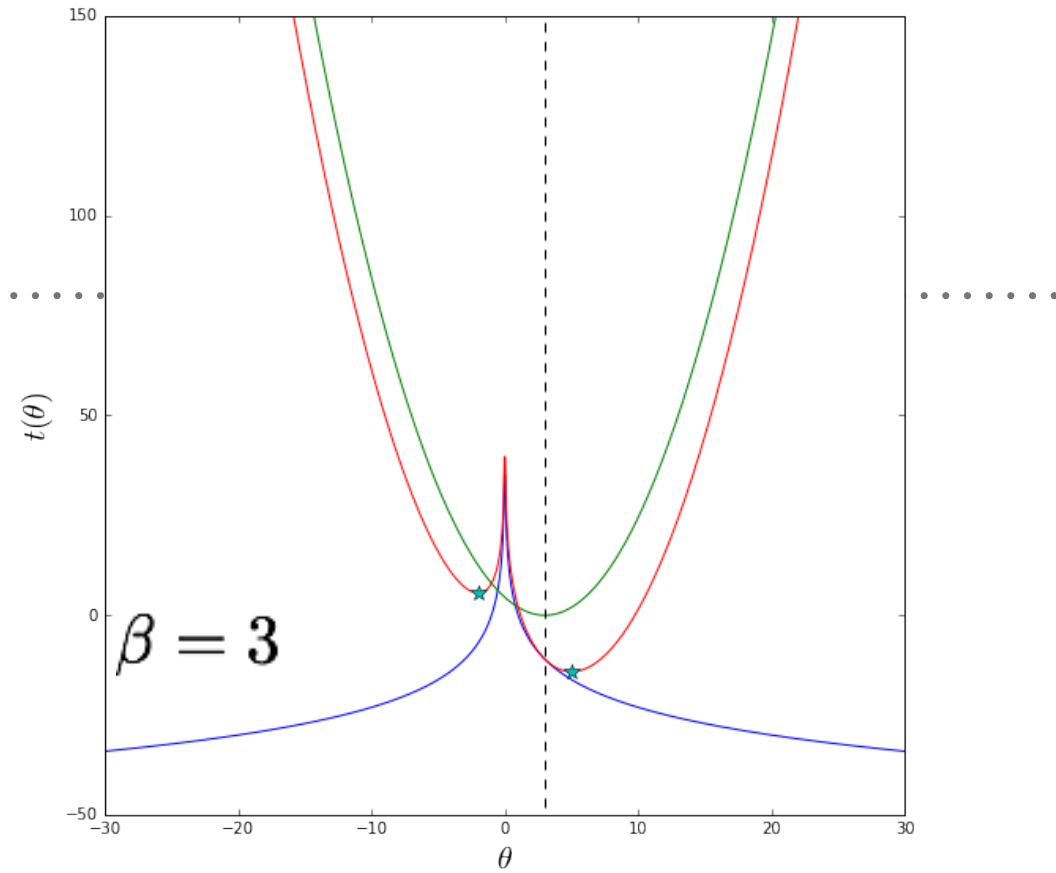
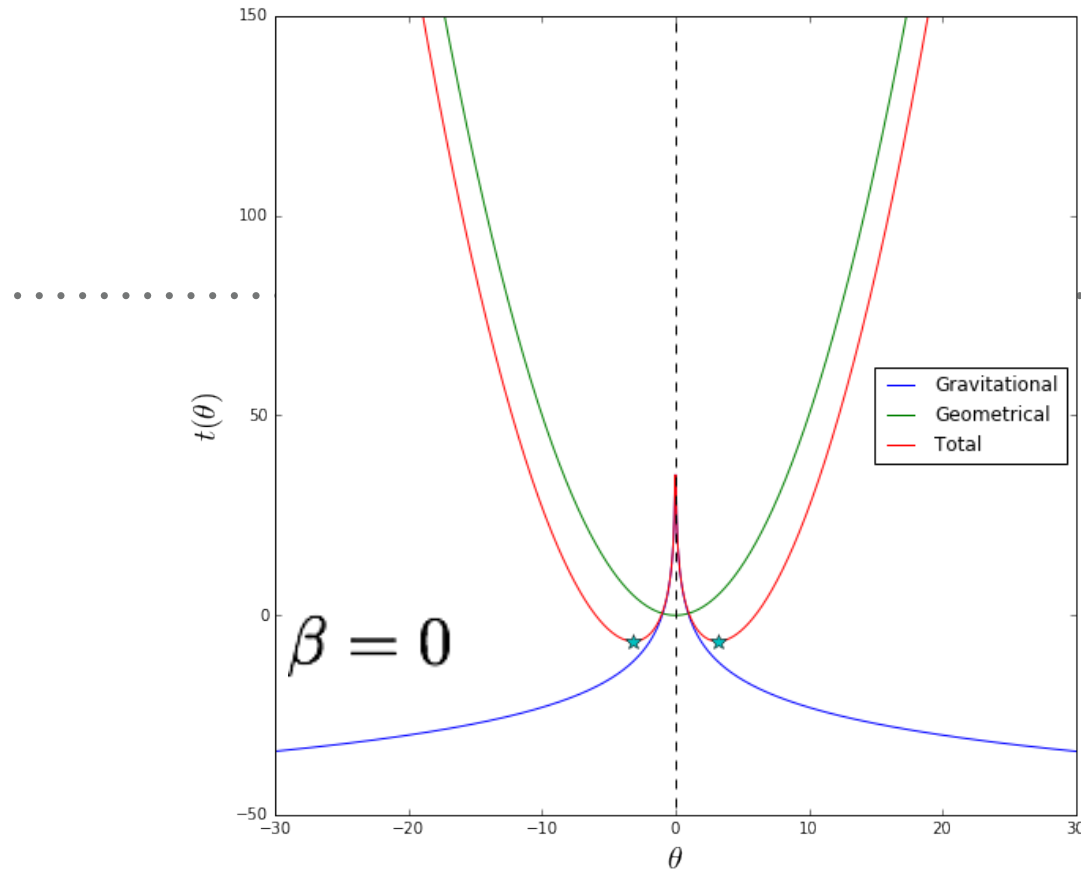


GRAVITATIONAL LENSING

8 – GRAVITATIONAL MICROLENSING I

R. Benton Metcalf
2022-2023

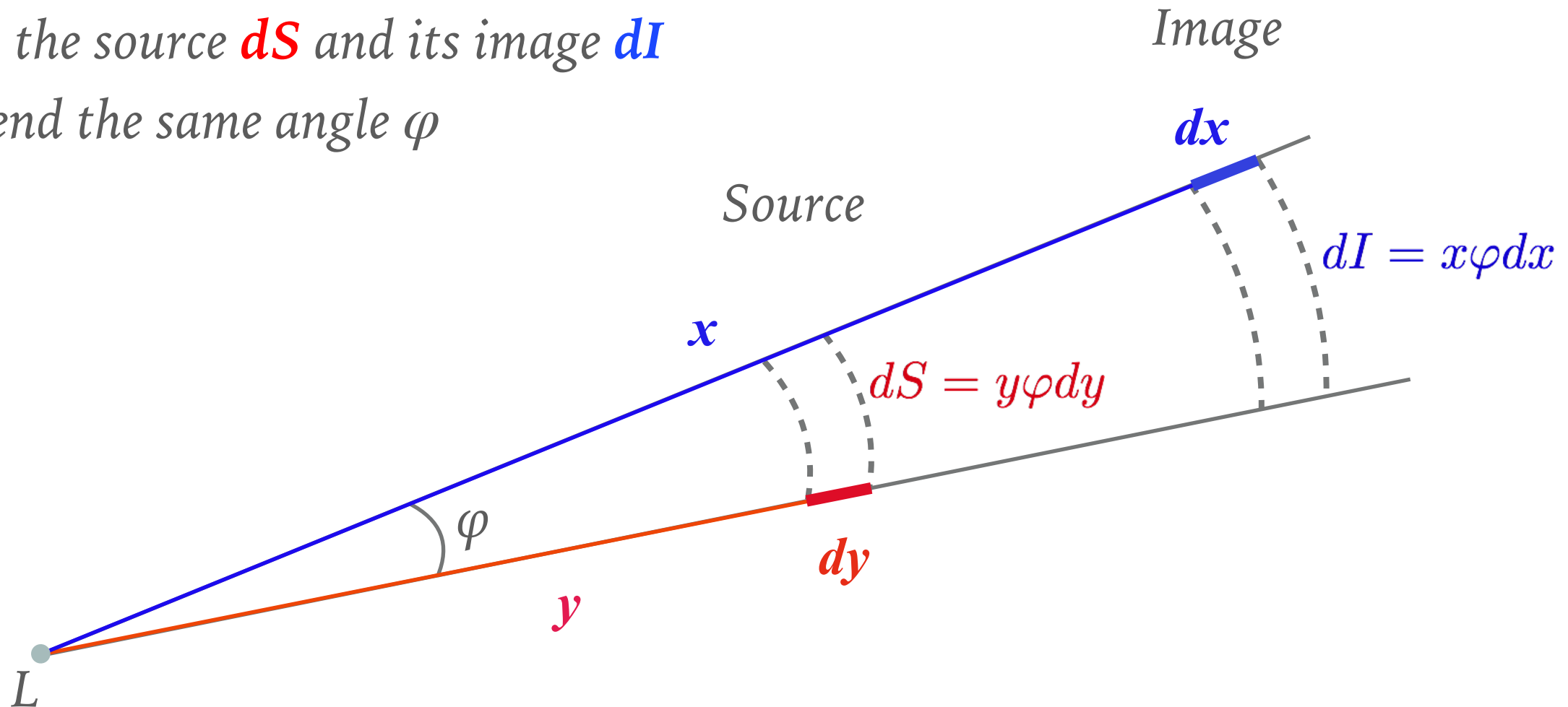
time-delay surfaces for a point mass



MAGNIFICATION

Remeber: \vec{x} , \vec{y} , $\vec{\alpha}(\vec{x})$ are parallel!

Thus the source dS and its image dI subtend the same angle φ



The figure shows that

$$\mu(x) = \frac{x}{y} \frac{dx}{dy} \quad \text{or} \quad \det A(x) = \frac{y}{x} \frac{dy}{dx}$$

CRITICAL LINES AND CAUSTICS

From the lens equation, it follows that:

$$y = x - \frac{1}{x}$$

$$\lambda_t(x) = \frac{y}{x} = 1 - \frac{1}{x^2}$$

$$\lambda_r(x) = \frac{dy}{dx} = 1 + \frac{1}{x^2}$$

The second eigenvalue is always positive (no critical line). The first is zero on the circle

$$x^2 = 1$$

Thus, the Einstein ring is the tangential critical line! The corresponding caustic is a point at $y=0$

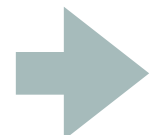
IMAGE MAGNIFICATION

Clearly,

$$\det A(x) = \frac{y}{x} \frac{dy}{dx}$$

$$\mu(x) = \det A^{-1}$$

$$\lambda_t(x) = \frac{y}{x} = 1 - \frac{1}{x^2}$$



$$\mu(x) = \left(1 - \frac{1}{x^4} \right)^{-1}$$

$$\lambda_r(x) = \frac{dy}{dx} = 1 + \frac{1}{x^2}$$

$$\det A(x) = \frac{y}{x} \frac{dy}{dx} = \left(1 - \frac{1}{x^4} \right)$$

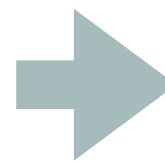
IMAGE PARITY

Note that:

$$y > 0 \quad \rightarrow \quad x_+ > 0$$
$$x_- < 0$$

$$\mu_t = \frac{x}{y} \quad \rightarrow \quad \mu_t(x_+) > 0$$
$$\mu_t(x_-) < 0$$

$$\mu_r = \frac{dx}{dy} > 0$$



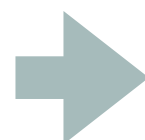
*Thus the parity of the images
is different!*

*Not surprising given that the
two images are separated by
the critical line*

SOURCE MAGNIFICATION

Let's compute now the image magnification as a function of the source position:

$$x_{\pm} = \frac{1}{2} \left[y \pm \sqrt{y^2 + 4} \right]$$



$$\frac{x}{y} = \frac{1}{2} \left(1 \pm \frac{\sqrt{y^2 + 4}}{y} \right)$$

$$\frac{dx}{dy} = \frac{1}{2} \left(1 \pm \frac{y}{\sqrt{y^2 + 4}} \right)$$

Thus, the magnifications at the two image positions are

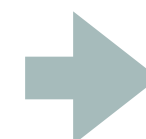
$$\mu = \frac{x}{y} \frac{dx}{dy}$$

$$\begin{aligned}\mu_{\pm}(y) &= \frac{1}{4} \left(1 \pm \frac{\sqrt{y^2 + 4}}{y} \right) \left(1 \pm \frac{y}{\sqrt{y^2 + 4}} \right) \\ &= \frac{1}{4} \left(1 \pm \frac{\sqrt{y^2 + 4}}{y} \pm \frac{y}{\sqrt{y^2 + 4}} + 1 \right) \\ &= \frac{1}{4} \left(2 \pm \frac{2y^2 + 4}{y\sqrt{y^2 + 4}} \right) = \frac{1}{2} \left(1 \pm \frac{y^2 + 2}{y\sqrt{y^2 + 4}} \right)\end{aligned}$$

SOURCE MAGNIFICATION

The total magnification is obtained by summing the magnifications of the images:

$$\begin{aligned}\mu_{\pm}(y) &= \frac{1}{4} \left(1 \pm \frac{\sqrt{y^2+4}}{y} \right) \left(1 \pm \frac{y}{\sqrt{y^2+4}} \right) \\ &= \frac{1}{4} \left(1 \pm \frac{\sqrt{y^2+4}}{y} \pm \frac{y}{\sqrt{y^2+4}} + 1 \right) \\ &= \frac{1}{4} \left(2 \pm \frac{2y^2+4}{y\sqrt{y^2+4}} \right) = \frac{1}{2} \left(1 \pm \frac{y^2+2}{y\sqrt{y^2+4}} \right)\end{aligned}$$



$$\mu(y) = \mu_+(y) + |\mu_-(y)| = \frac{y^2 + 2}{y\sqrt{y^2 + 4}}$$

inverse

$$y(\mu) = \sqrt{2 \left(\frac{\mu}{\sqrt{\mu^2 - 1}} - 1 \right)}$$

The sum of the signed magnification is one!

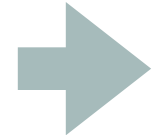
We can take a series expansion of the magnification to see that $\mu \propto 1 + 2/y^4$ for $y \rightarrow \infty$

Thus, the magnification drops quickly as the source moves away from the lens!

SOURCE MAGNIFICATION

In addition:

$$\begin{aligned}\left| \frac{\mu_+}{\mu_-} \right| &= \frac{1 + \frac{y^2+2}{y\sqrt{y^2+4}}}{\frac{y^2+2}{y\sqrt{y^2+4}} - 1} \\ &= \frac{y^2+2+y\sqrt{y^2+4}}{y^2+2-y\sqrt{y^2+4}}\end{aligned}$$



$$\begin{aligned}\left| \frac{\mu_+}{\mu_-} \right| &= \left(\frac{y + \sqrt{y^2 + 4}}{y - \sqrt{y^2 + 4}} \right)^2 \\ &= \left(\frac{x_+}{x_-} \right)^2.\end{aligned}$$

Laurent series expansion at infinity:

$$\left| \frac{\mu_+}{\mu_-} \right| \propto y^4$$

$$\frac{1}{2} (y + \sqrt{y^2 + 4})^2 = y^2 + 2 + y\sqrt{y^2 + 4}$$

$$\frac{1}{2} (y - \sqrt{y^2 + 4})^2 = y^2 + 2 - y\sqrt{y^2 + 4}$$

As we move the source away from the lens, the image in x_+ dominates the flux budget very soon.

$$\lim_{y \rightarrow \infty} \mu_- = 0$$

$$\lim_{y \rightarrow \infty} \mu_+ = 1$$

A SOURCE ON THE EINSTEIN RING

For a source on the Einstein ring:

$$x_{\pm} = \frac{1}{2} \left[y \pm \sqrt{y^2 + 4} \right] \rightarrow y = 1 \rightarrow x_{\pm} = \frac{1}{2}(1 \pm \sqrt{5}) \Rightarrow \mu_{\pm} = \left[1 - \left(\frac{2}{1 \pm \sqrt{5}} \right)^4 \right]^{-1}$$

Therefore $\mu = \mu_+ + |\mu_-| = 1.17 + 0.17 = 1.34$:

$$\Delta m = -2.5 \log_{10} \mu \simeq 0.3$$

Given how quickly the magnification drops by moving the source away from the lens, we can assume that only sources within the Einstein radius are magnified in a significant way.

For this reason, the circle within the Einstein radius is assumed to be the cross section for microlensing.

MICROLENSING OBSERVABLES?

- typical Einstein radii for lenses in the MW are ~ 1 mas
- thus, the image separation is too small to resolve the images
- magnification is small also for relatively close pairs of lenses and sources
- how to detect a microlensing event?

MICROLENSING LIGHT CURVE

Assume a linear trajectory of the source relative to the lens, with impact parameter y_0

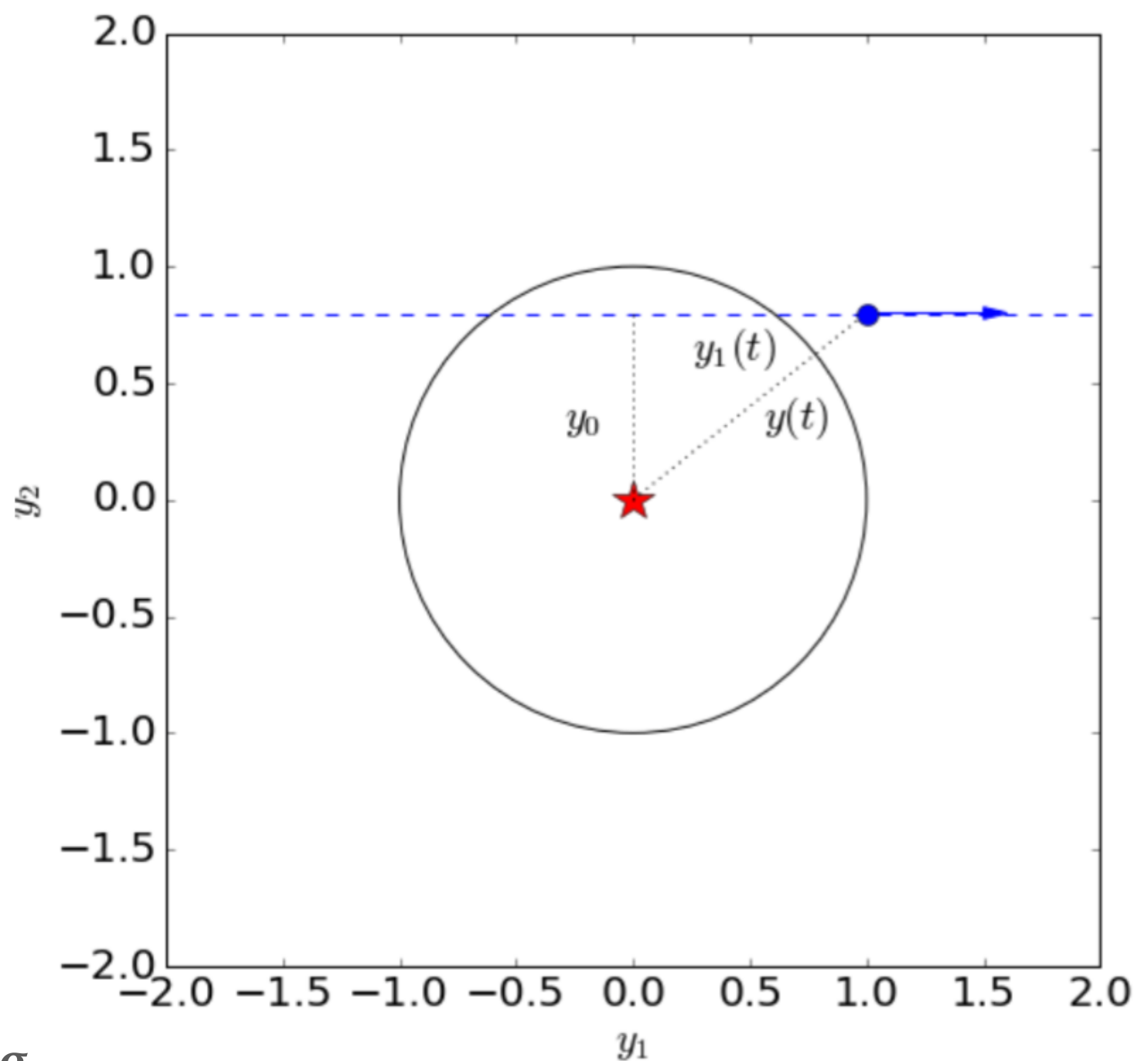
Assume also constant transverse velocity v :

$$y_1(t) = \frac{v(t - t_0)}{D_L \theta_E}$$

We can define a characteristic time of the event:

$$t_E = \frac{D_L \theta_E}{v} = \frac{\theta_E}{\mu_{rel}}$$

This is the Einstein radius crossing time



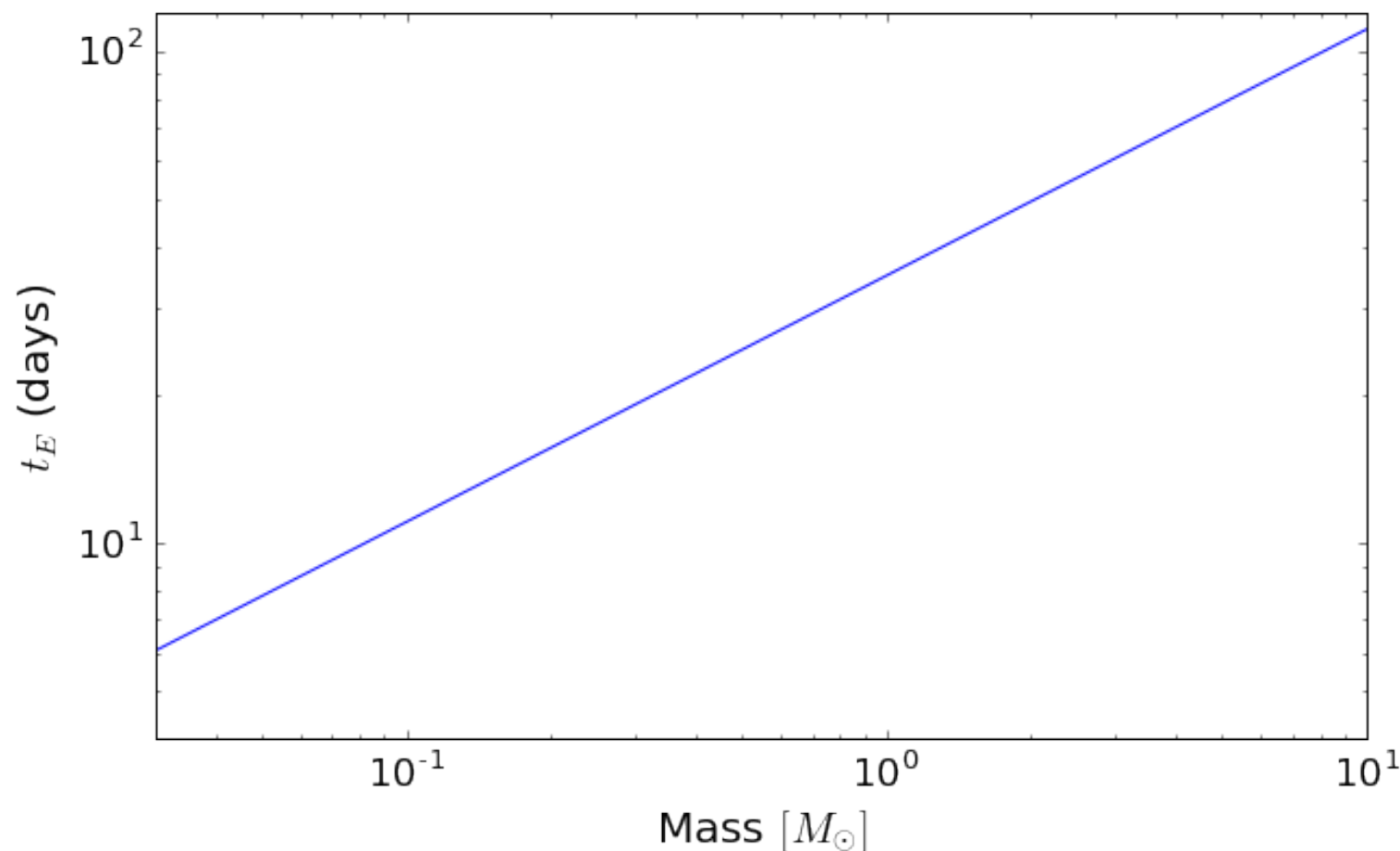
MICROLENSING LIGHT CURVE

Given the definition of Einstein radius

$$\theta_E = \sqrt{\frac{4GM}{c^2} \frac{D_{LS}}{D_L D_S}}$$

The order of magnitude of the t_E is

$$t_E \approx 19 \text{ days} \sqrt{4 \frac{D_L}{D_S} \left(1 - \frac{D_L}{D_S}\right) \left(\frac{D_S}{8 \text{kpc}}\right)^{1/2} \left(\frac{M}{0.3 M_\odot}\right)^{1/2} \left(\frac{v}{200 \text{km/s}}\right)^{-1}}$$



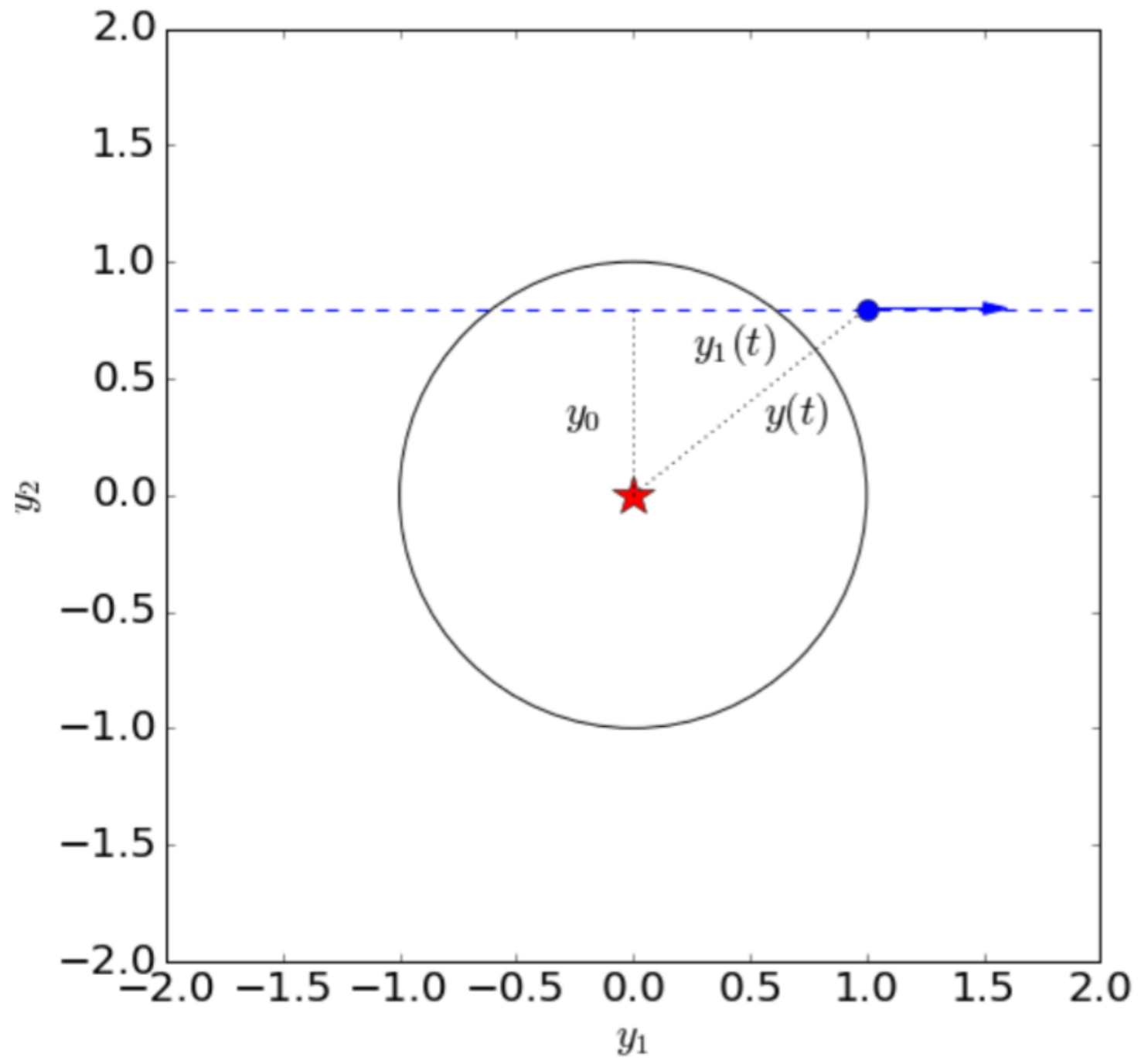
MICROLENSING LIGHT CURVE

We obtain

$$y_1(t) = \frac{v(t - t_0)}{D_L \theta_E} = \frac{t - t_0}{t_E}$$

Thus:

$$y(t) = \sqrt{y_0^2 + y_1^2(t)} = \sqrt{y_0^2 + \frac{(t - t_0)^2}{t_E^2}}$$



MICROLENSING LIGHT CURVE

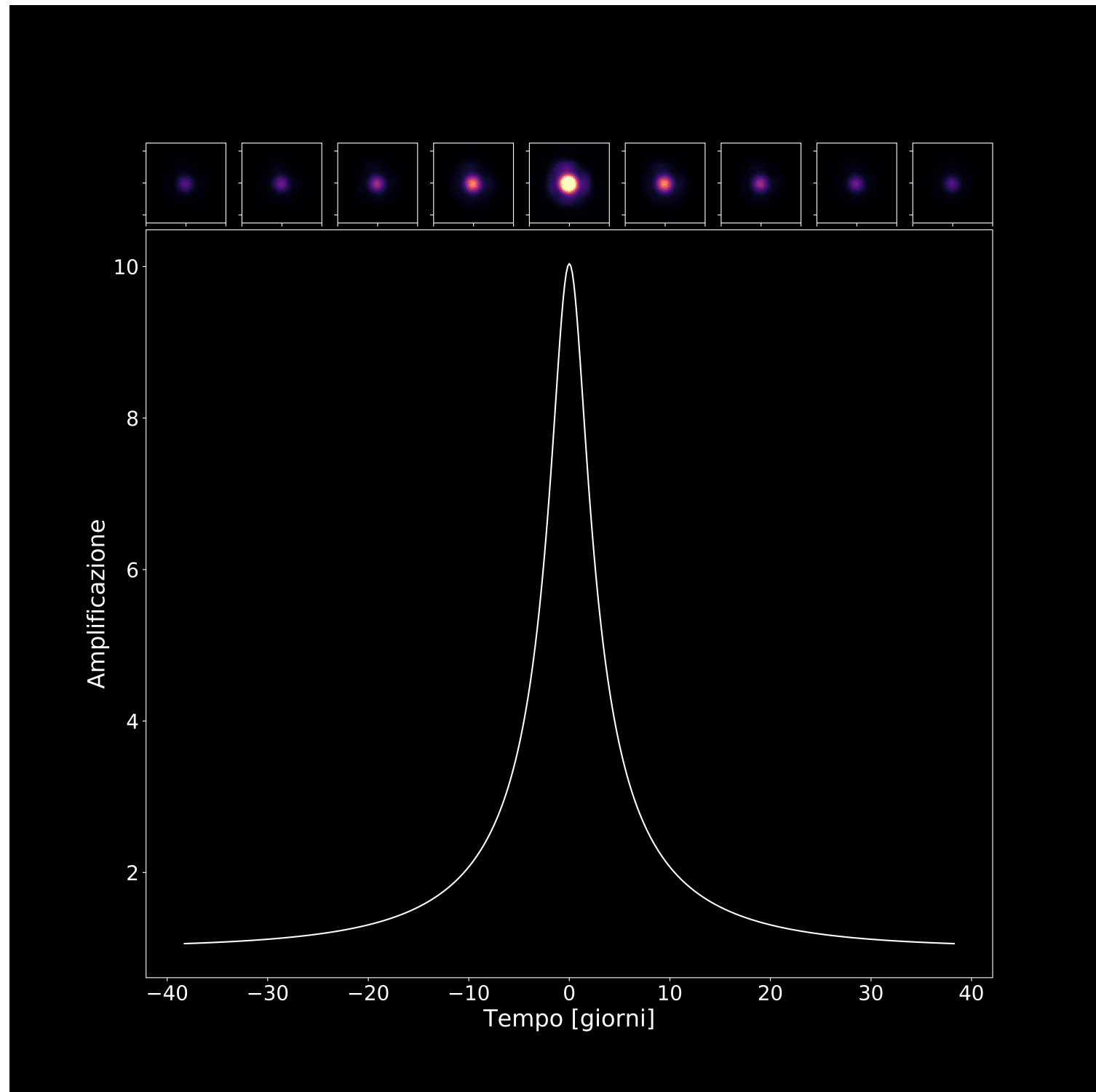
Combine

$$y(t) = \sqrt{y_0^2 + y_1^2(t)} = \sqrt{y_0^2 + \frac{(t - t_0)^2}{t_E^2}}$$

with

$$\mu(y) = \frac{y^2 + 2}{y\sqrt{y^2 + 4}}$$

And obtain $\mu(t)$



Possible gravitational microlensing of a star in the Large Magellanic Cloud

C. Alcock^{*†}, C. W. Akerlof^{†¶}, R. A. Allsman^{*},
T. S. Axelrod^{*}, D. P. Bennett^{*†}, S. Chan[‡],
K. H. Cook^{*†}, K. C. Freeman[‡], K. Griest^{†||},
S. L. Marshall^{†§}, H-S. Park^{*}, S. Perlmutter[†],
B. A. Peterson[†], M. R. Pratt^{†§}, P. J. Quinn[†],
A. W. Rodgers[†], C. W. Stubbs^{†§}
& W. Sutherland[†]

* Lawrence Livermore National Laboratory, Livermore, California 94550, USA

† Center for Particle Astrophysics, University of California, Berkeley, California 94720, USA

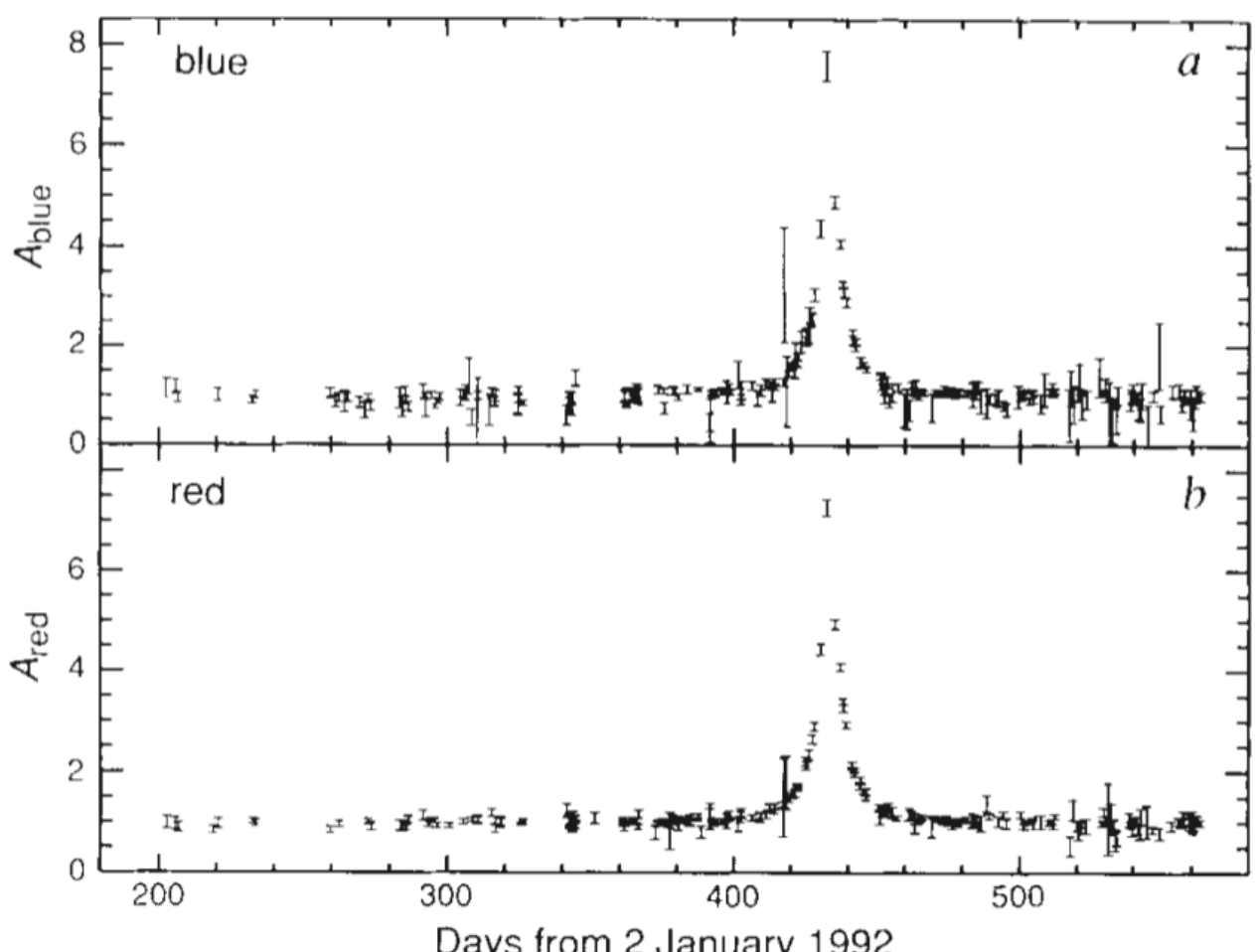
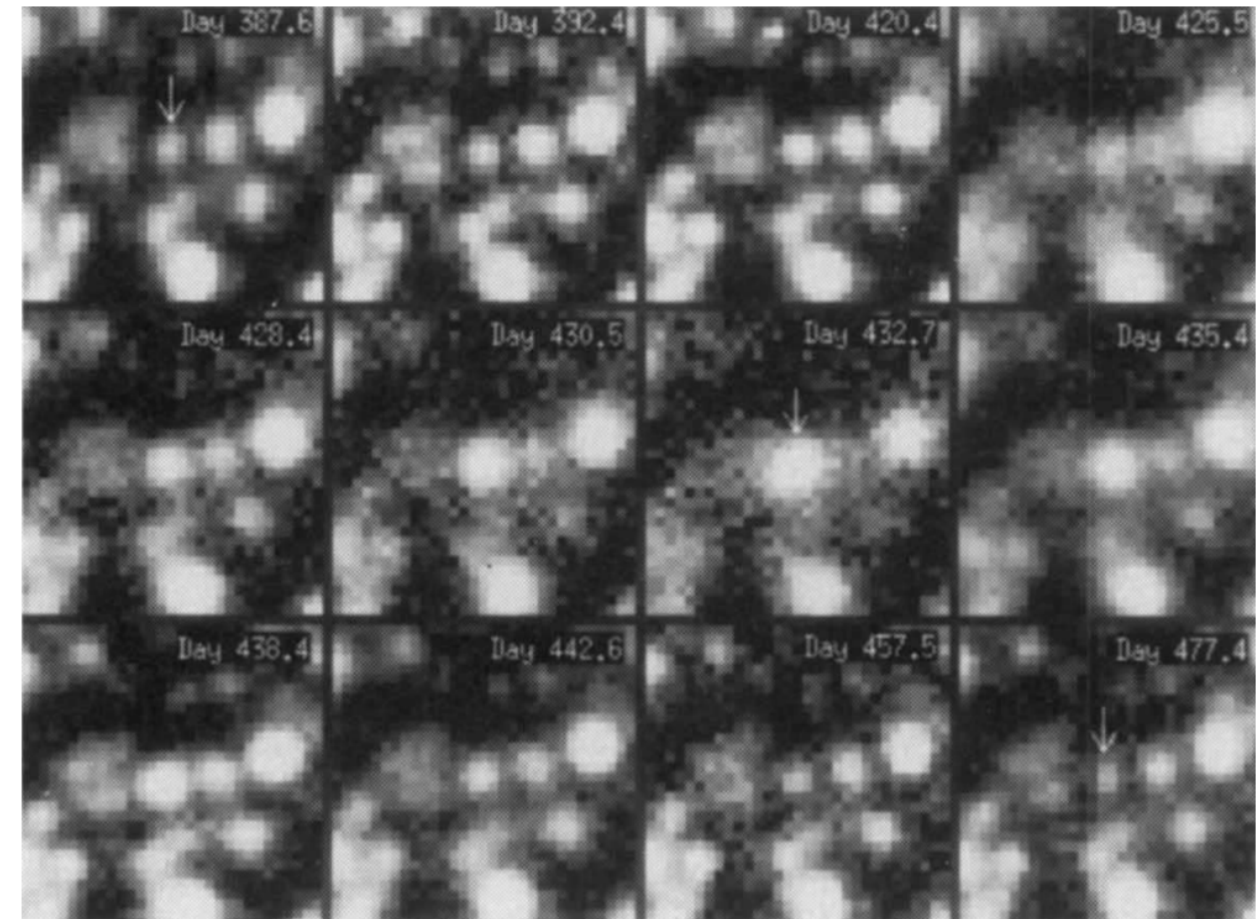
‡ Mt Stromlo and Siding Spring Observatories, Australian National University, Weston, ACT 2611, Australia

§ Department of Physics, University of California, Santa Barbara, California 93106, USA

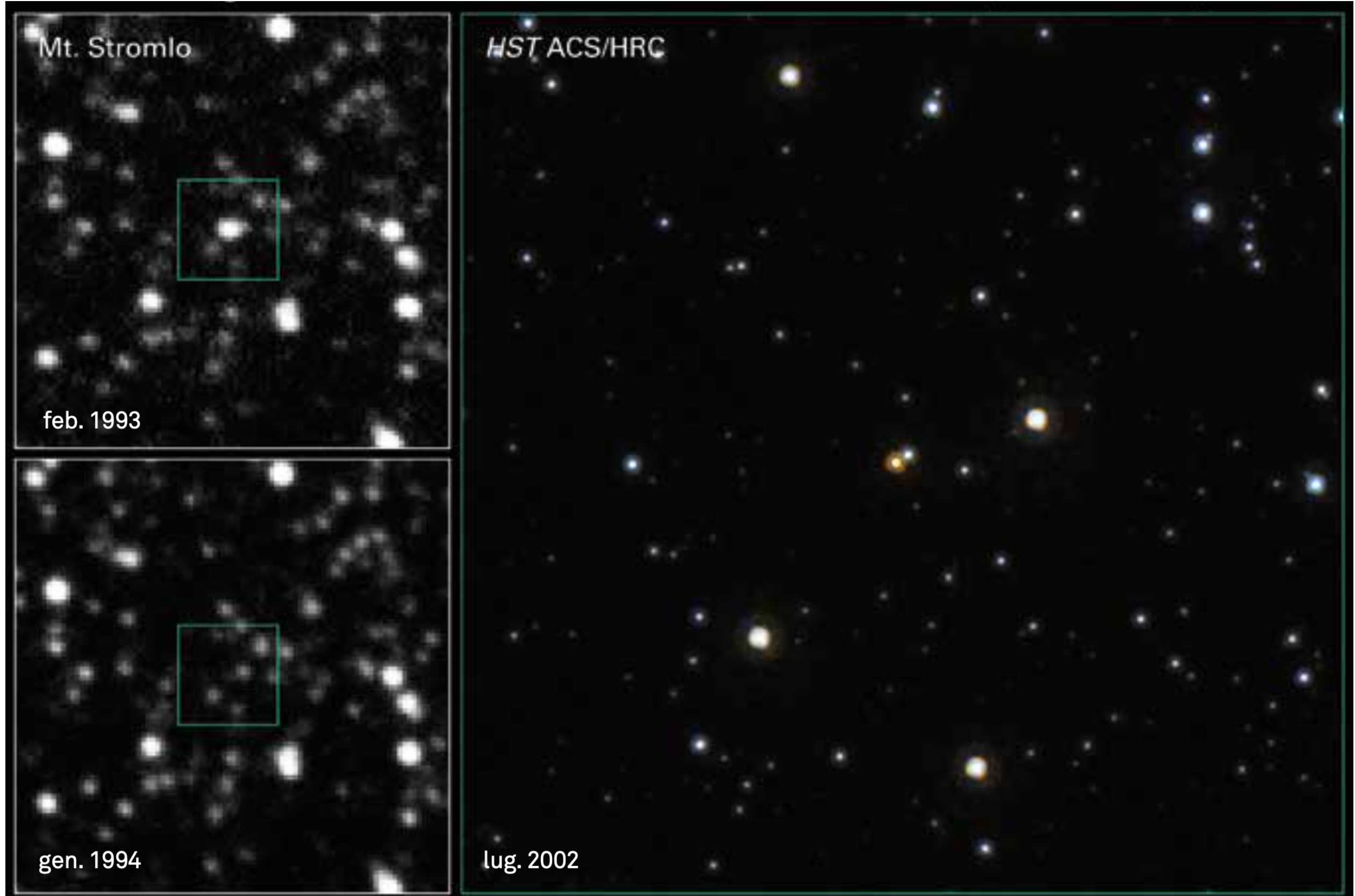
¶ Department of Physics, University of California, San Diego, California 92039, USA

|| Department of Physics, University of Michigan, Ann Arbor, Michigan 48109, USA

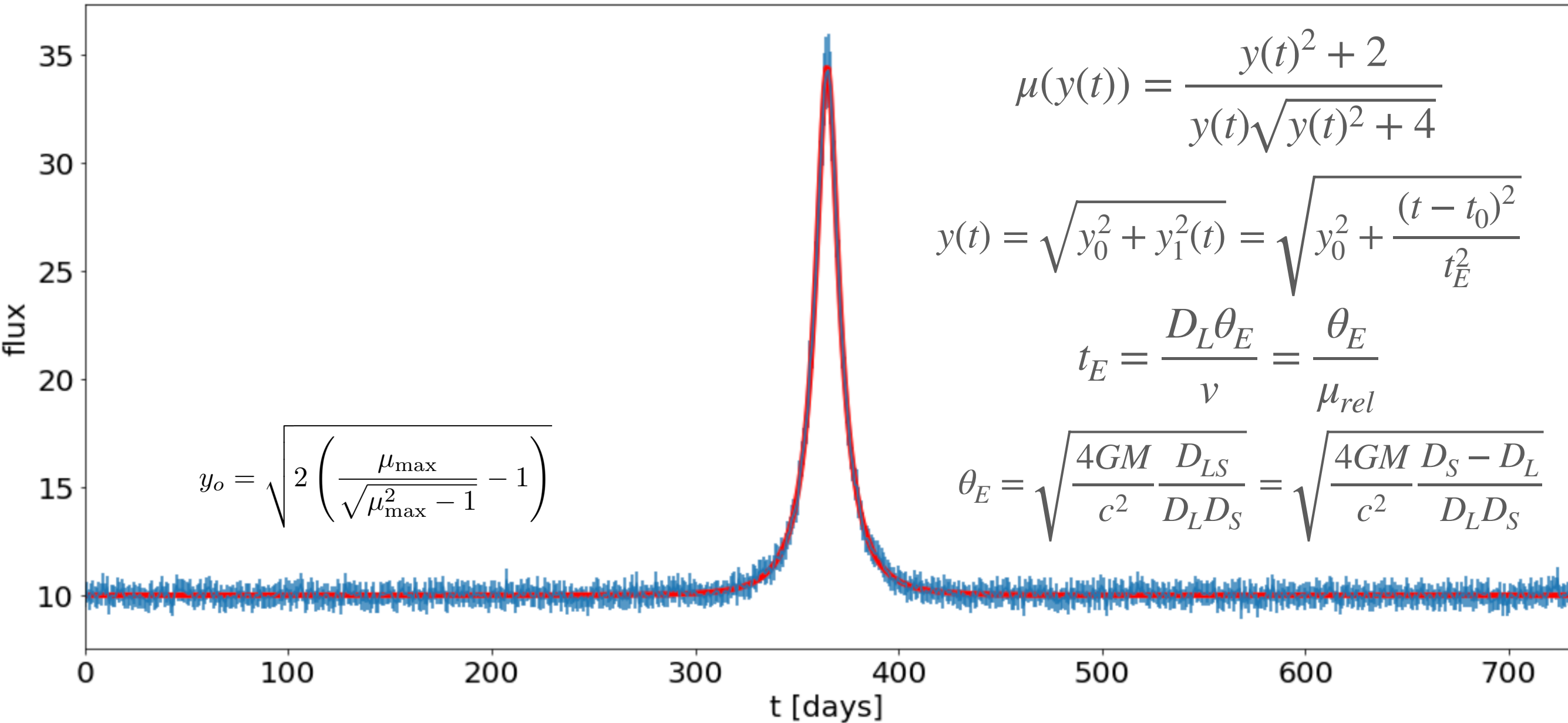
THERE IS NOW ABUNDANT EVIDENCE FOR THE PRESENCE OF LARGE QUANTITIES OF UNSEEN MATTER SURROUNDING NORMAL GALAXIES, INCLUDING OUR OWN^{1,2}. THE NATURE OF THIS 'DARK MATTER' IS UNKNOWN, EXCEPT THAT IT CANNOT BE MADE OF NORMAL STARS, DUST OR GAS, AS THEY WOULD BE EASILY DETECTED. EXOTIC PARTICLES SUCH AS AXIONS, MASSIVE NEUTRINOS OR OTHER WEAKLY INTERACTING MASSIVE PARTICLES (COLLECTIVELY KNOWN AS WIMPS) HAVE BEEN PROPOSED^{3,4}, BUT HAVE YET TO BE DETECTED. A LESS EXOTIC ALTERNATIVE IS NORMAL MATTER IN THE FORM OF BODIES WITH MASSES RANGING FROM THAT OF A LARGE PLANET TO A FEW SOLAR MASSES. SUCH OBJECTS, KNOWN COLLECTIVELY AS MASSIVE COMPACT HALO OBJECTS⁵ (MACHOS), MIGHT BE BROWN DWARFS OR 'JUPITERS' (BODIES TOO SMALL TO PRODUCE THEIR OWN ENERGY BY FUSION), NEUTRON STARS, OLD WHITE DWARFS OR BLACK HOLES. PACZYNSKI⁶ SUGGESTED THAT MACHOS MIGHT ACT AS GRAVITATIONAL MICROLENSES, TEMPORARILY AMPLIFYING THE APPARENT BRIGHTNESS OF BACKGROUND STARS IN NEARBY GALAXIES. WE ARE CONDUCTING A MICROLENSING EXPERIMENT TO DETERMINE WHETHER THE DARK MATTER HALO OF OUR GALAXY IS MADE UP OF MACHOS. HERE WE REPORT A CANDIDATE FOR SUCH A MICROLENSING EVENT, DETECTED BY MONITORING THE LIGHT CURVES OF 1.8 MILLION STARS IN THE LARGE MAGELLANIC CLOUD FOR ONE YEAR. THE LIGHT CURVE SHOWS NO VARIATION FOR MOST OF THE YEAR OF DATA TAKING, AND AN UPWARD EXCURSION LASTING OVER 1 MONTH, WITH A MAXIMUM INCREASE OF ~2 MAG. THE MOST PROBABLE LENS MASS, INFERRED FROM THE DURATION OF THE CANDIDATE MICROLENSING EVENT, IS ~0.1 SOLAR MASS.



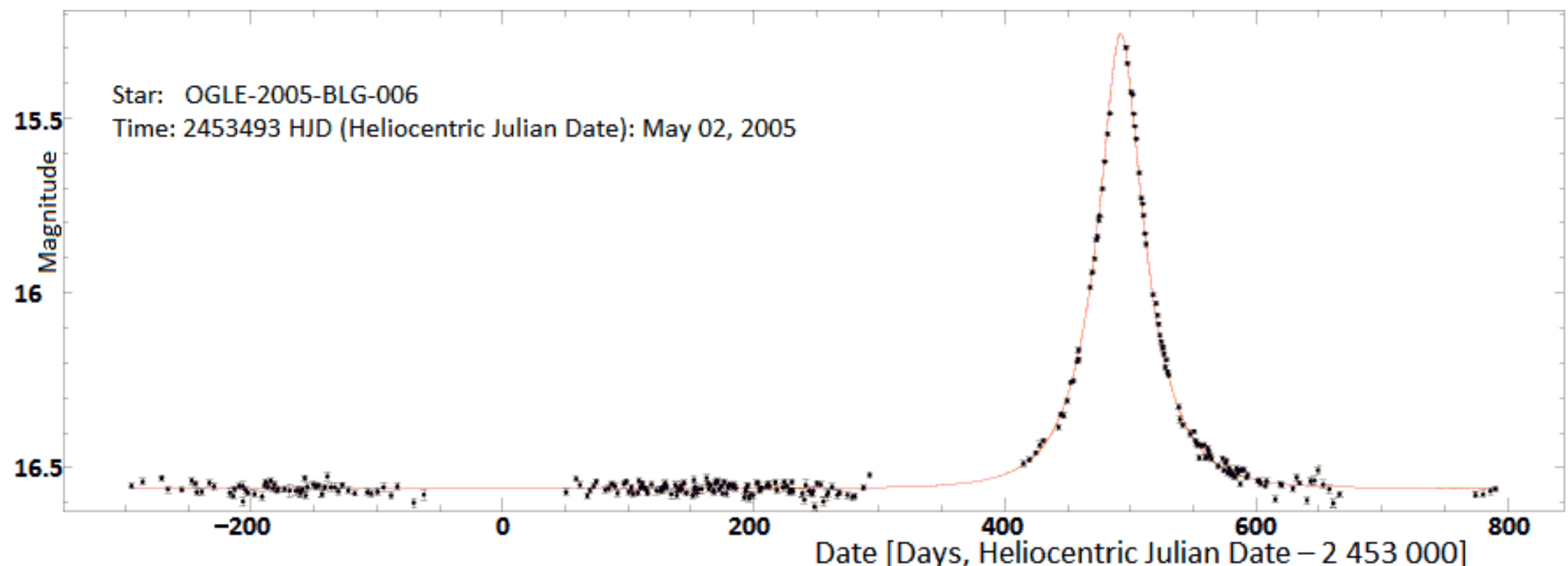
DETECTION OF THE LENS STAR IN A MICROLENSING EVENT



EXAMPLE DISCUSSED IN THE NOTEBOOK



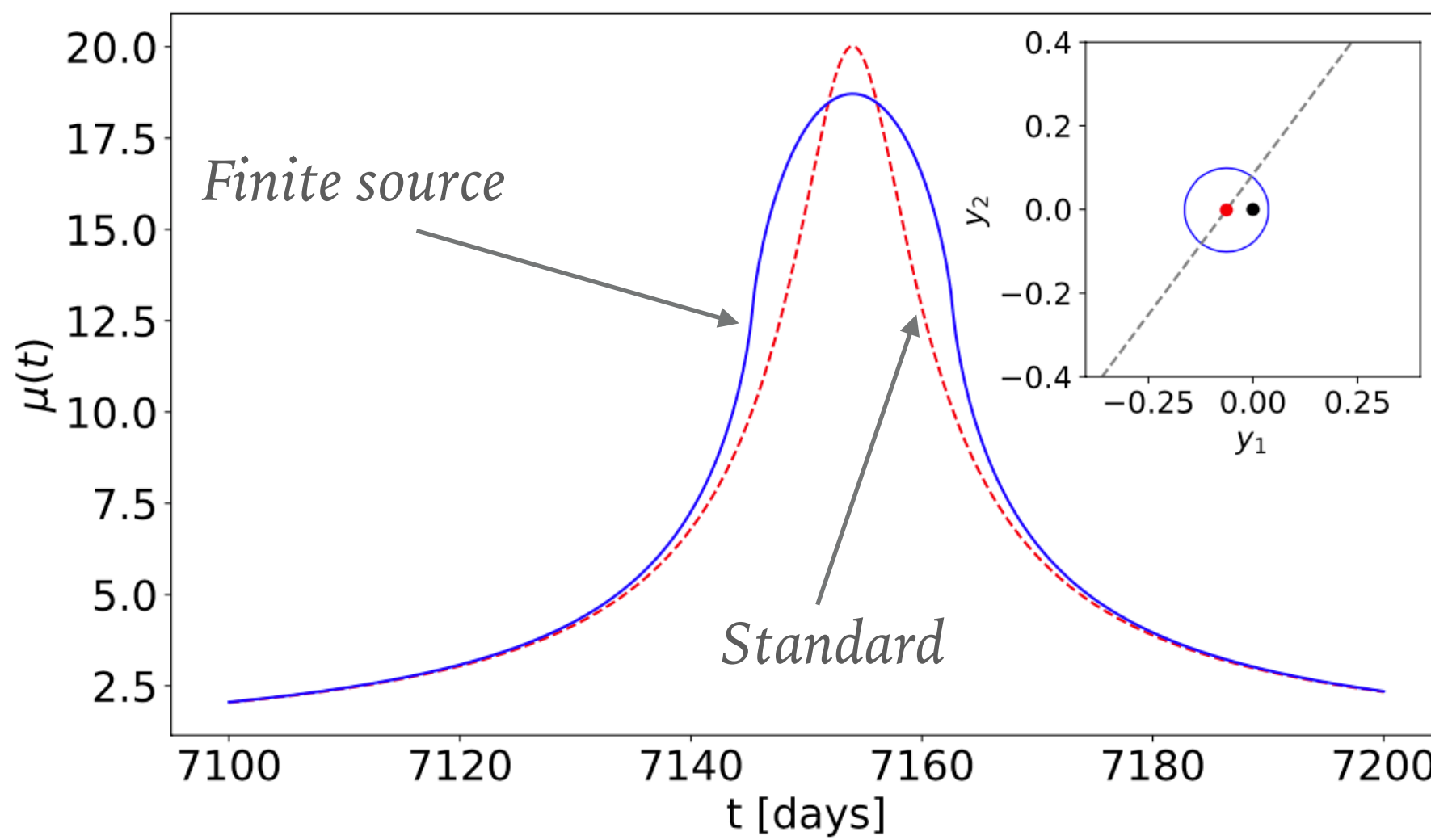
EXAMPLE OF REAL STANDARD LIGHT CURVE



MICROLENSING DEGENERACY AND ITS BREAKERS

- As seen, from the standard light curve we can measure the Einstein crossing time, which is a degenerate combination of the lens mass, distance and velocity
- Thus it is impossible to characterise the lens and the source of a single event through light curve measurement alone...
- ... unless special circumstances are present!

FINITE SOURCE EFFECTS

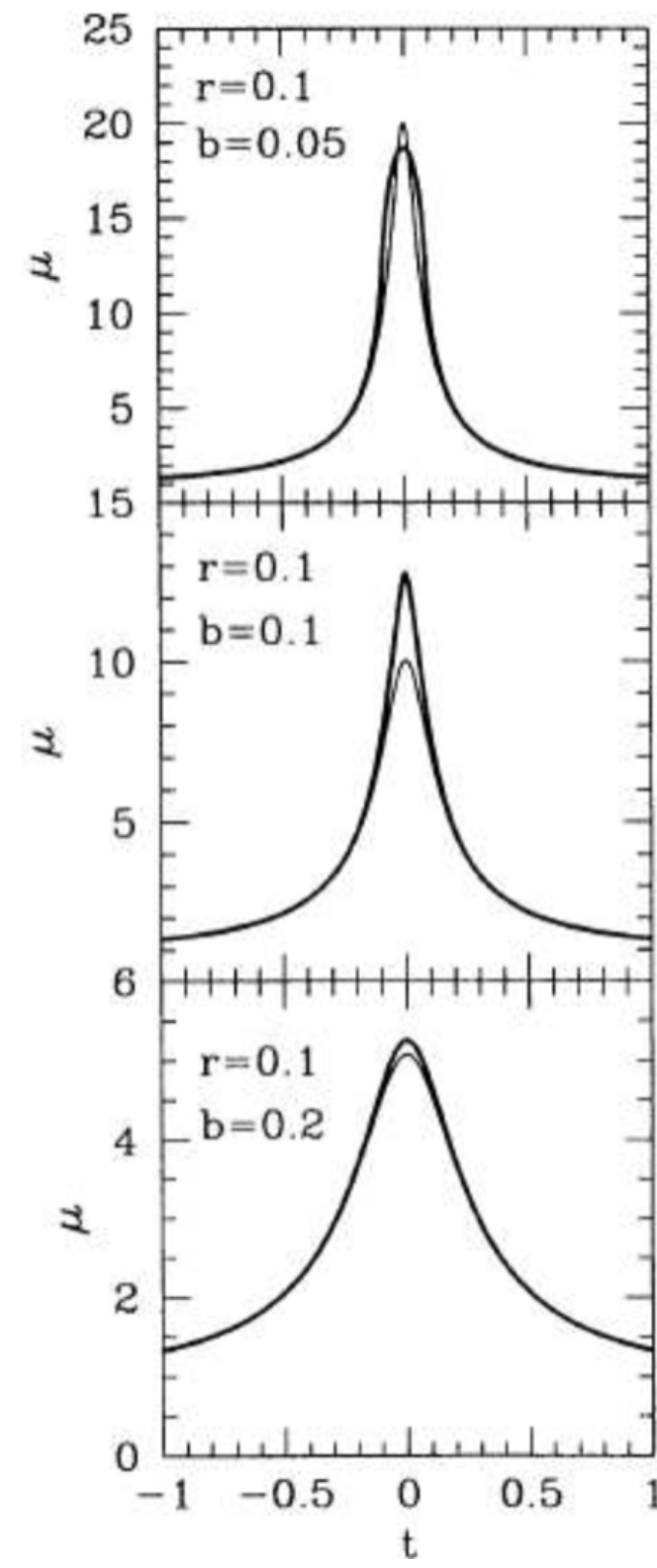
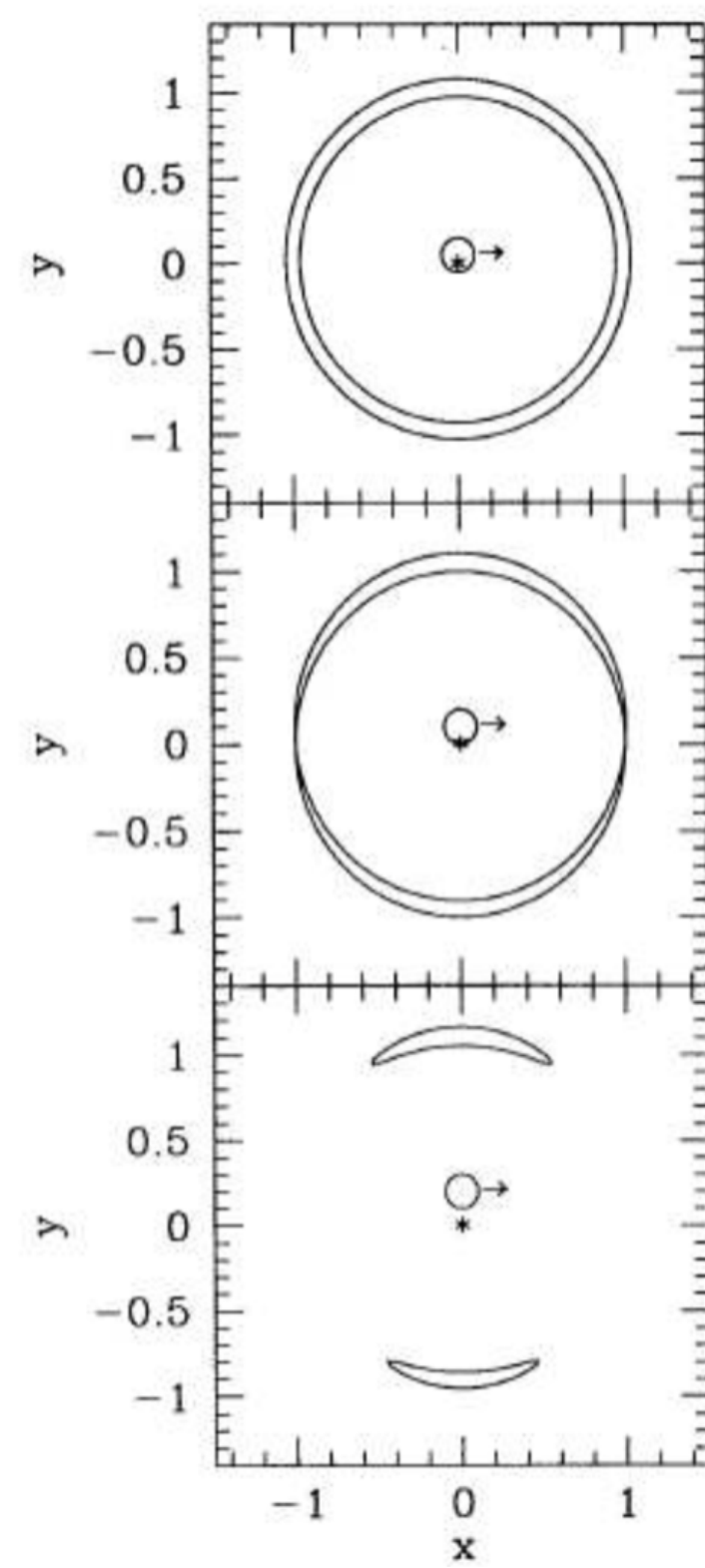


We can fit the light curve with an additional parameter (ρ_s), and use some empirical relation to measure the source size from the source color and magnitude. For example, Kervella et al. (2004) find:

$$\log(2\beta_*) = 0.0755(V - K) + 0.517 - 0.2K$$

Then, we can infer the Einstein radius.

FINITE SOURCE EFFECTS



MICROLENSING PARALLAX

As seen:

$$\theta_E = \sqrt{\frac{4GM}{c^2} \frac{D_{LS}}{D_L D_S}} = \sqrt{\frac{4GM}{c^2} \frac{D_S - D_L}{D_L D_S}} = \sqrt{\frac{4GM}{c^2} \left(\frac{1}{D_L} - \frac{1}{D_S} \right)} = \sqrt{\frac{4GM}{c^2} \pi_{rel}}$$

This illustrates that in a microlensing event we are sensitive to the relative parallax of lens and source.

In addition, note that:

$$\theta_E = \frac{4GM}{c^2} \frac{\pi_{rel}}{\theta_E} = \frac{4GM}{c^2} \pi_E \quad , \quad \pi_E = \frac{\pi_{rel}}{\theta_E}$$

This gives us another relation between the Einstein radius and the mass of the lens:

$$\theta_E = kM\pi_E \Rightarrow M = \frac{\theta_E}{k\pi_E} \quad k = 8.14 \text{ mas M}_\odot^{-1}$$

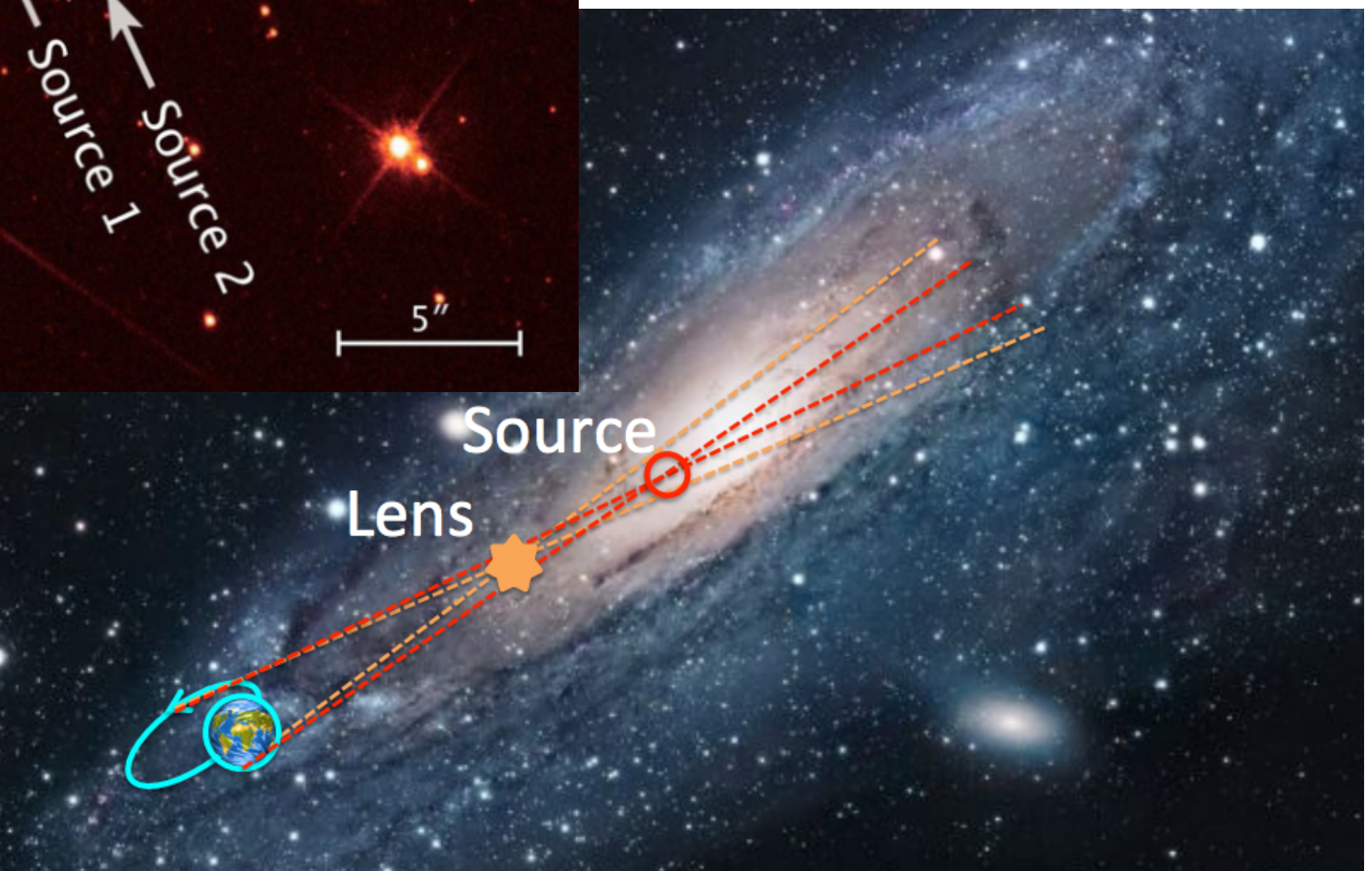
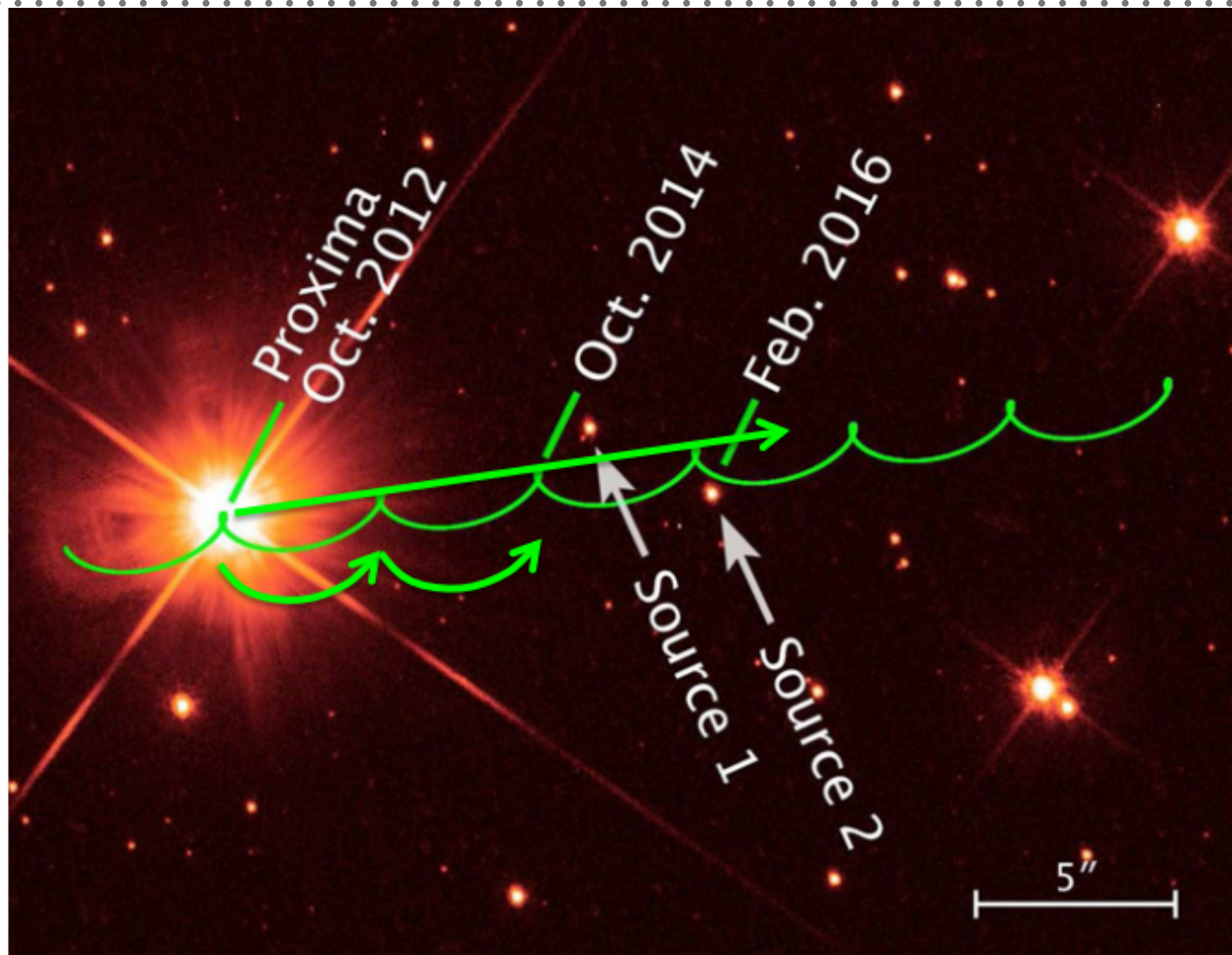
WHAT KIND OF MEASURABLE EFFECTS DOES PARALLAX CAUSE?

Parallax causes a difference in the relative position of lens and source depending on the observer point of view. Since the observable in a microlensing event depends on the relative separation between source and lens, parallax effects are very relevant.

In microlensing, parallax effects can be observed in two ways:

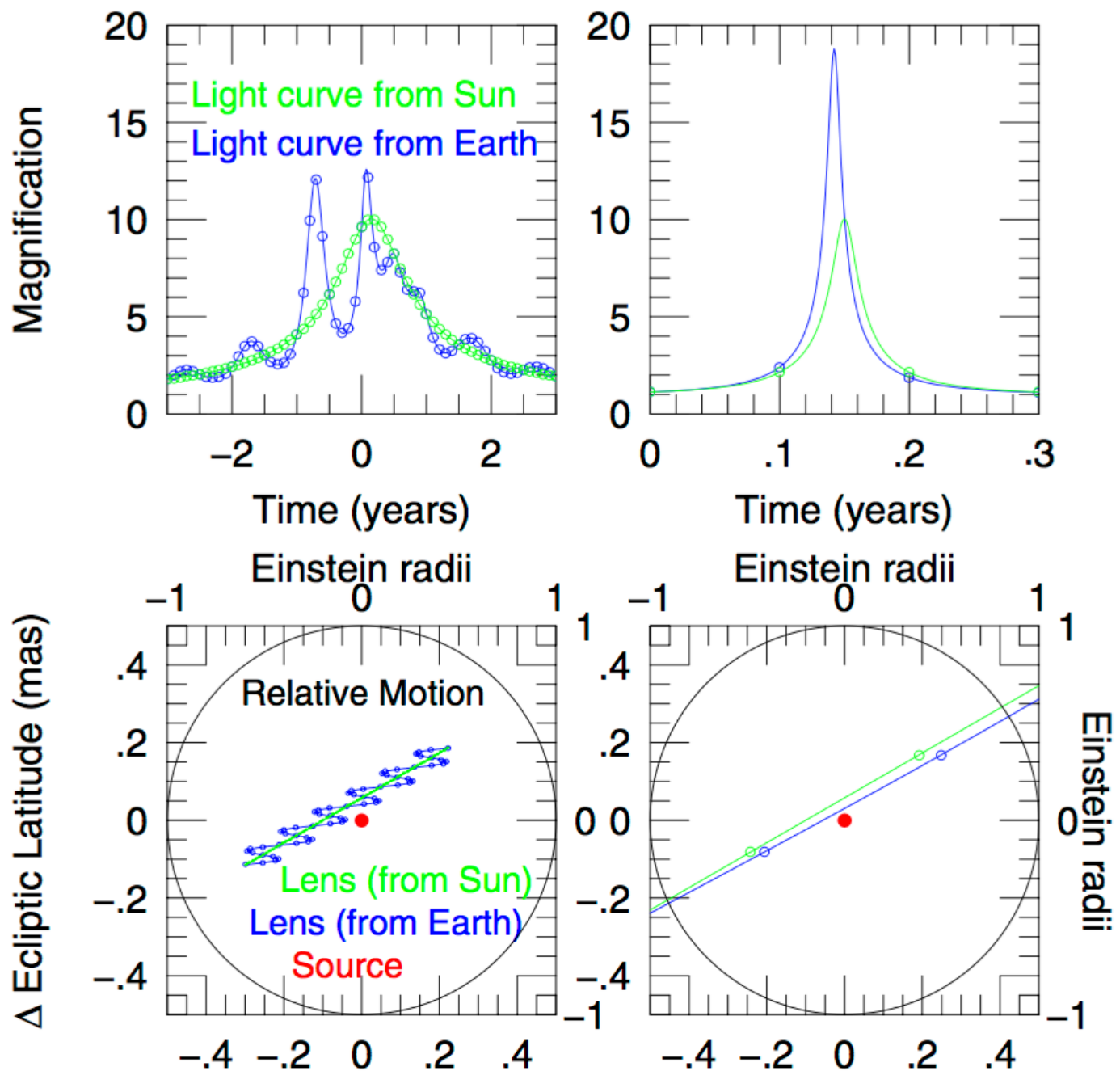
- *Because the observer move during the microlensing event*
- *Because two observers look at the same pair of lens and source from different positions*

ORBITAL PARALLAX

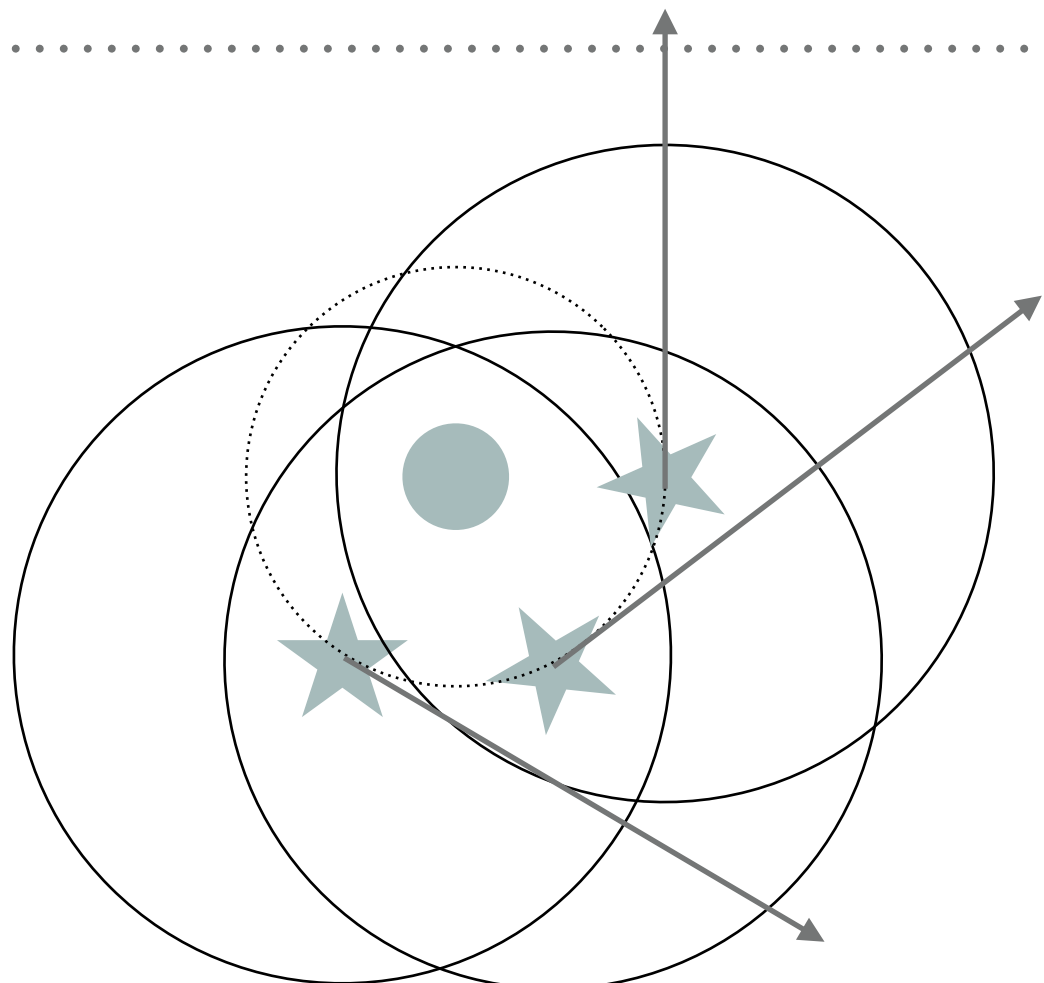


ORBITAL PARALLAX

- on the left: what we would see if the $\mu_{\text{hel}}=0.1$ mas/year
- on the right: the typical $\mu_{\text{hel}}=5$ mas/year



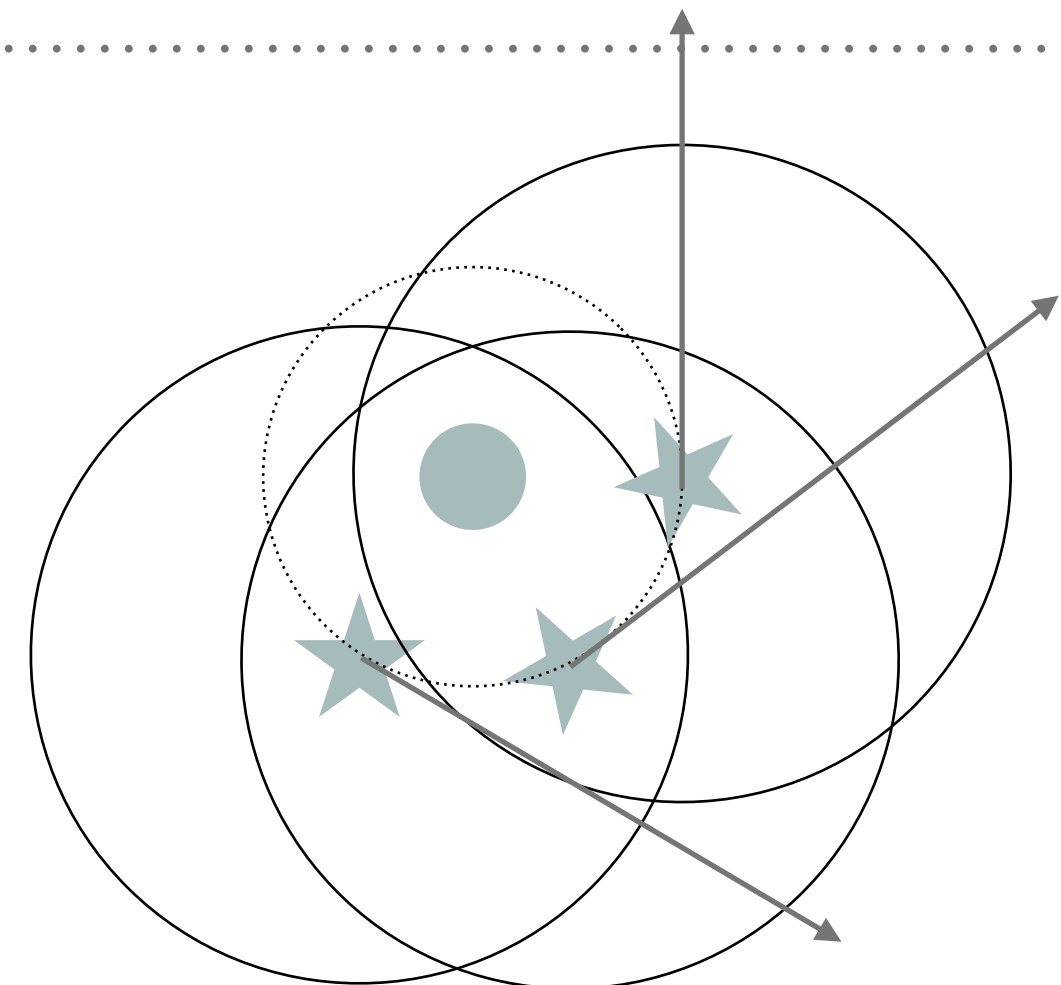
IMPORTANT: MICROLENSING PARALLAX IS A VECTOR!



*Magnification does not depend on
the direction of proper motion*

$$\mu(t) = \frac{y^2(t) + 2}{y(t)\sqrt{y^2(t) + 4}}$$

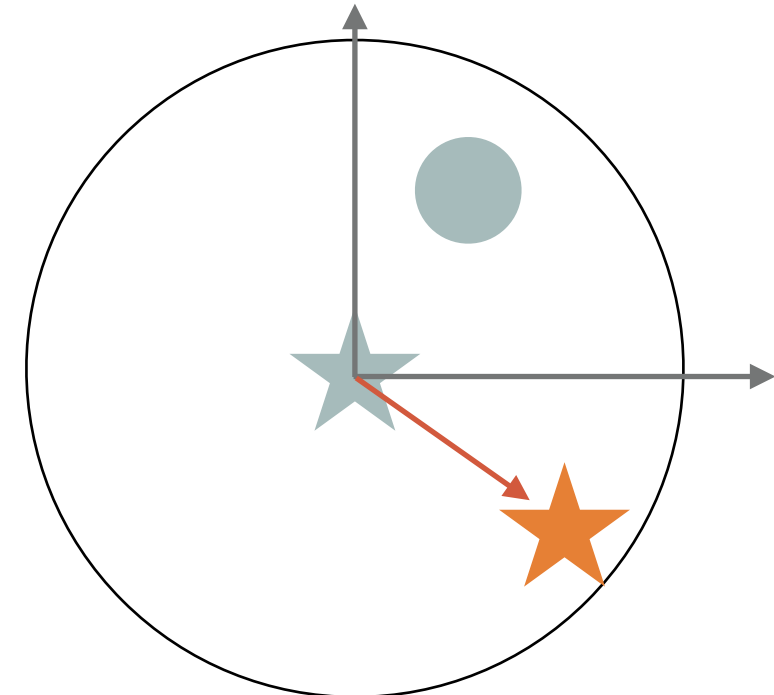
IMPORTANT: MICROLENSING PARALLAX IS A VECTOR!



Magnification does not depend on the direction of proper motion

$$\mu(t) = \frac{y^2(t) + 2}{y(t)\sqrt{y^2(t) + 4}}$$

$$\vec{\pi}_E = \pi_E \frac{\vec{\mu}_{rel}}{\mu_{rel}}$$

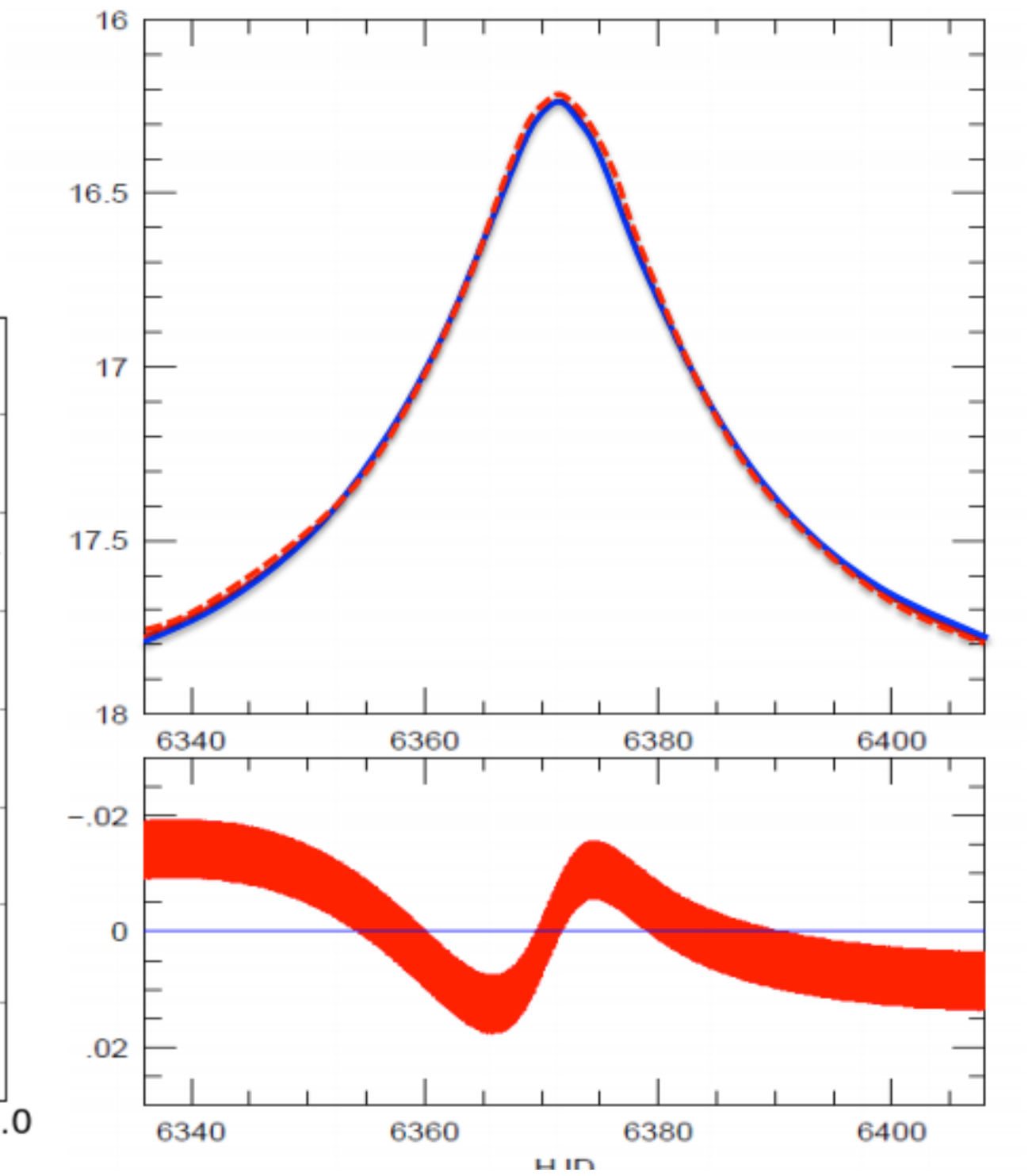
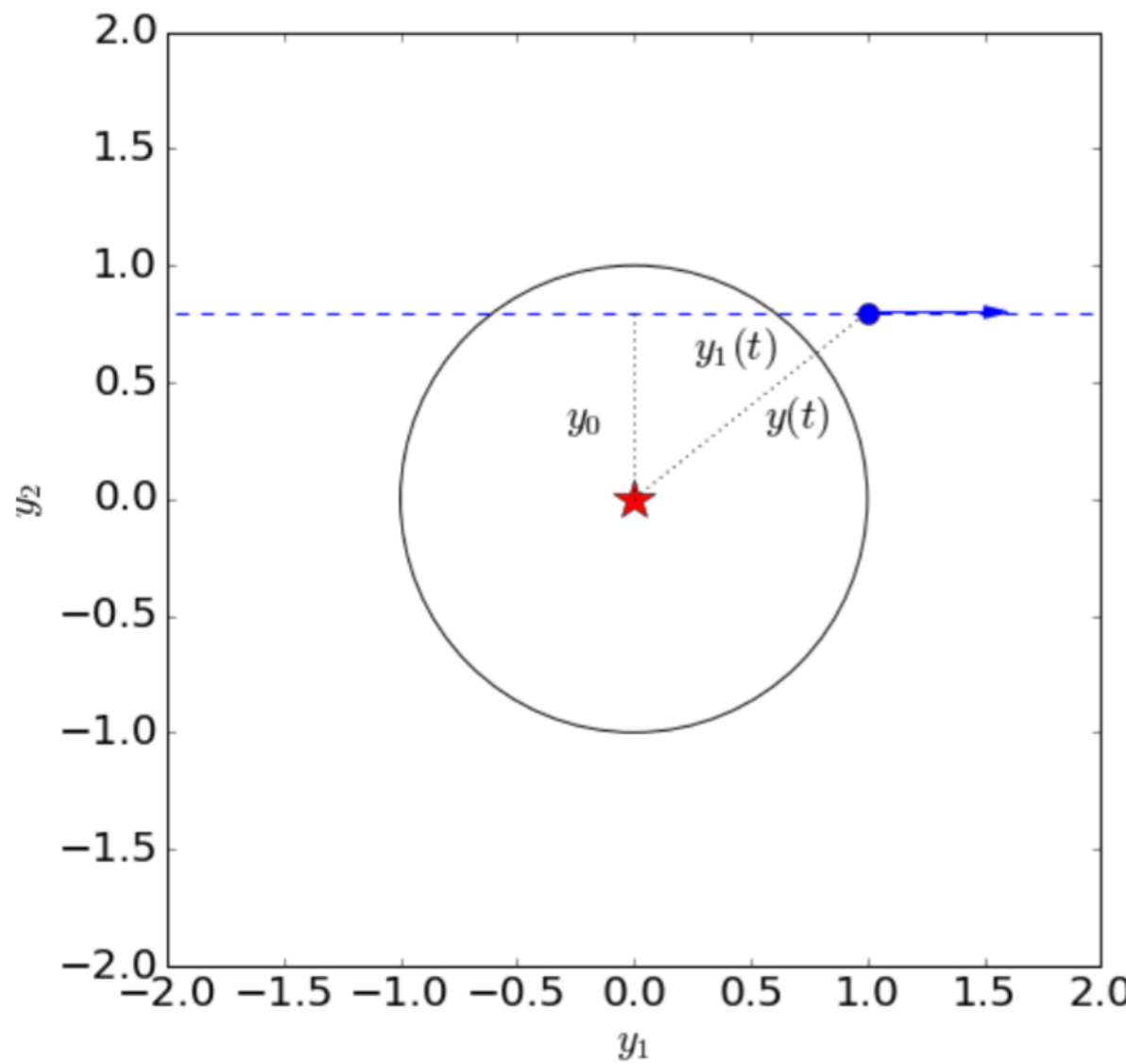


...but microlensing parallax does!

Depending on the lens displacement relative to the source (parallel or perpendicular to the proper motion), we will see different effects

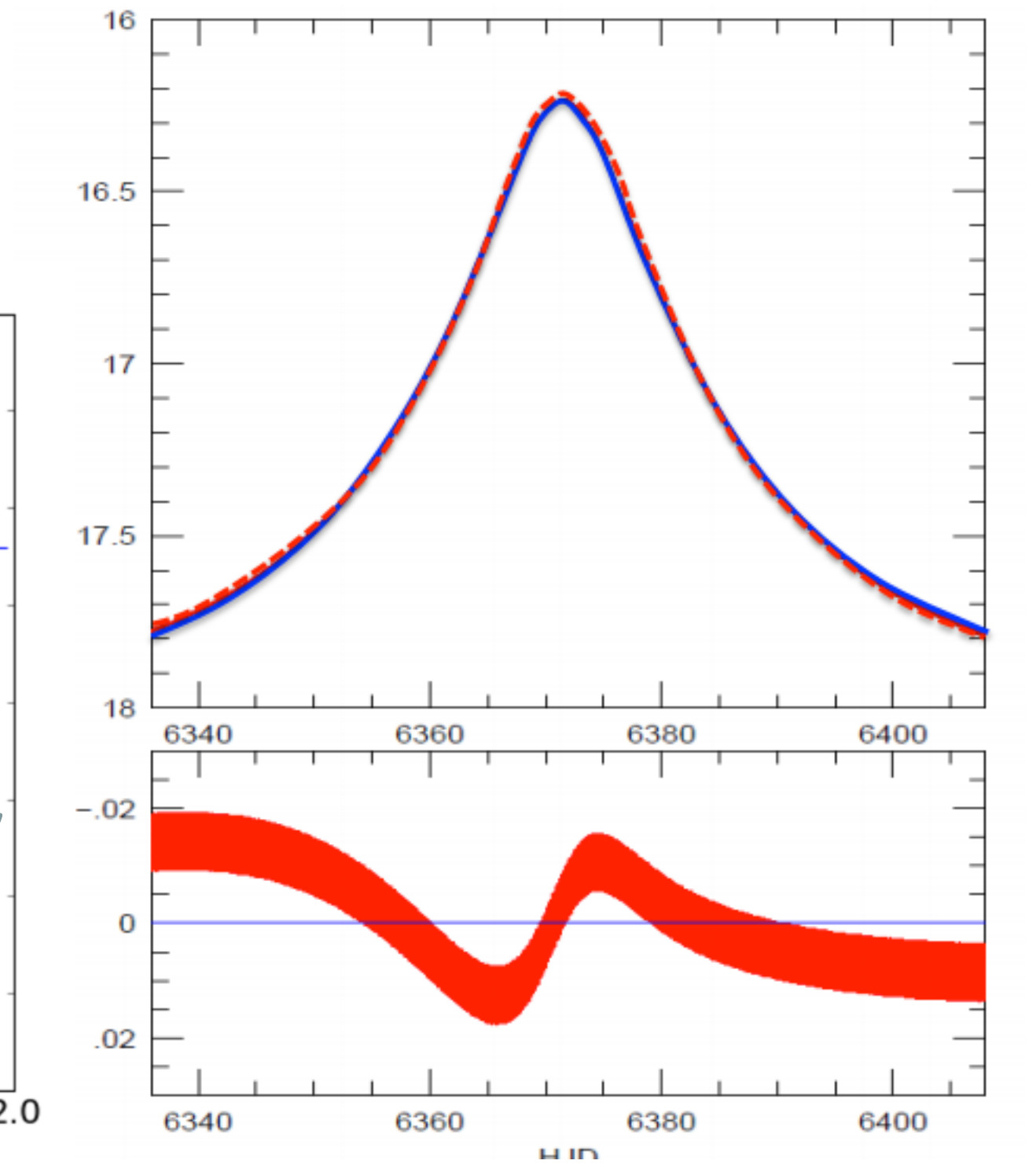
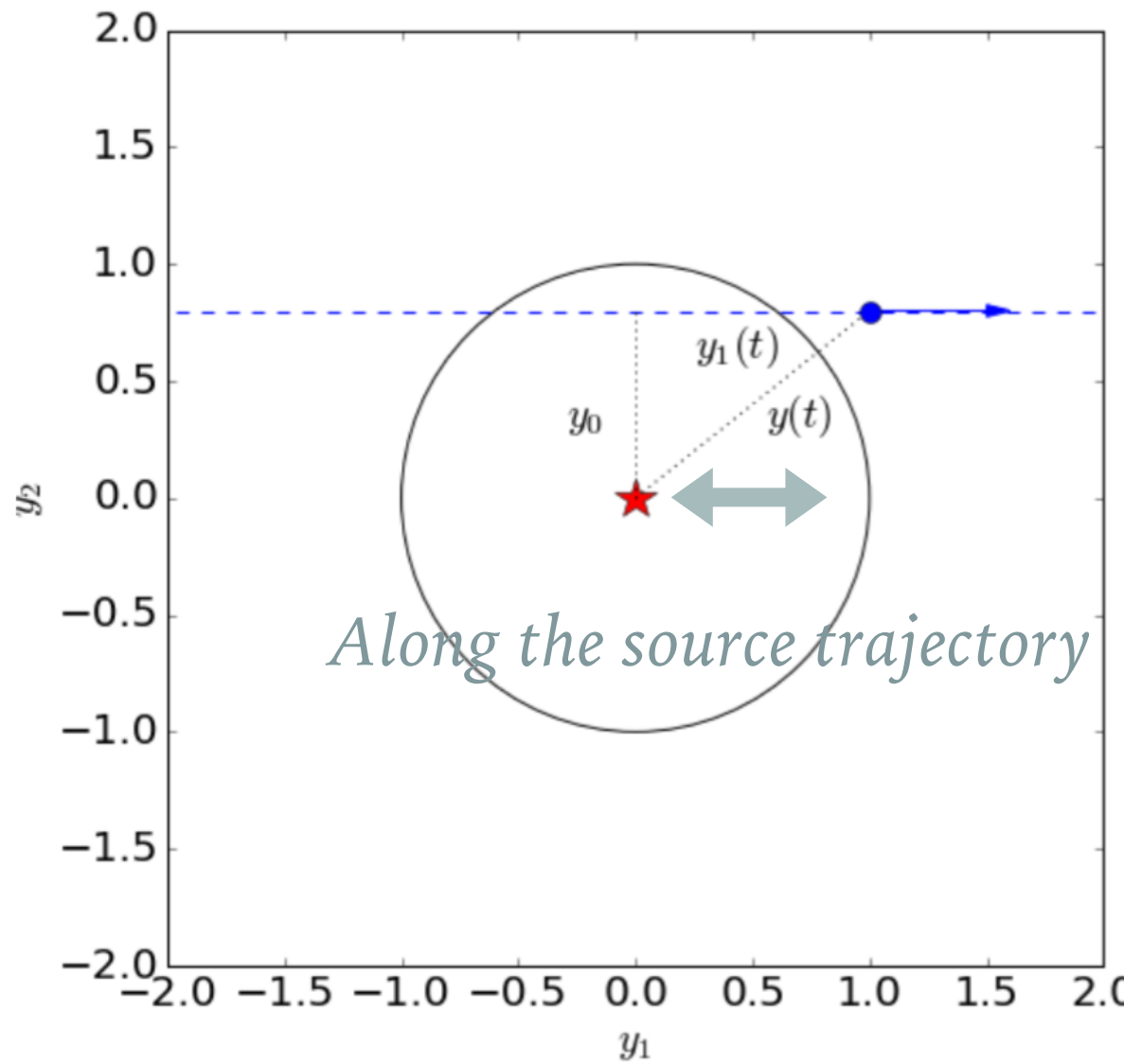
COMPONENT PARALLEL TO THE LENS TRAJECTORY

Asymmetric distortion of the light curve due to acceleration of the lens



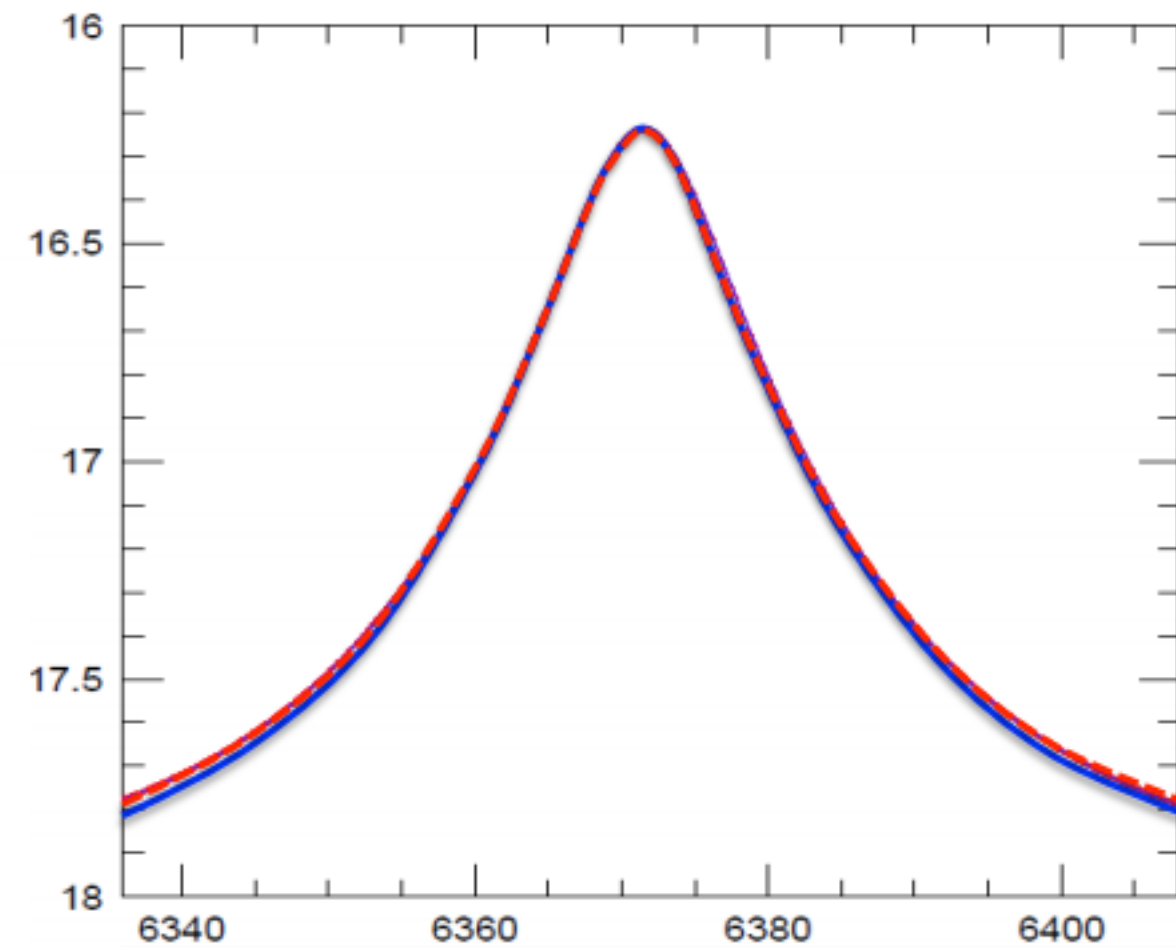
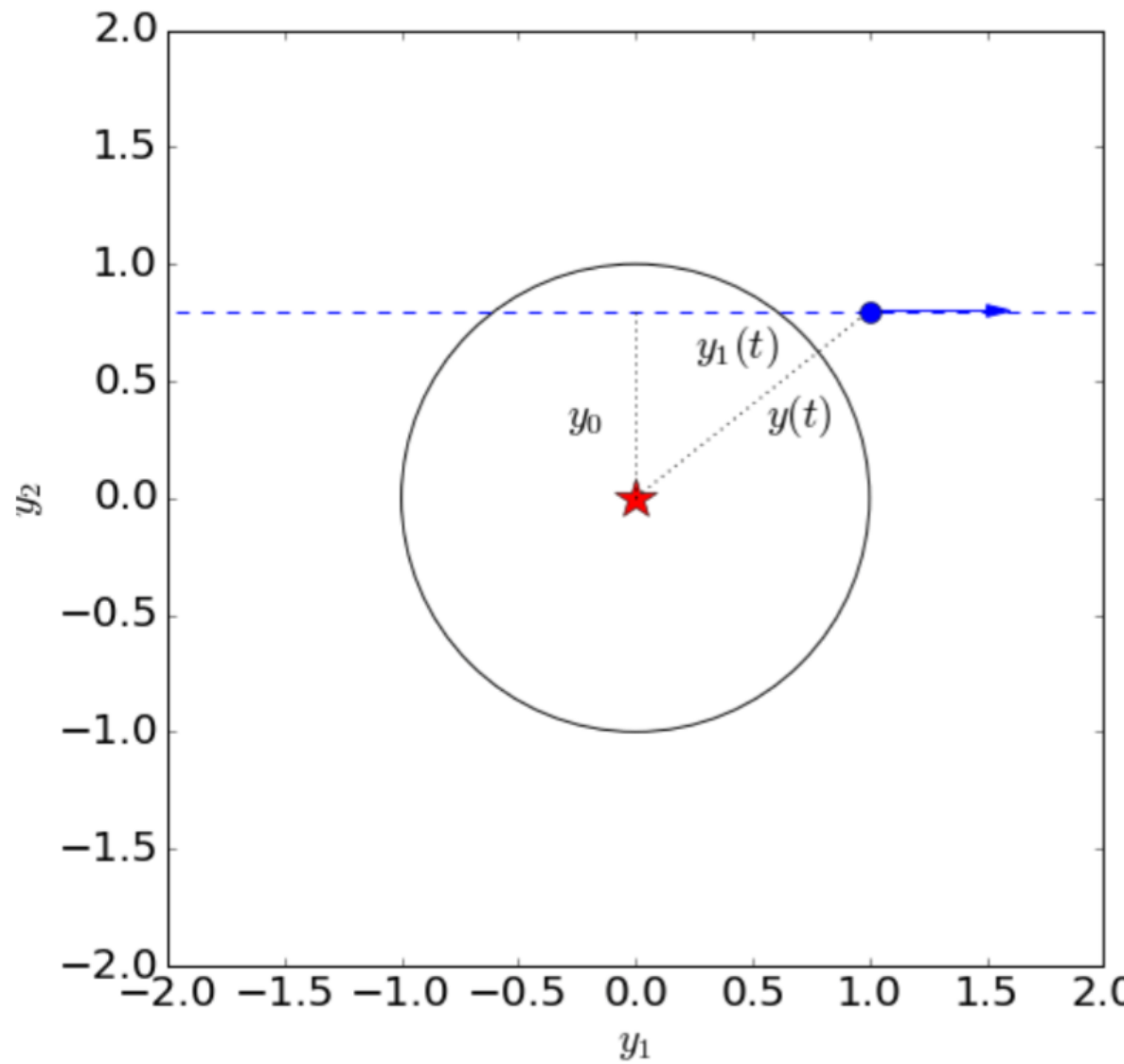
COMPONENT PARALLEL TO THE LENS TRAJECTORY

Asymmetric distortion of the light curve due to acceleration of the lens



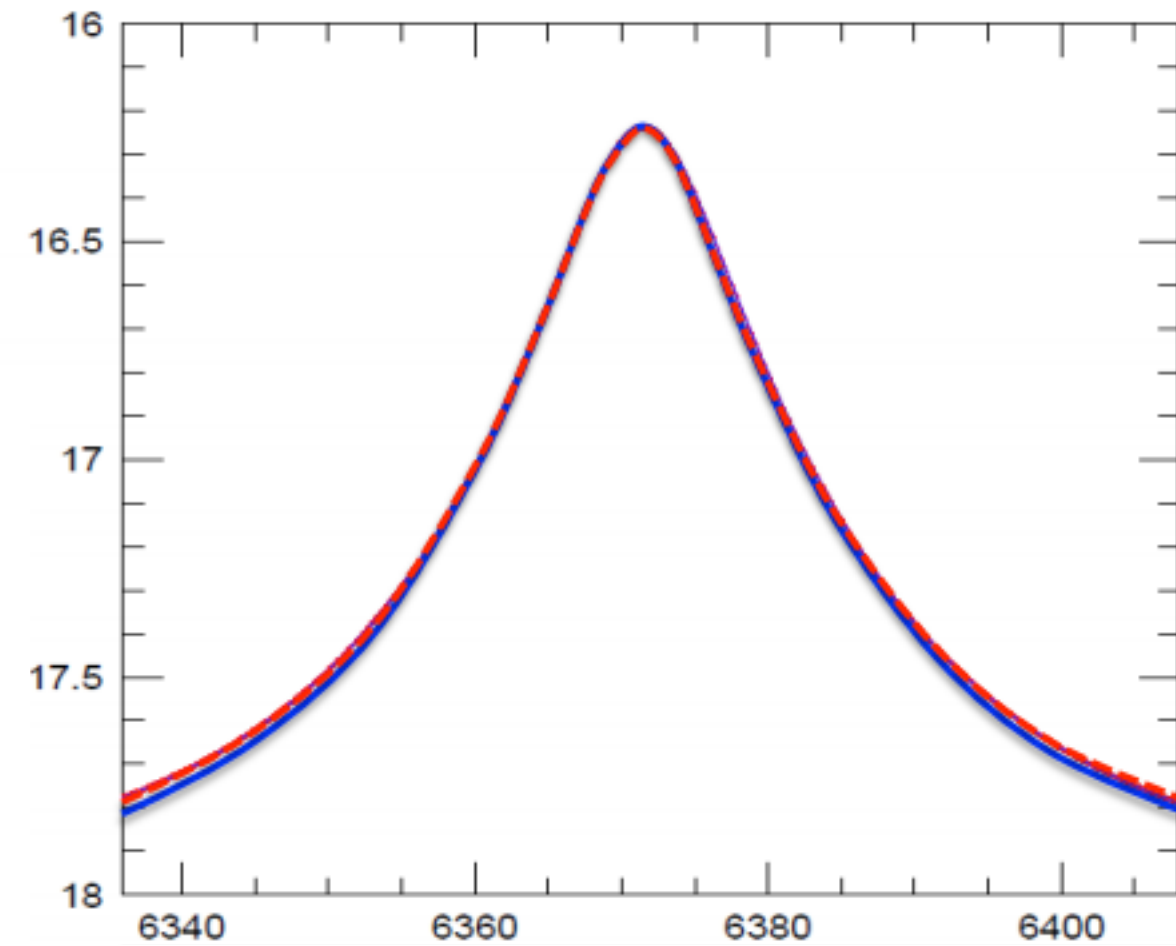
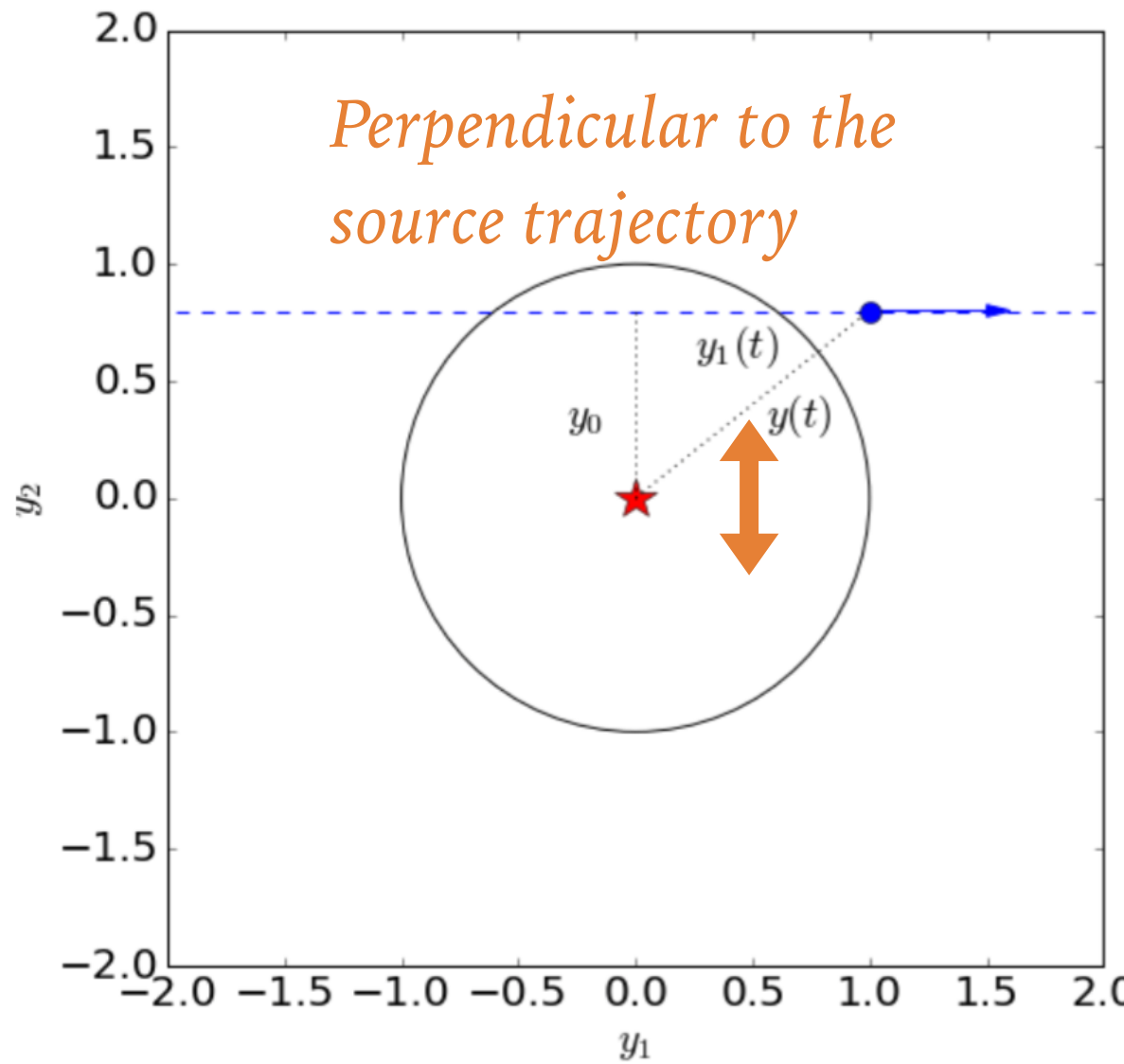
COMPONENT PERPENDICULAR TO THE LENS TRAJECTORY

Symmetric distortion of the light curve due to motion perpendicular to lens trajectory



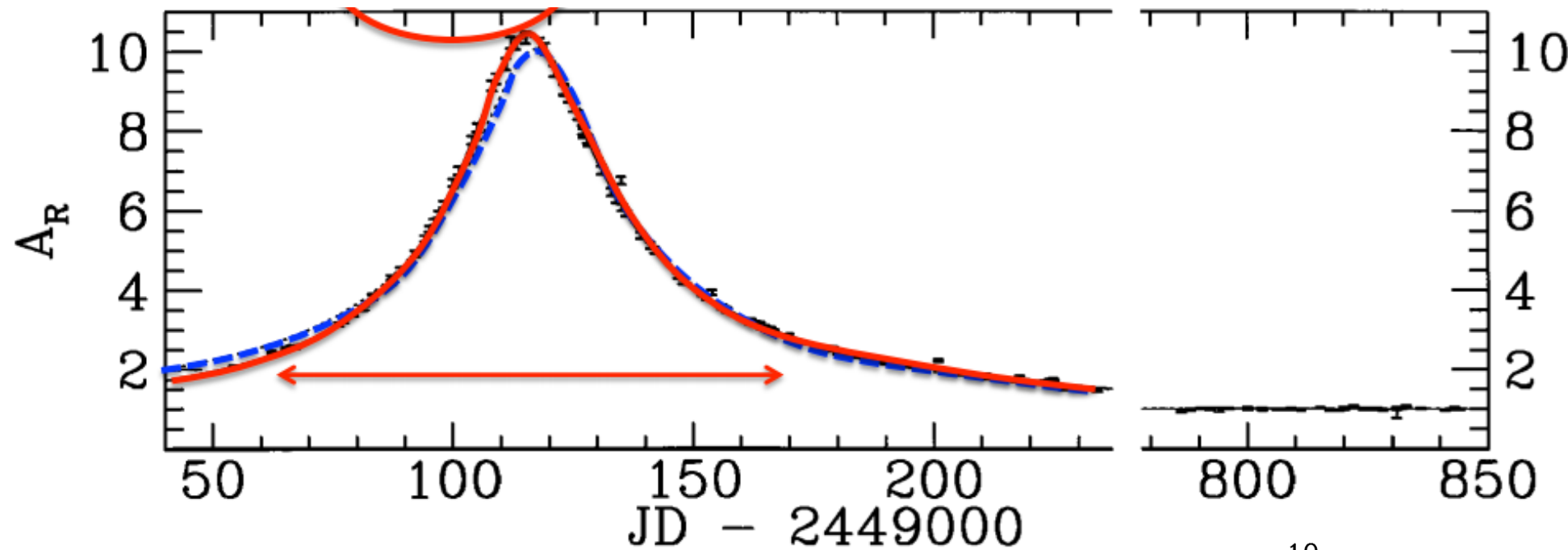
COMPONENT PERPENDICULAR TO THE LENS TRAJECTORY

Symmetric distortion of the light curve due to motion perpendicular to lens trajectory

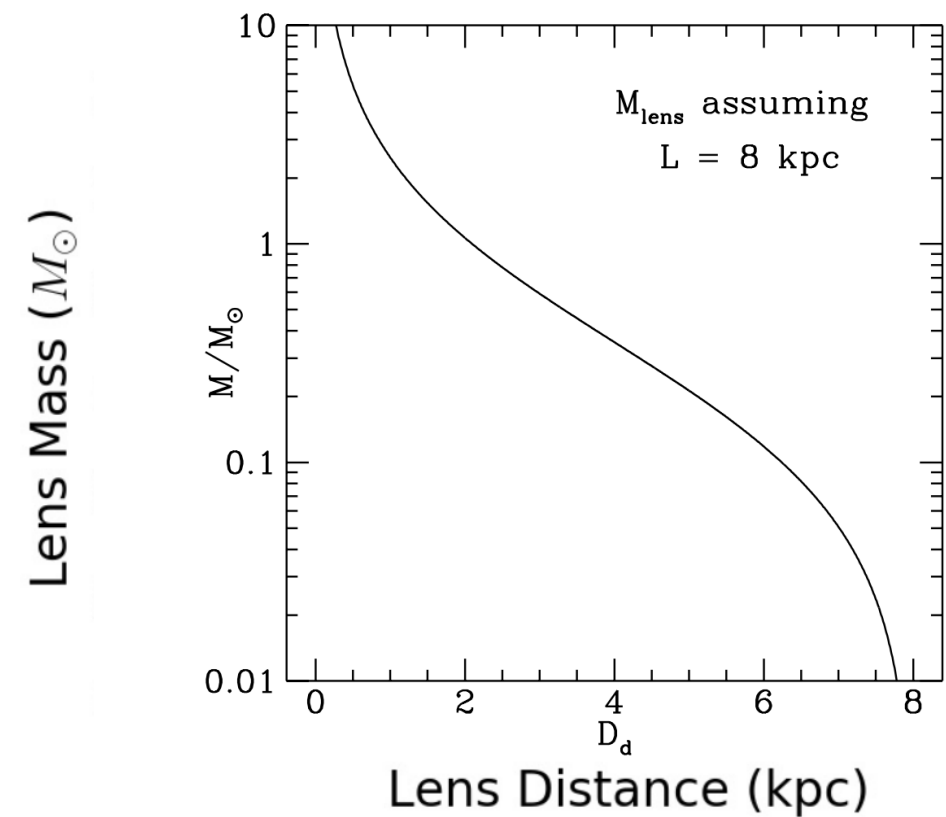


FIRST DETECTION OF ORBITAL PARALLAX

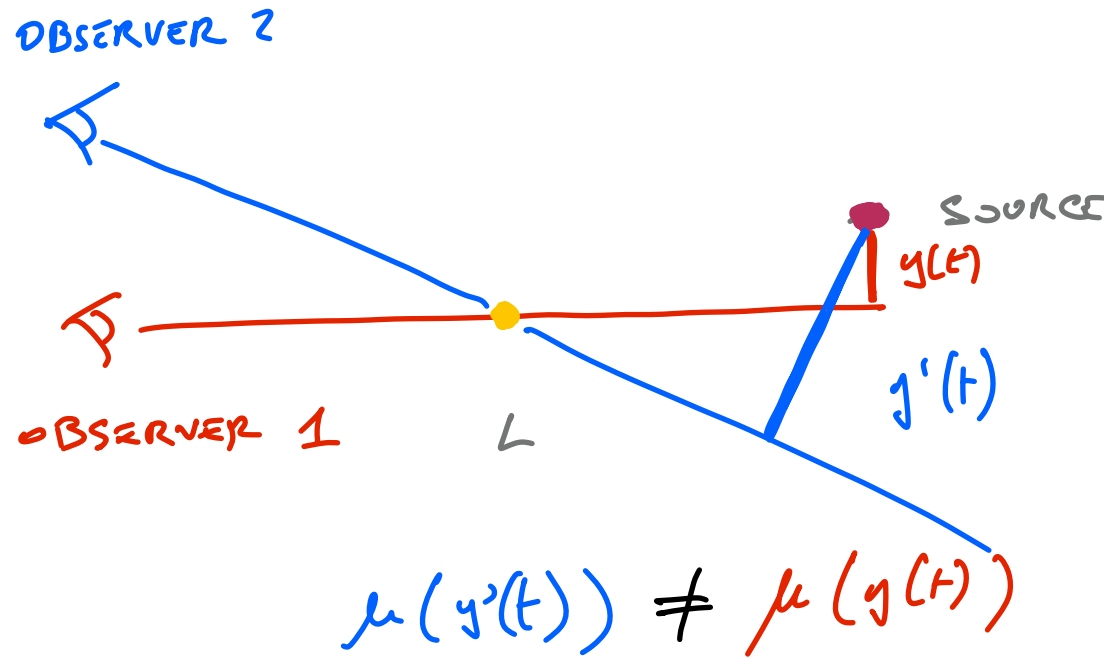
Alcock et al. 1995



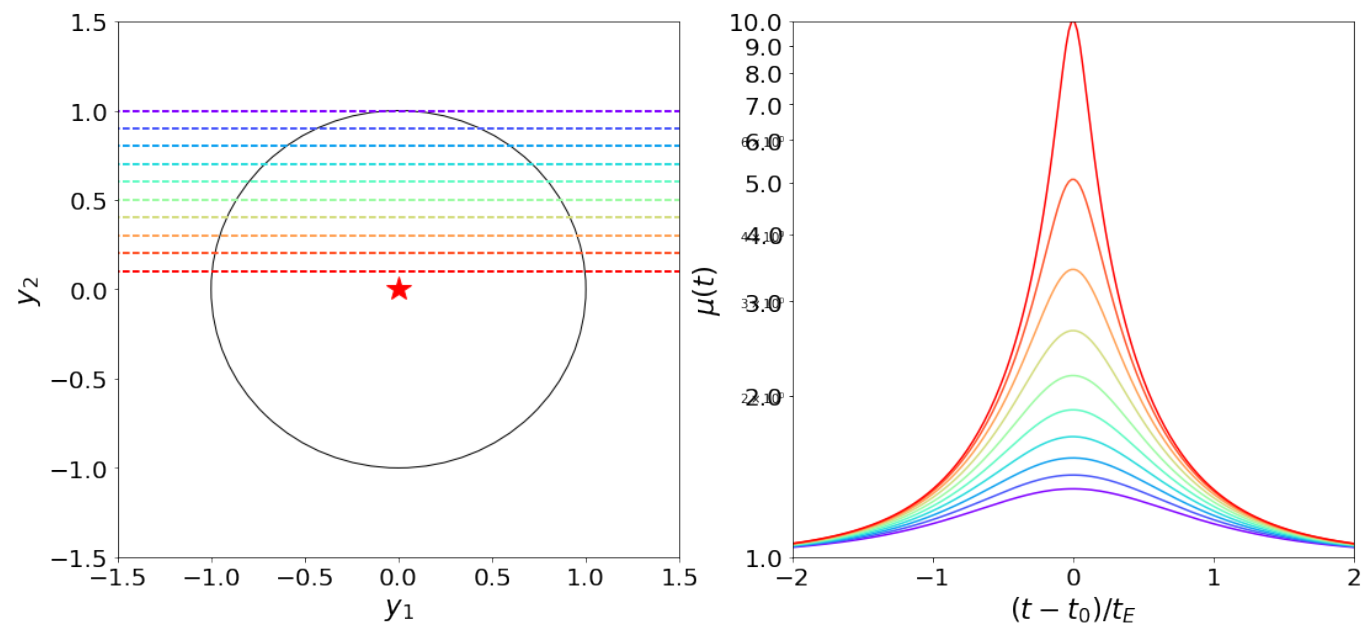
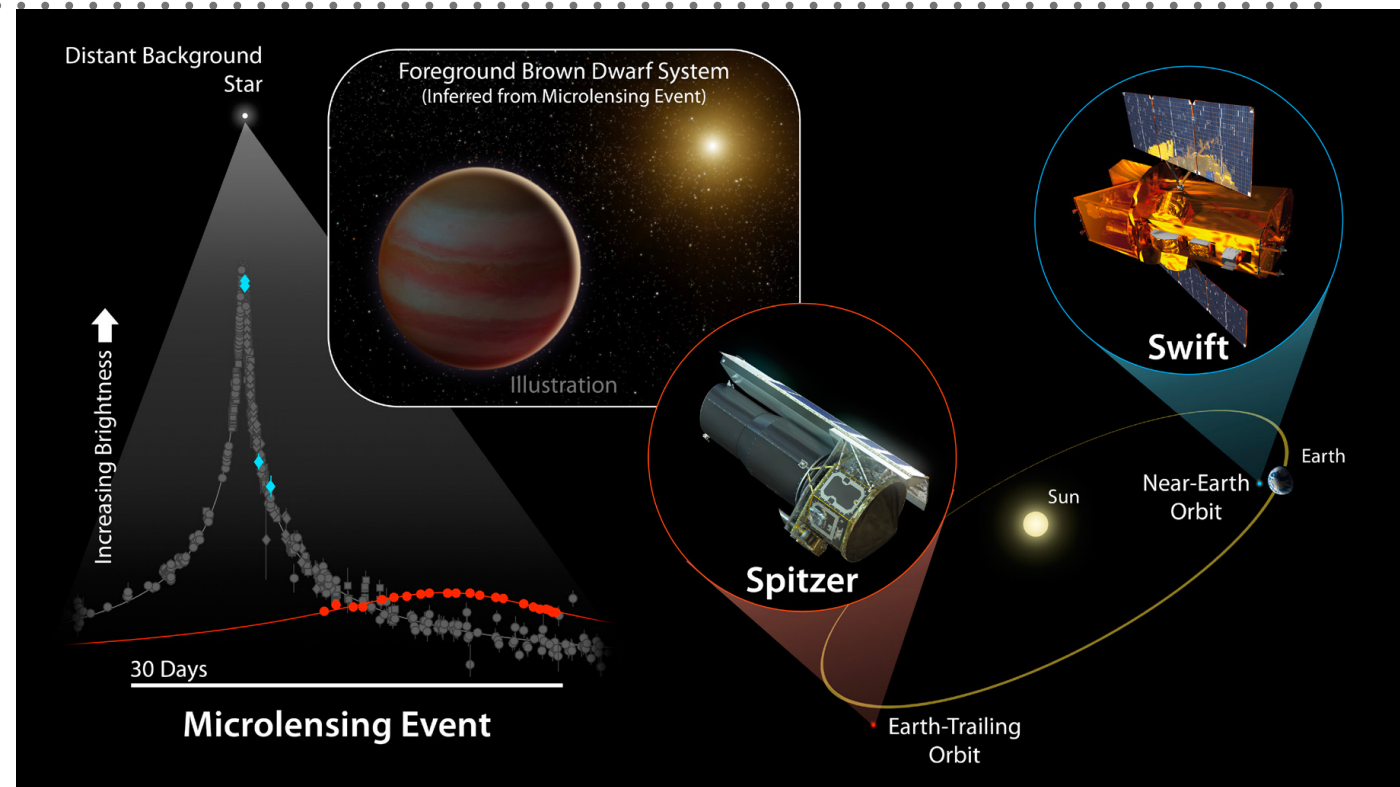
*Even without an estimate of θ_E ,
measuring the parallax still allows
to measure the mass vs distance*



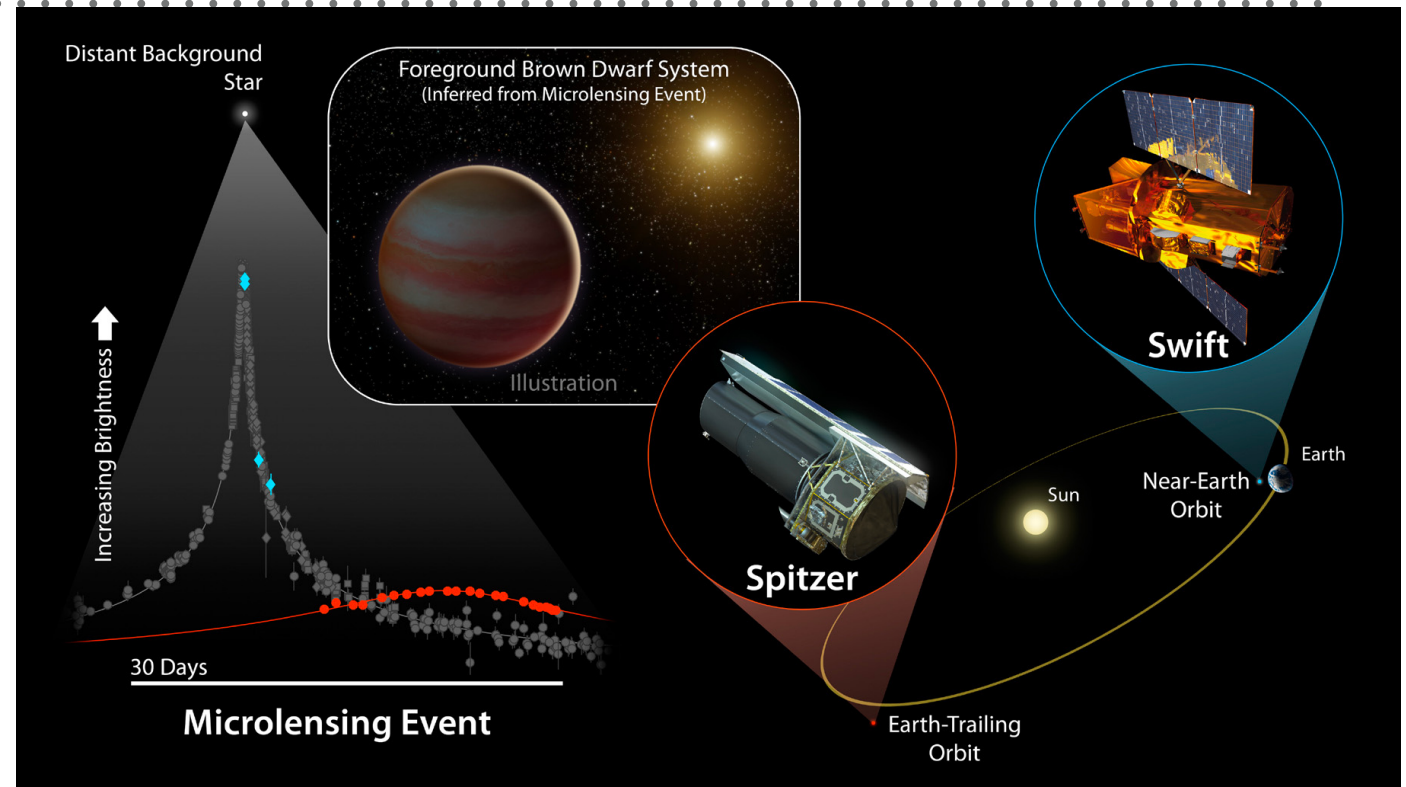
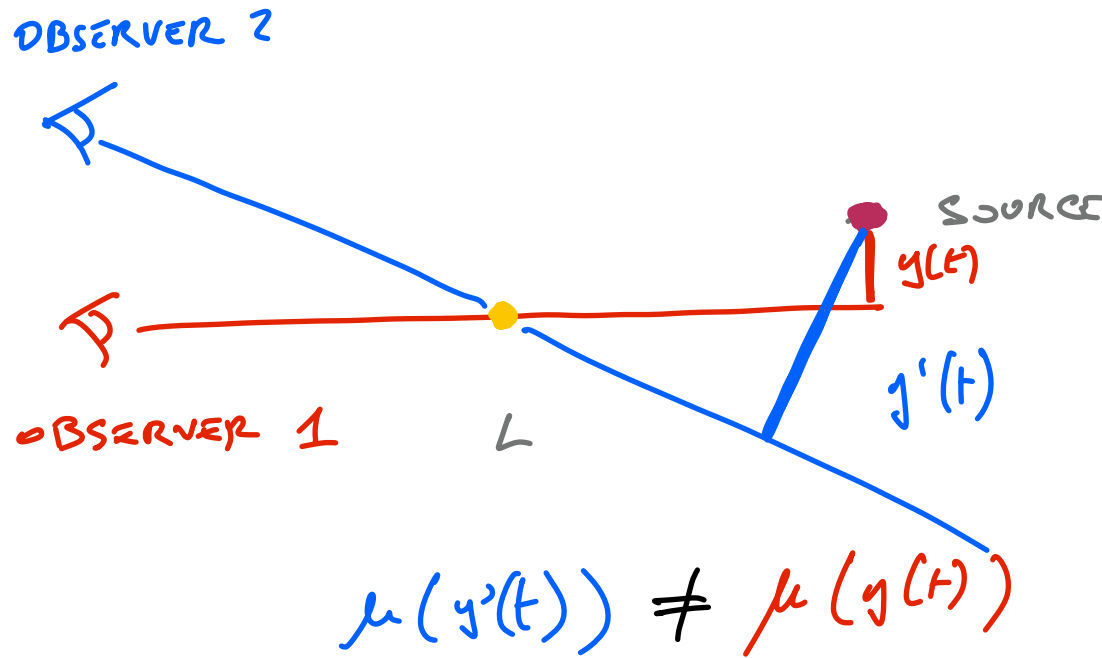
SATELLITE PARALLAX



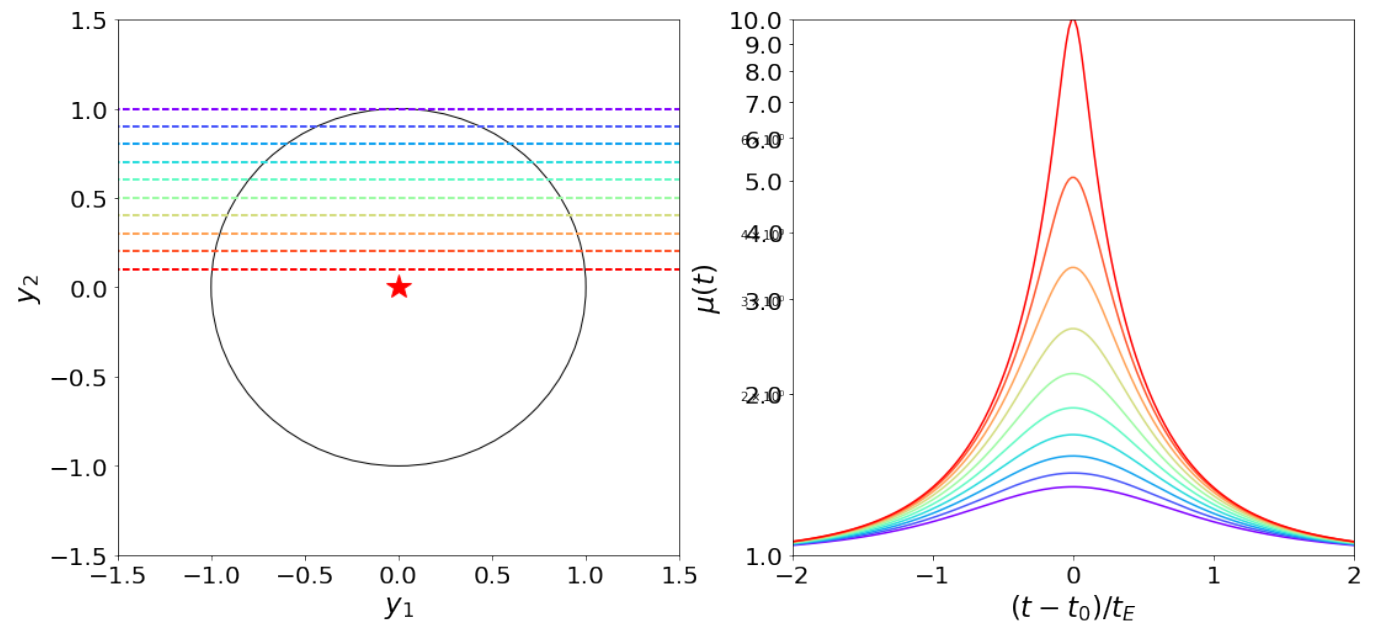
$$\mu(y(t)) = \frac{y(t)^2 + 2}{y(t)\sqrt{y(t)^2 + 4}}$$



SATELLITE PARALLAX

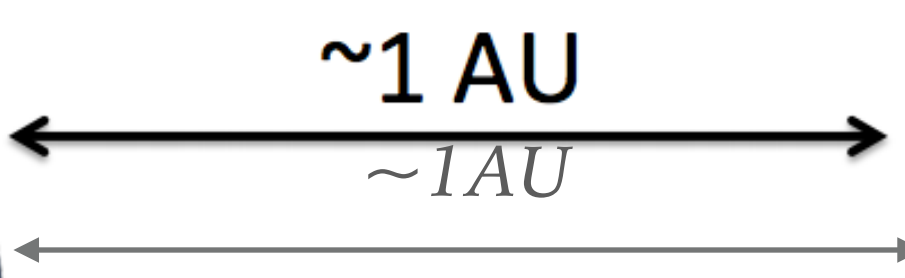


$$\mu(y(t)) = \frac{y(t)^2 + 2}{y(t)\sqrt{y(t)^2 + 4}}$$



Two observers looking at the same Microlensing event will see two different light curves (under some circumstances).

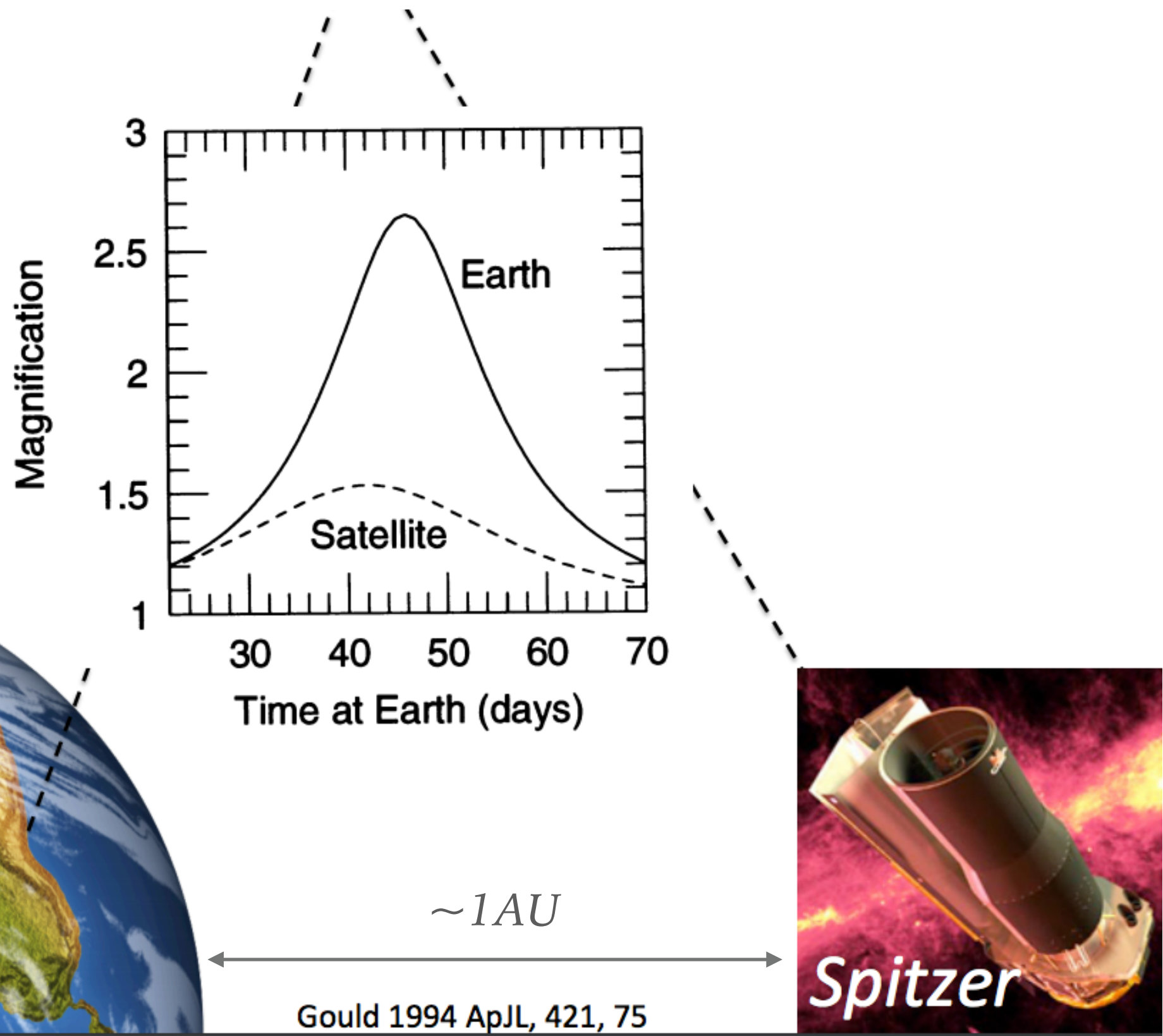
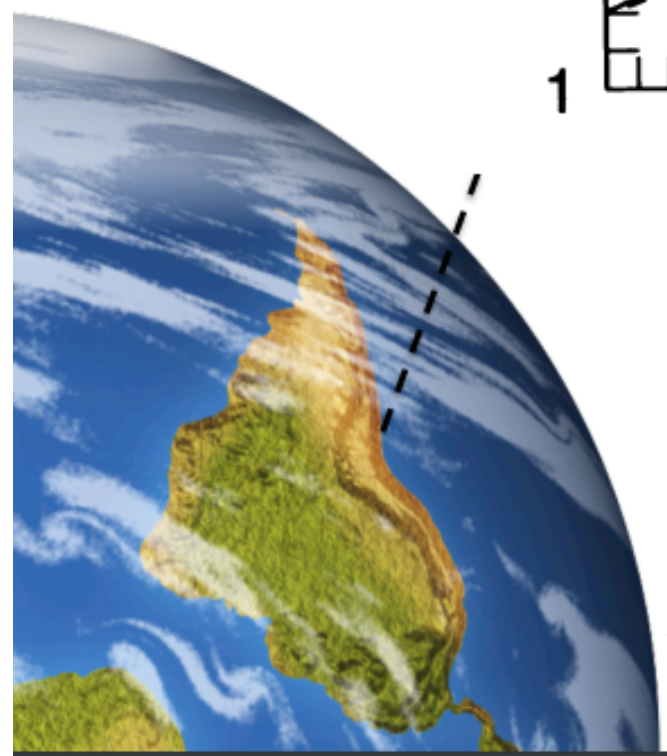
SATELLITE PARALLAX



Gould 1994 ApJL, 421, 75



SATELLITE PARALLAX



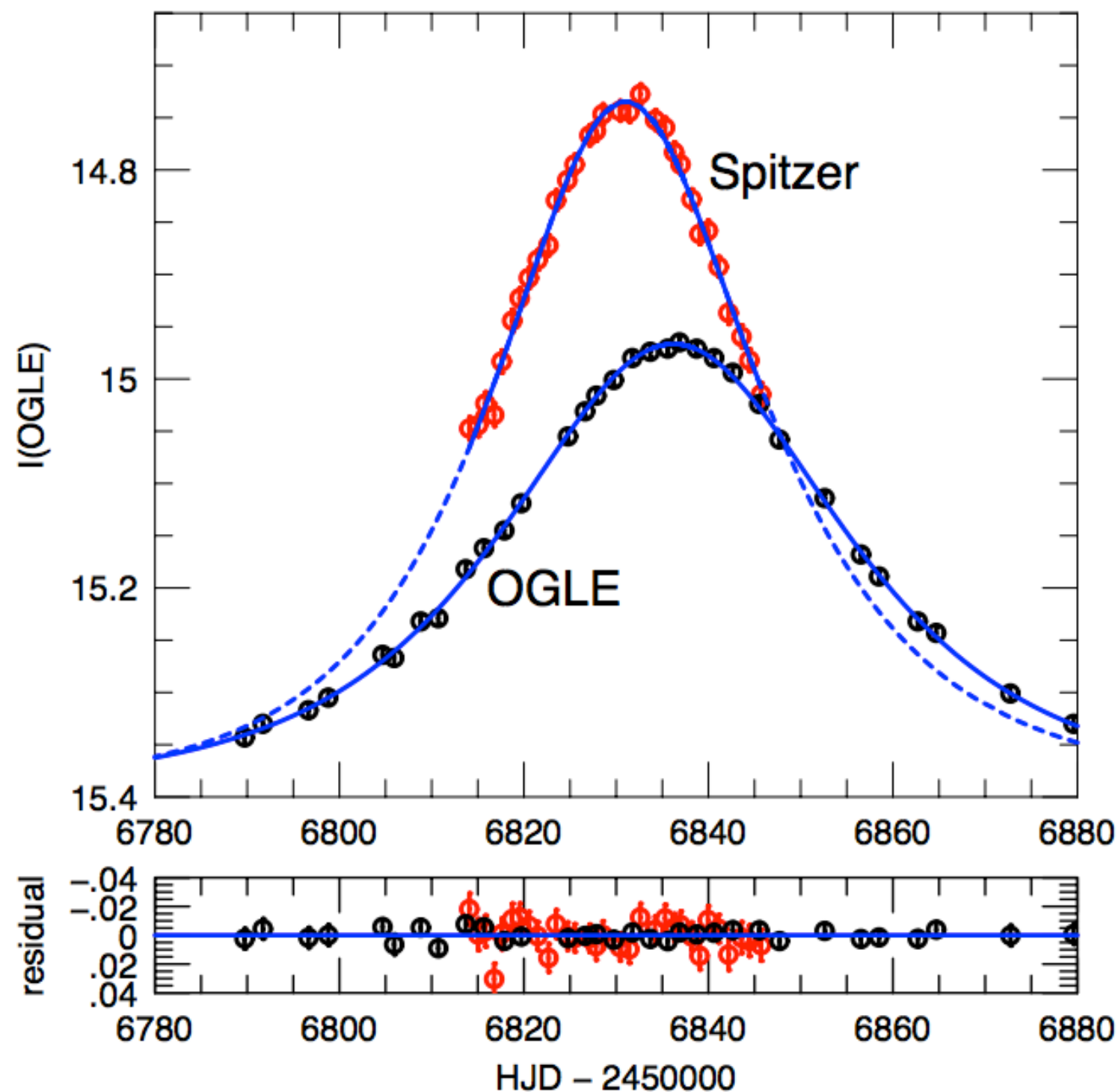
ORBITAL PARALLAX

Similarly, in the case of orbital parallax, what matters is the Einstein crossing time:

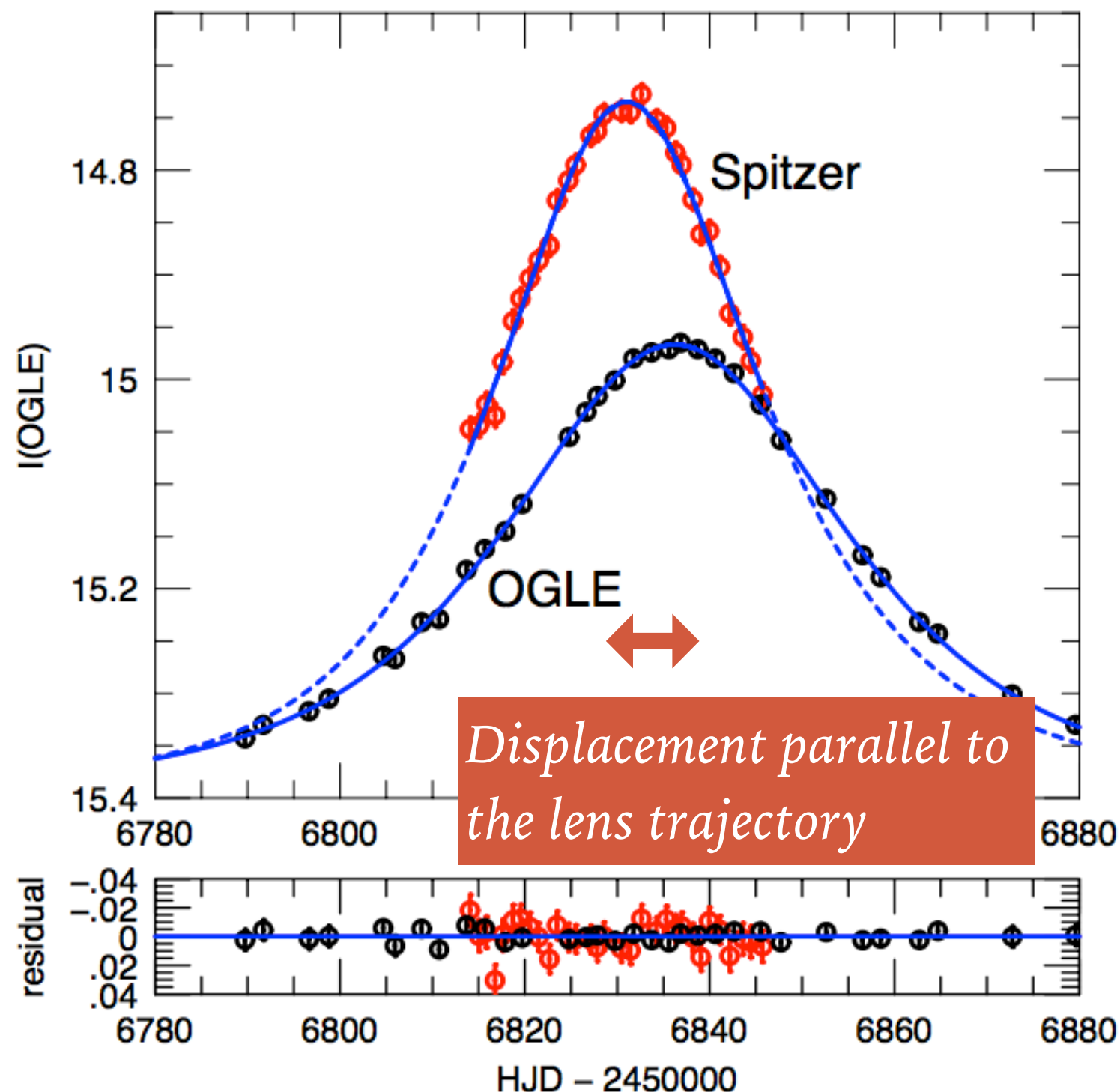
Are we likely to see annual parallax effects for an event with $t_E \sim 10$ days?

And for an event with $t_E \sim 100$ days?

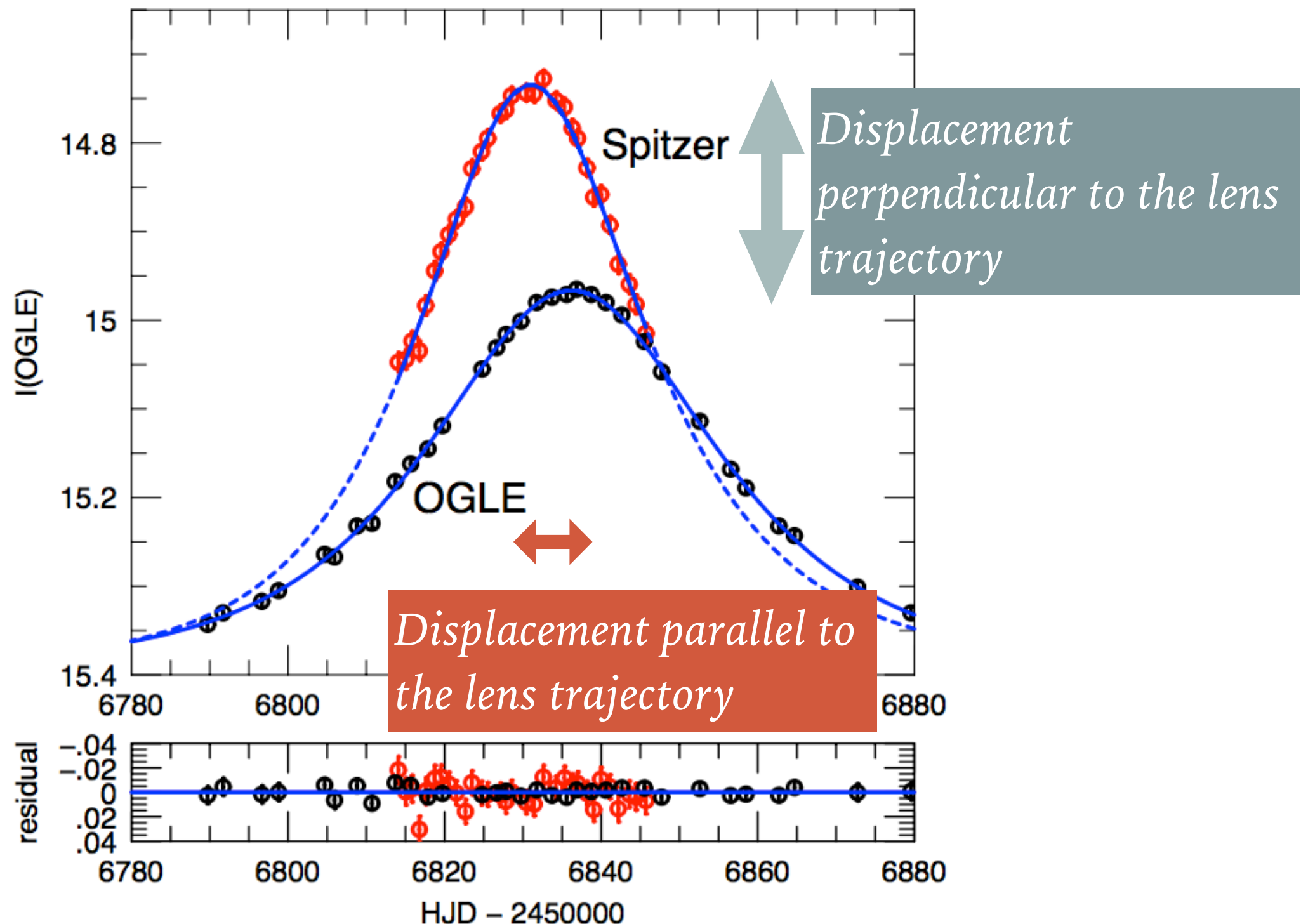
SATELLITE PARALLAX



SATELLITE PARALLAX



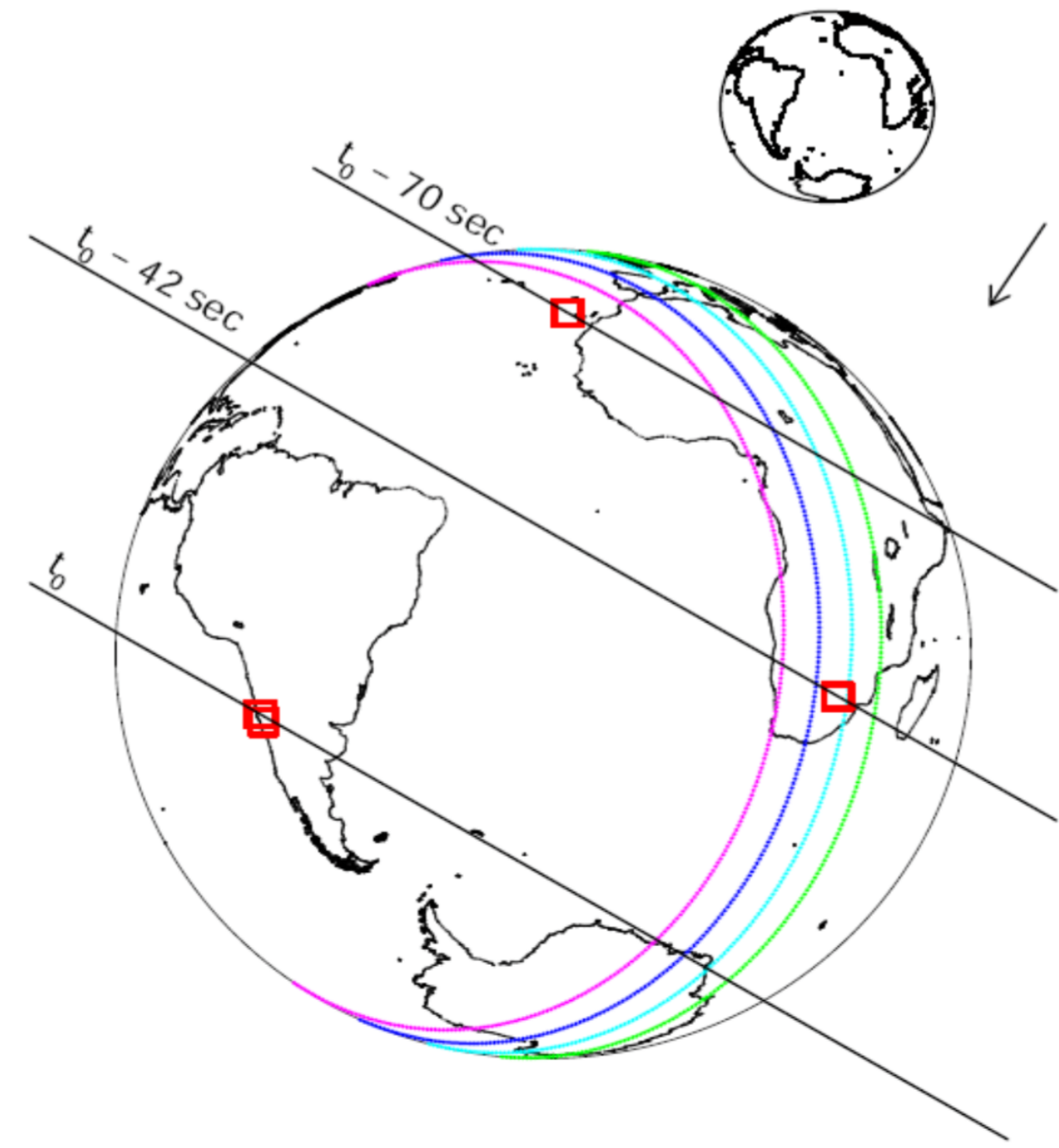
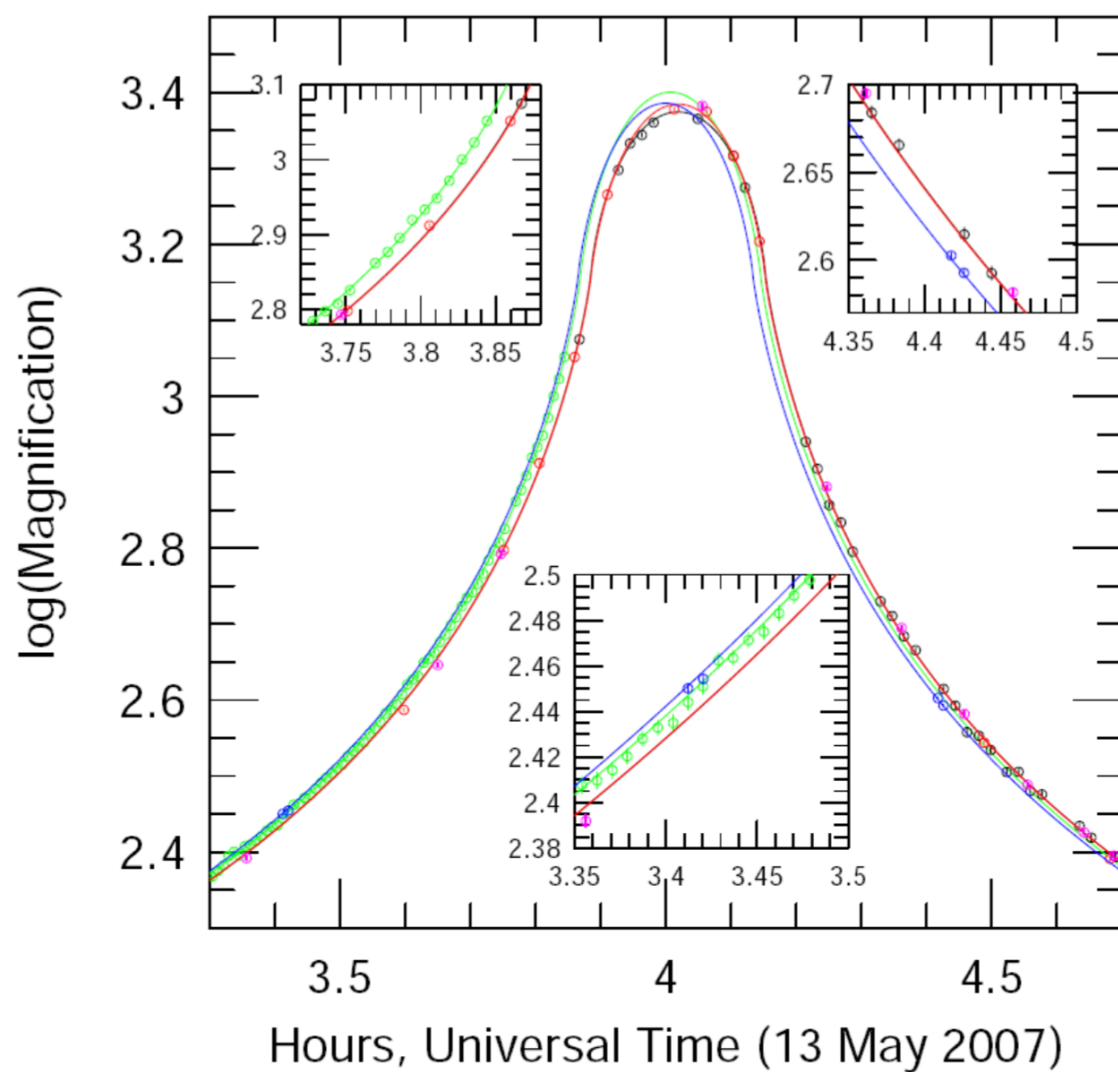
SATELLITE PARALLAX



MICROLENS PARALLAX (TERRESTRIAL)

OGLE-2007-BLG-224

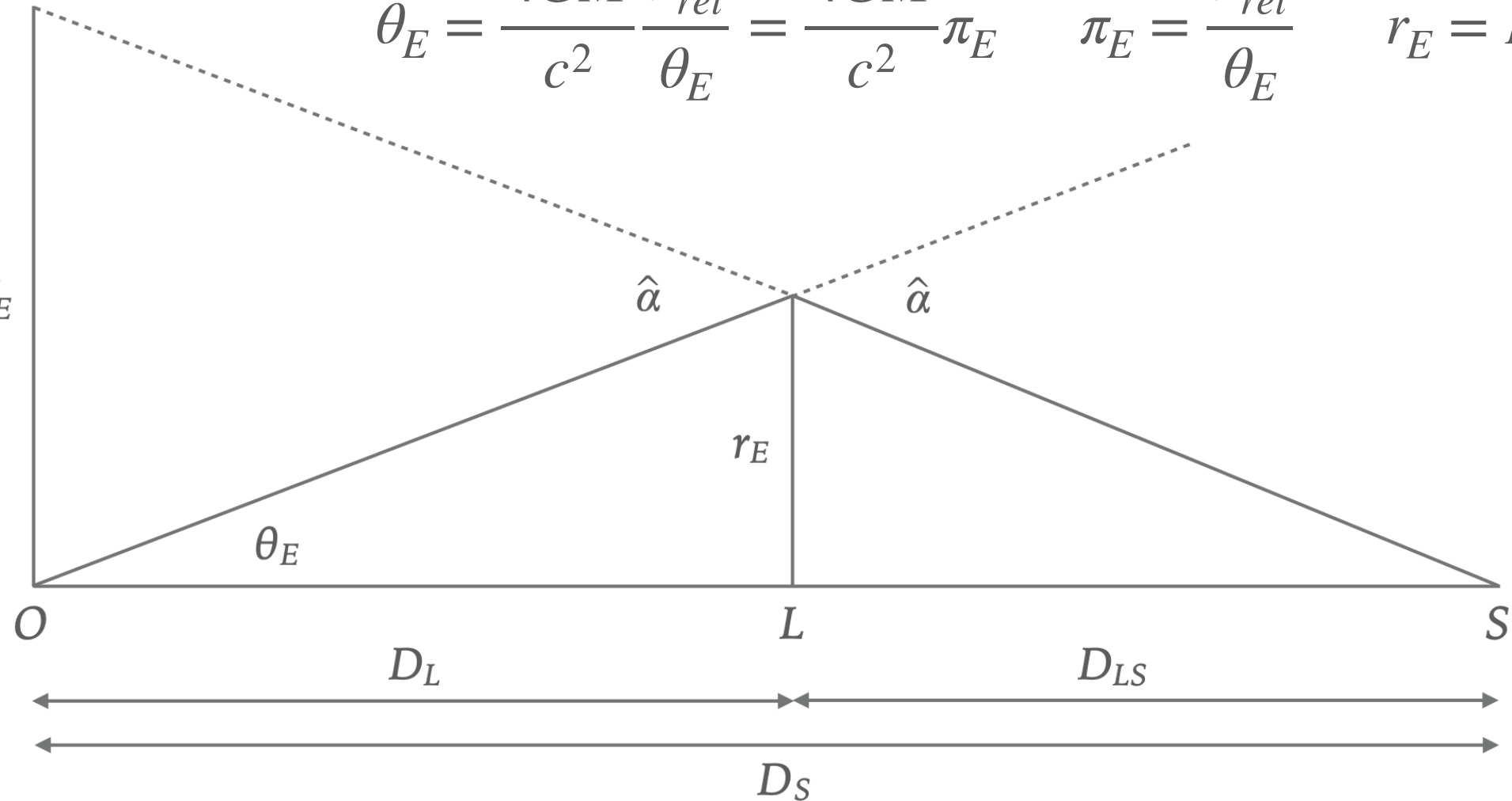
Canaries South Africa Chile



RELEVANT BASELINE

$$\theta_E = \frac{4GM}{c^2} \frac{\pi_{rel}}{\theta_E} = \frac{4GM}{c^2} \pi_E \quad \pi_E = \frac{\pi_{rel}}{\theta_E} \quad r_E = D_L \theta_E$$

Few-10 AU \tilde{r}_E



The relevant scale for parallax is the size of the Einstein radius on the observer plane

$$\tilde{r}_E = D_L \hat{\alpha}(\theta_E) = D_L \frac{4GM}{c^2 D_L \theta_E} = \frac{1}{\pi_E}$$

ASTROMETRIC MEASUREMENT OF THE RELATIVE PROPER MOTION

- Another method to measure the Einstein radius is by measuring the relative proper motion of source and lens.
- This requires to see the lens!
- If we have high resolution imaging with HST or ground based AO, we can measure the position of lens and source at some time after the maximum of the light curve Δt
- If we measure a shift $\Delta\theta$ then $\mu_{rel} = \Delta\theta/\Delta t$ and

$$\theta_E = t_E \times \mu_{rel}$$

ASTROMETRIC MICROLENSING

Position of the image centroid relative to the unlensed position.

$$\delta \vec{x} = \frac{|\mu_1| \vec{x}_1 + |\mu_2| \vec{x}_2}{|\mu_1| + |\mu_2|} - \vec{y}$$

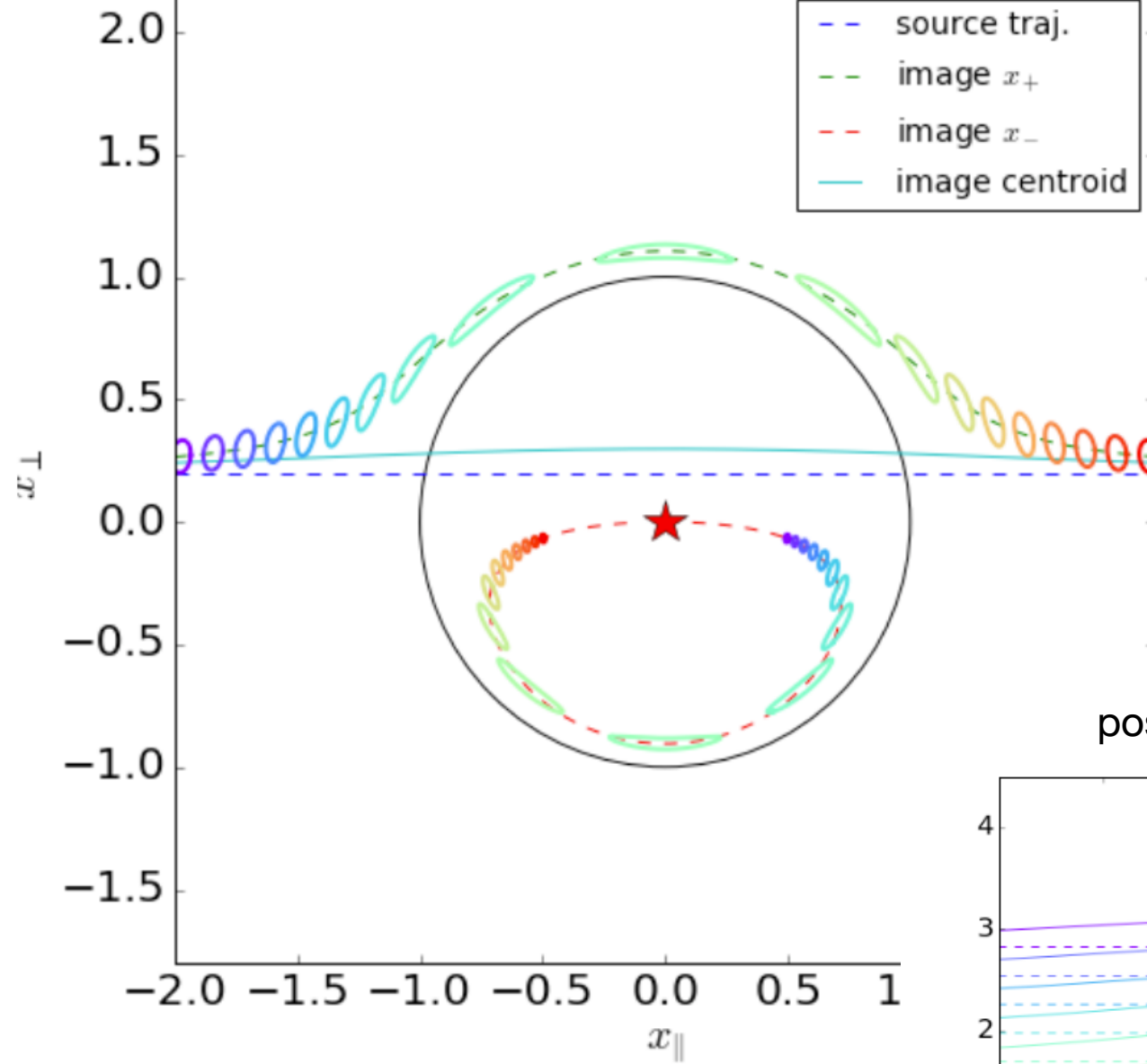
$$|\delta \vec{x}| = \frac{y}{y^2 + 2}$$

Components that are parallel and perpendicular to the motion of the star relative to the lens.

$$\vec{x}_{\parallel} = \delta \vec{x} \cdot \hat{y} = \frac{y_{\parallel}}{y^2 + 2} = \frac{(t - t_o)/t_E}{(t - t_o)^2/t_E^2 + y_o^2 + 2}$$

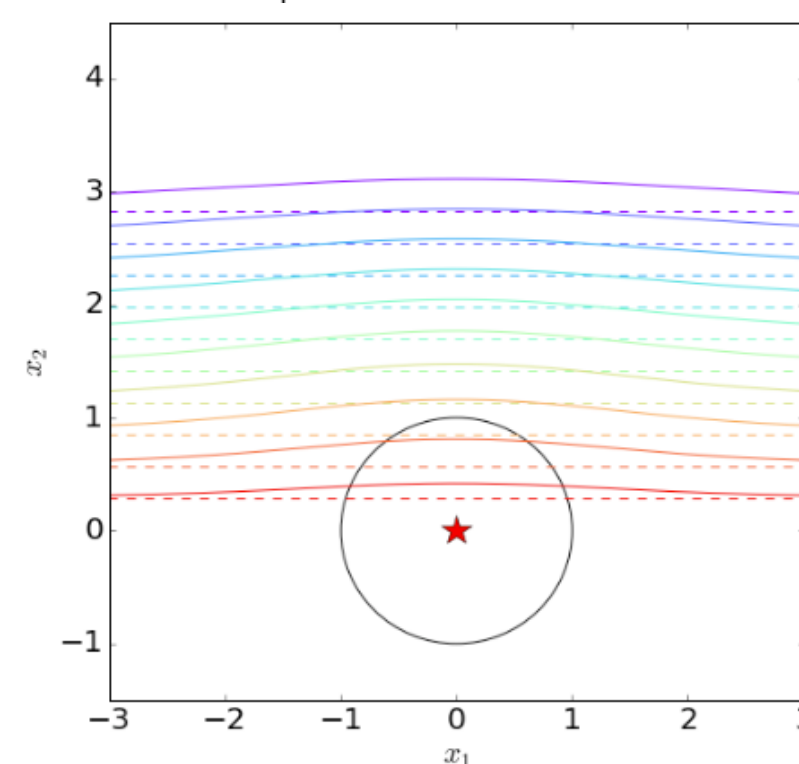
$$\vec{x}_{\perp} = \delta \vec{x} - (\delta \vec{x} \cdot \hat{y}) \hat{y} = \frac{y_{\perp}}{y^2 + 2} = \frac{y_o}{(t - t_o)^2/t_E^2 + y_o^2 + 2}$$

ASTROMETRIC MICROLENSING

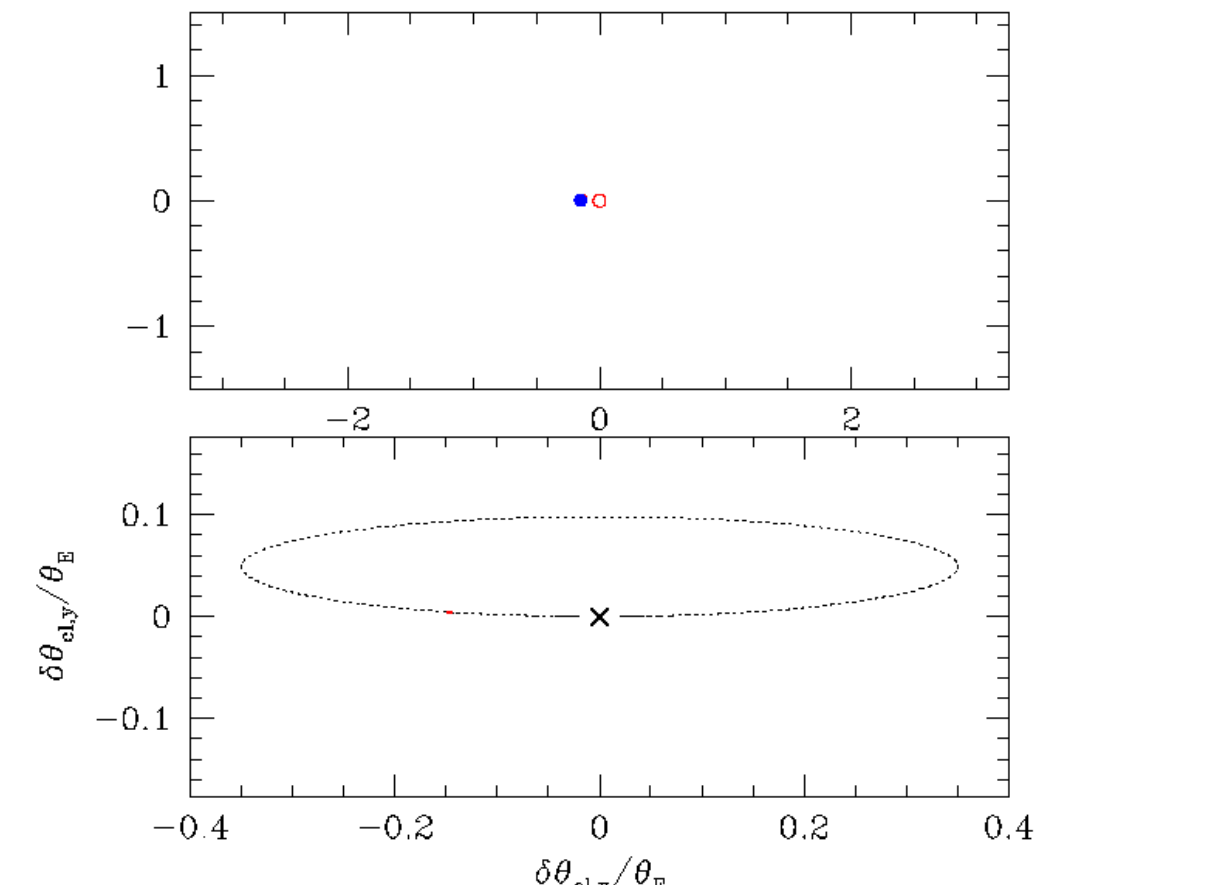


position relative to lens

$$\vec{x}_c = \frac{\vec{x}_+ \mu_+ + \vec{x}_- |\mu_-|}{\mu_+ + |\mu_-|}$$



position relative to unlensed
source position



GRAVITATIONAL LENSING

9- GRAVITATIONAL MICROLENSING II : STATISTICS

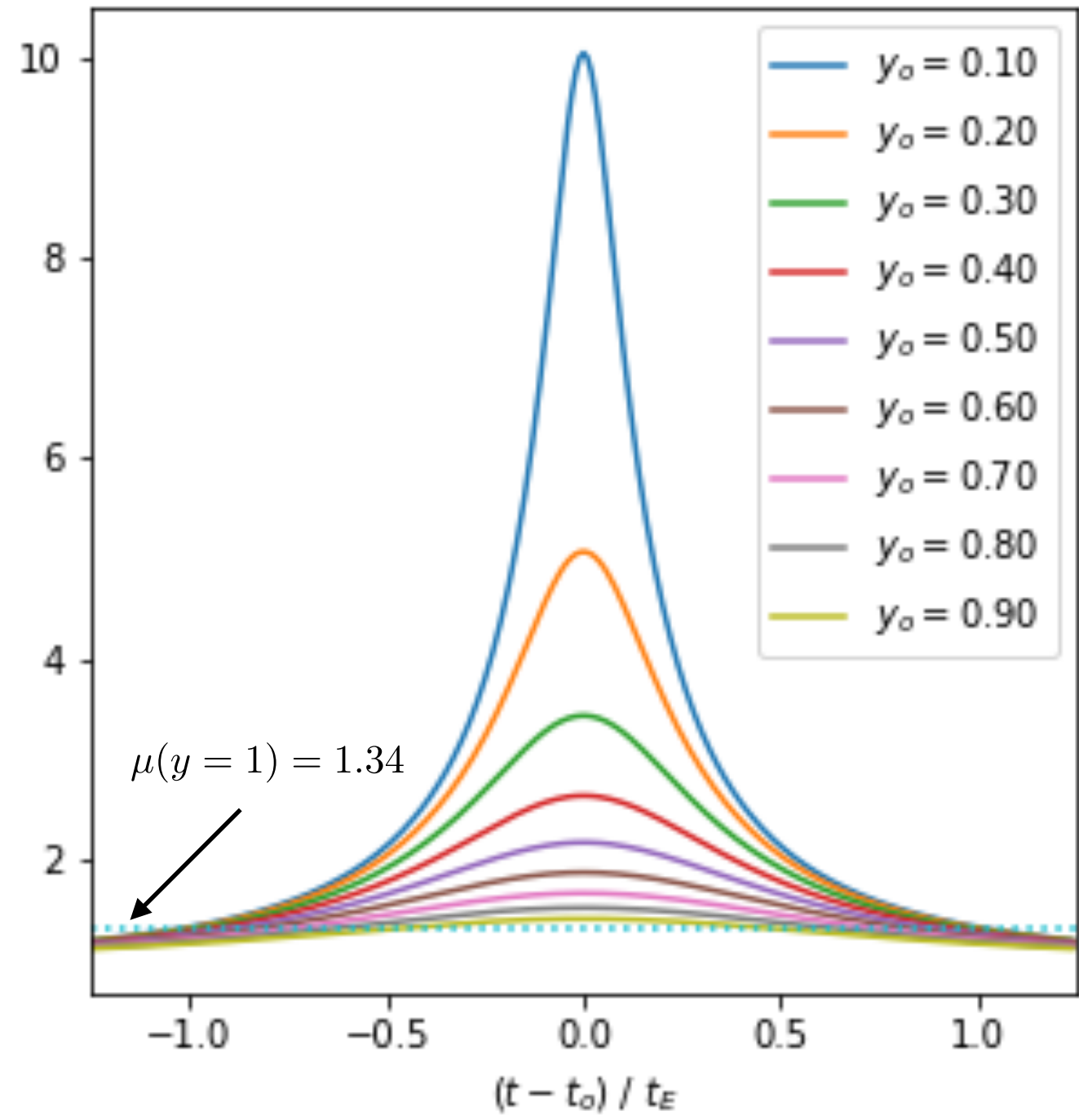
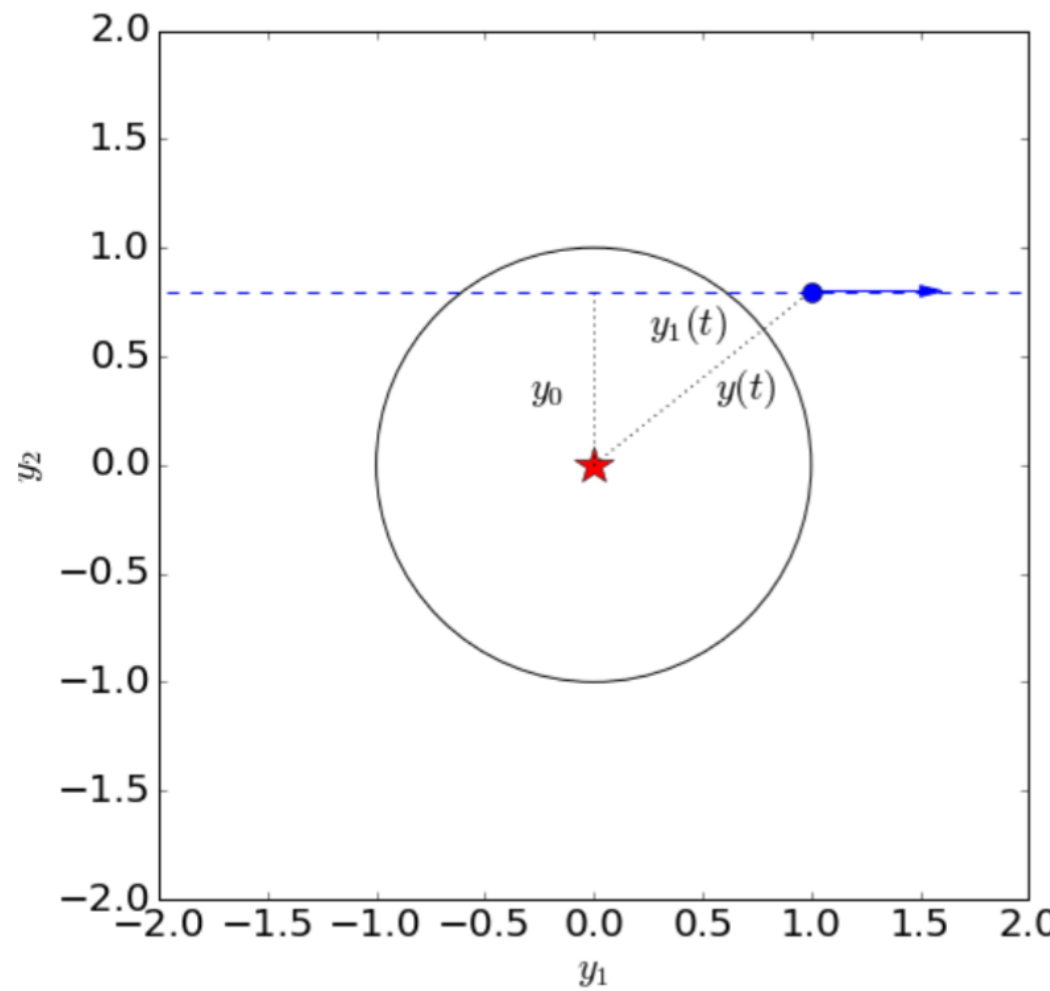
R. Benton Metcalf
2022-2023

MICROLENSING LIGHT CURVE

magnification

$$\mu(y) = \frac{y^2 + 2}{y\sqrt{y^2 + 4}}$$

$$y(t) = \sqrt{y_o^2 + y_1(t)^2} = \sqrt{y_o^2 + \frac{(t - t_o)^2}{t_E^2}}$$



MICROLENSING STATISTICS

Einstein radius

$$R_E = D_l \theta_E = \sqrt{\frac{4GM}{c^2} \frac{D_{ls} D_l}{D_s}} = \sqrt{\frac{4GM}{c^2} D_s x(1-x)}$$

Einstein crossing time

$$t_E = \frac{R_E}{|v_\perp|}$$

OPTICAL DEPTH - probability that a star is being microlensed.

$$\tau = \frac{4\pi G}{c^2} D_s^2 \int_0^1 dx \ x(1-x) \rho(xD_s)$$

EVENT RATE

$$\begin{aligned} \Gamma &= 2N_* \int_0^{D_s} dD \int_0^\infty dM \int d^3v \ f(v) f(M) \ |v_\perp| R_E(M, D) \frac{\rho(D)}{M} \\ &= 2N_* \sqrt{\frac{4G}{c^2}} D_s^{3/2} \int_0^\infty dM \int_0^1 dx f(M) \ \sqrt{\frac{x(1-x)}{M}} \rho(D_s x) \langle |v_\perp| \rangle \end{aligned}$$

MICROLENSING STATISTICS

Einstein radius

$$R_E = D_l \theta_E = \sqrt{\frac{4GM}{c^2} \frac{D_{ls} D_l}{D_s}} = \sqrt{\frac{4GM}{c^2} D_s x(1-x)}$$

Einstein crossing time

$$t_E = \frac{R_E}{|v_\perp|}$$

Einstein crossing time distribution

$$\frac{d\Gamma}{dt_E} = -2N_* \int_0^{D_s} dD \int_0^\infty dM f(M) f_v \left(\frac{R_E}{t_E}\right) \left(\frac{R_E}{t_E}\right)^3 \frac{\rho(D)}{M}$$

For an isotropic Maxwellian velocity distribution $f_v(v_\perp) = \frac{v_\perp}{\sigma^2} \exp\left[-\frac{v_\perp^2}{2\sigma^2}\right]$

$$\frac{d\Gamma}{dt_E} = -\frac{2N_*}{\sigma^2} \frac{1}{t_E^4} \int_0^{D_s} dD \int_0^\infty dM f(M) R_E^4 \frac{\rho(D)}{M} \exp\left[-\frac{1}{2\sigma^2} \left(\frac{R_E}{t_E}\right)^2\right]$$

MICROLENSING STATISTICS

$$D_s = 8 \text{ kpc}$$

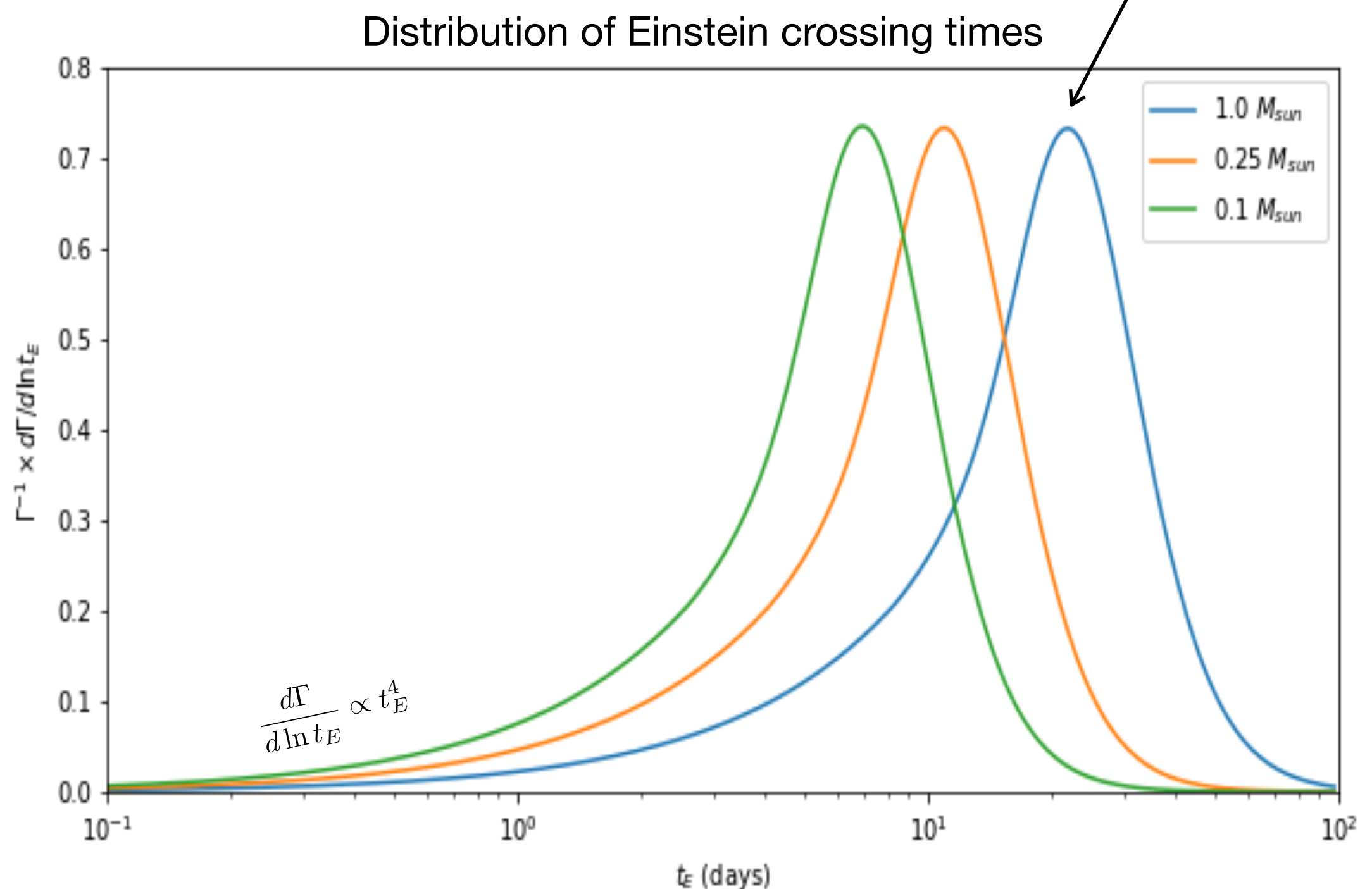
$\sigma_v = 120 \text{ km/s}$ Gaussian distributed

$$\rho(D) = \text{const.}$$

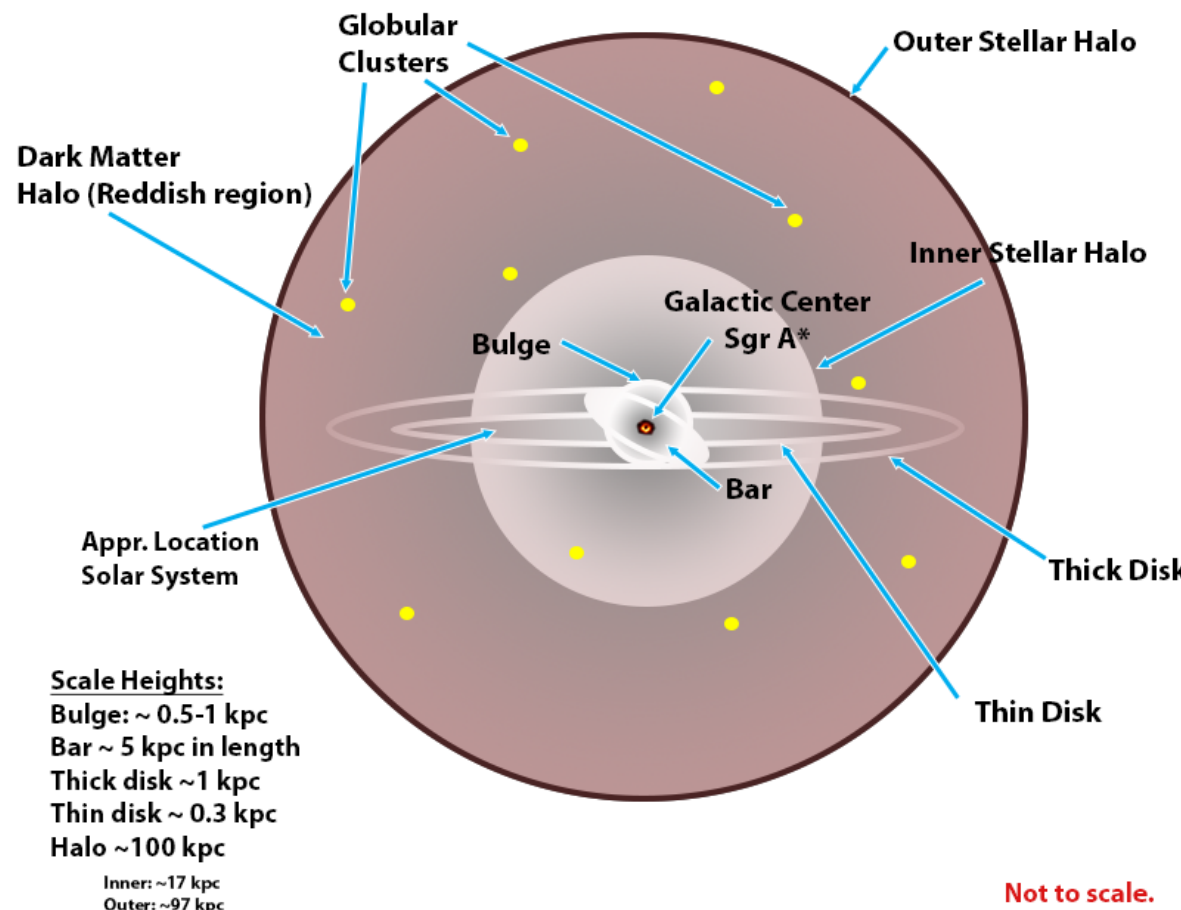
$$t_E^{\max} \sim \frac{t_o}{5.25} = 0.38 \sqrt{\frac{GMD_s}{c^2\sigma^2}}$$

$$f(M') = \delta_D(M' - M) \text{ mass distribution}$$

$$\frac{1}{\Gamma} \frac{d\Gamma}{d \ln t_E}$$



A MODEL FOR OUR GALAXY



All these components have their own optical depths...

I) thin & thick disk (young stars & gas)

$$\rho^D(R, z) = \rho_0^D \exp\left(-\frac{R - R_0}{h_R} - \frac{|z|}{h_z}\right)$$

$$\sigma^D \simeq 20 \text{ km/s} \quad v_{rot}^D \simeq 220 \text{ km/s}$$

$$\sigma^{TD} \simeq 40 \text{ km/s} \quad v_{rot}^{TD} \simeq 180 \text{ km/s}$$

II) Spheroid (old star halo)

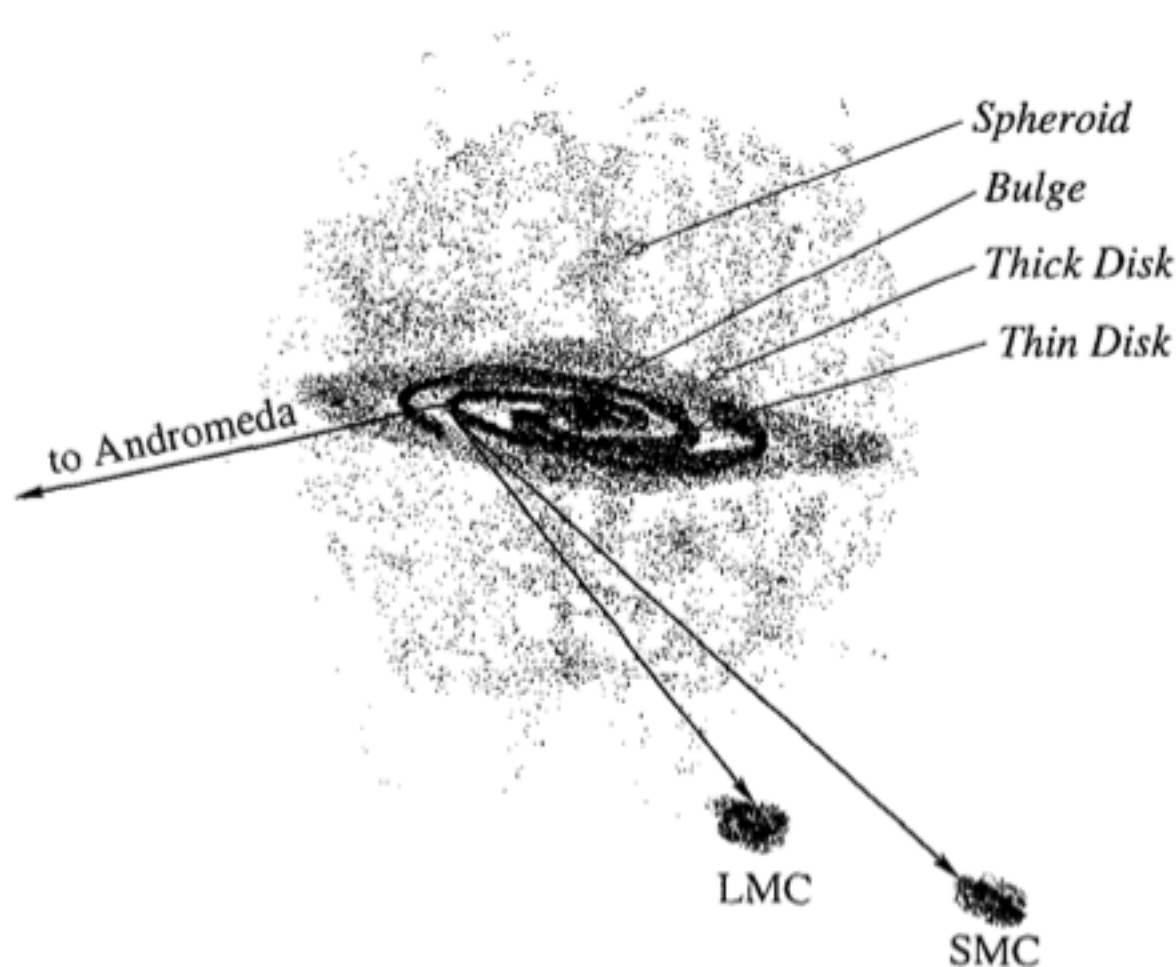
$$\rho^S \propto r^{-3.5} \quad \sigma^S \simeq 120 \text{ km/s}$$

III) Bulge (contains a bar)

$$\rho^B(s) = \frac{M_0}{8\pi abc} \exp\left[-\frac{s^2}{2}\right]$$

$$s^4 \equiv [(x'/a)^2 + (y'/b)^2]^2 + (z'/c)^4$$

A MODEL FOR OUR GALAXY



All these components have their own optical depths...

I) thin & thick disk (young stars & gas)

$$\rho^D(R, z) = \rho_0^D \exp\left(-\frac{R - R_0}{h_R} - \frac{|z|}{h_z}\right)$$

$$\sigma^D \simeq 20 \text{ km/s} \quad v_{rot}^D \simeq 220 \text{ km/s}$$

$$\sigma^{TD} \simeq 40 \text{ km/s} \quad v_{rot}^{TD} \simeq 180 \text{ km/s}$$

II) Spheroid (old star halo)

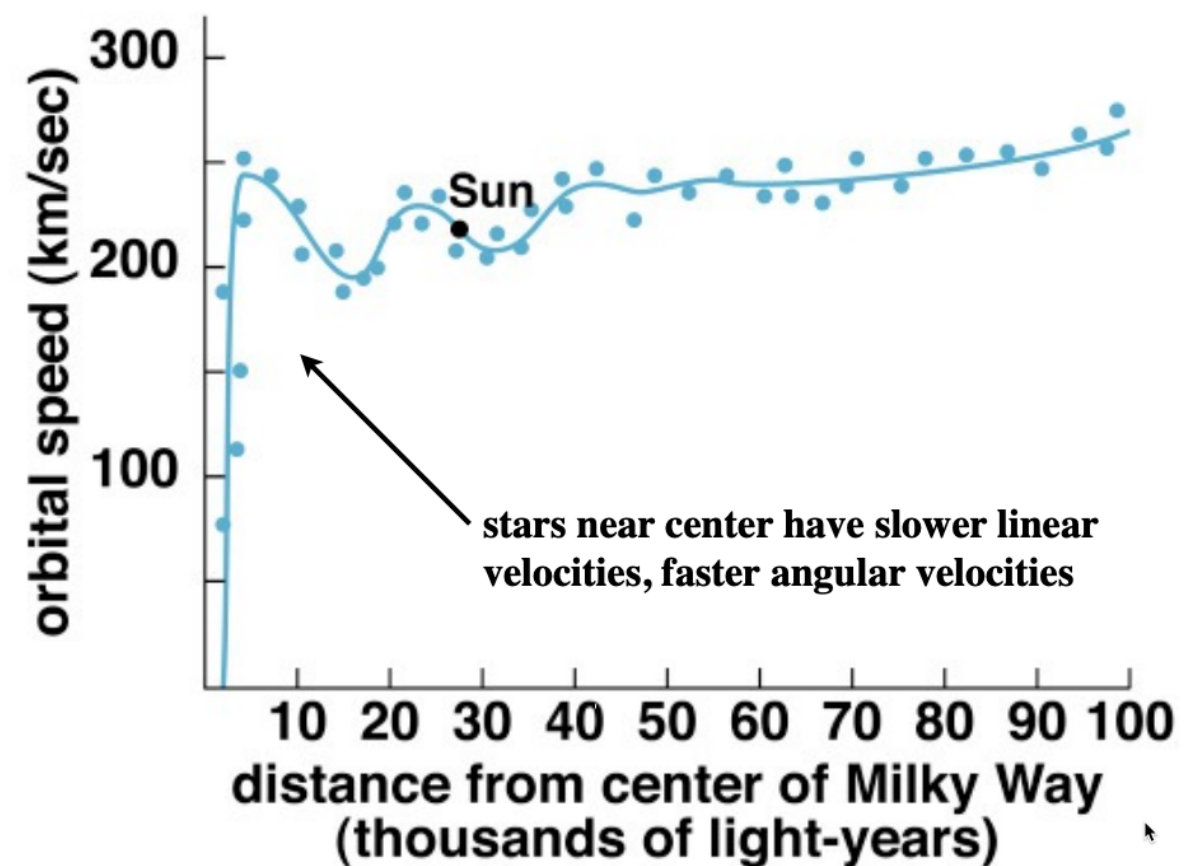
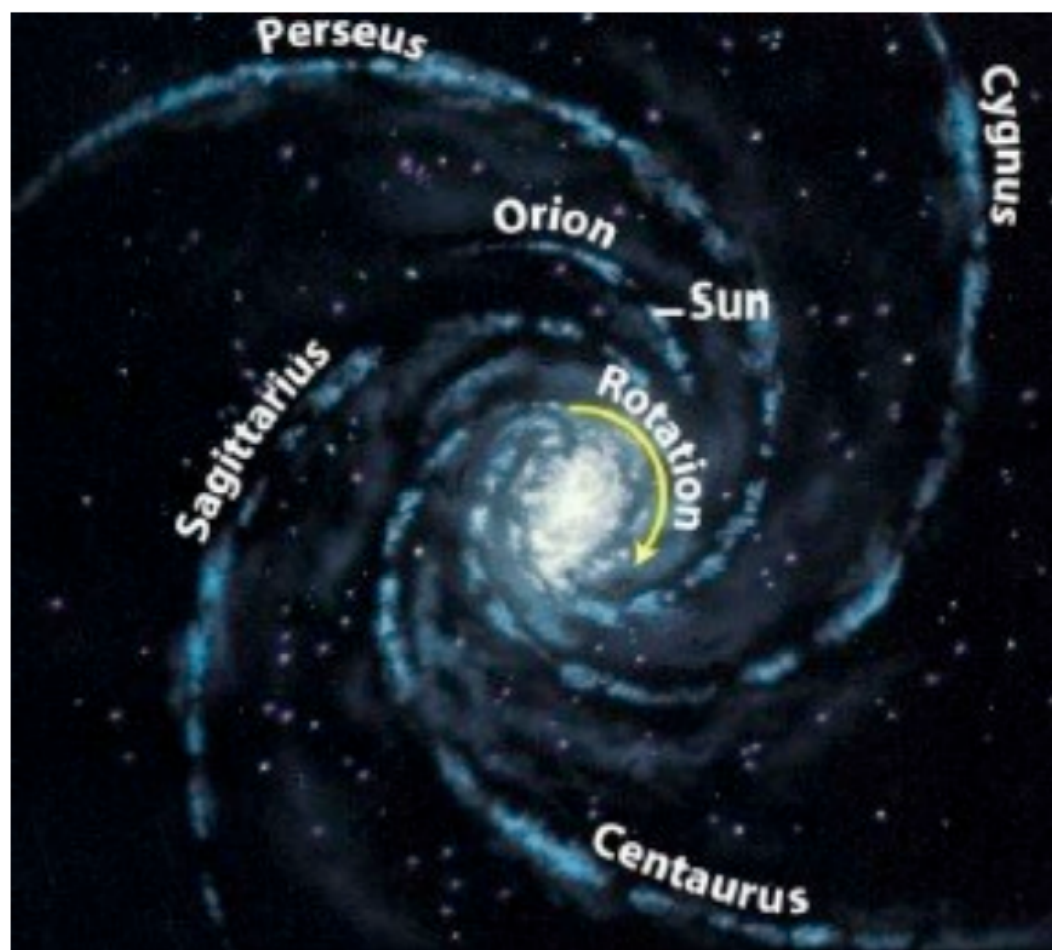
$$\rho^S \propto r^{-3.5} \quad \sigma^S \simeq 120 \text{ km/s}$$

III) Bulge (contains a bar)

$$\rho^B(s) = \frac{M_0}{8\pi abc} \exp\left[-\frac{s^2}{2}\right]$$

$$s^4 \equiv [(x'/a)^2 + (y'/b)^2]^2 + (z'/c)^4$$

DIFFERENTIAL ROTATION



MICROLENSING SURVEYS: THE OGLE PROJECT



[The main OGLE Homepage](#)

[Recent Scientific Results:](#)

[Real Time Data Analysis Systems:](#)

[OGLE Collection of](#)

[Variable Stars](#)

[opens in new window]

[OGLE-II Photometry](#)

[Databases](#)

[opens in new window]

[Main OGLE Results:](#)

[Sky Coverage:](#)

[GB Interstellar Extinction Calculator](#)

[GB Microlensing Event Rate Maps](#)

[Data Download Site](#)

[Publications:](#)

[OGLE related grants:](#)

[Miscellaneous Information:](#)

[Links to other](#)

[Microlensing Teams:](#)

[opens in new window]

[OGLE Photo Gallery](#)

25 years of OGLE

July
24-28
2017

Warsaw
Poland

- A free-floating or wide-orbit planet in the microlensing event OGLE-2019-BLG-0551
- Mapping the Northern Galactic Disk Warp with Classical Cepheids
- Over 78 000 RR Lyrae Stars in the Galactic Bulge and Disk
- Discovery of an Outbursting 12.8 Minute Ultracompact X-Ray Binary
- A three-dimensional map of the Milky Way using classical Cepheid variable stars
- OGLE Collection of Galactic Cepheids
- Microlensing optical depth and event rate toward the Galactic bulge from eight years of OGLE-IV observations
- 12 660 spotted stars toward the OGLE Galactic bulge fields
- Two new free-floating or wide-orbit planets from microlensing
- Rotation curve of the Milky Way from Classical Cepheids
- more...

OGLE-IV IN OPERATION

[OGLE Variable Stars](#) | [On-line Data](#) | [Project description and history](#) | [Telescope information](#)

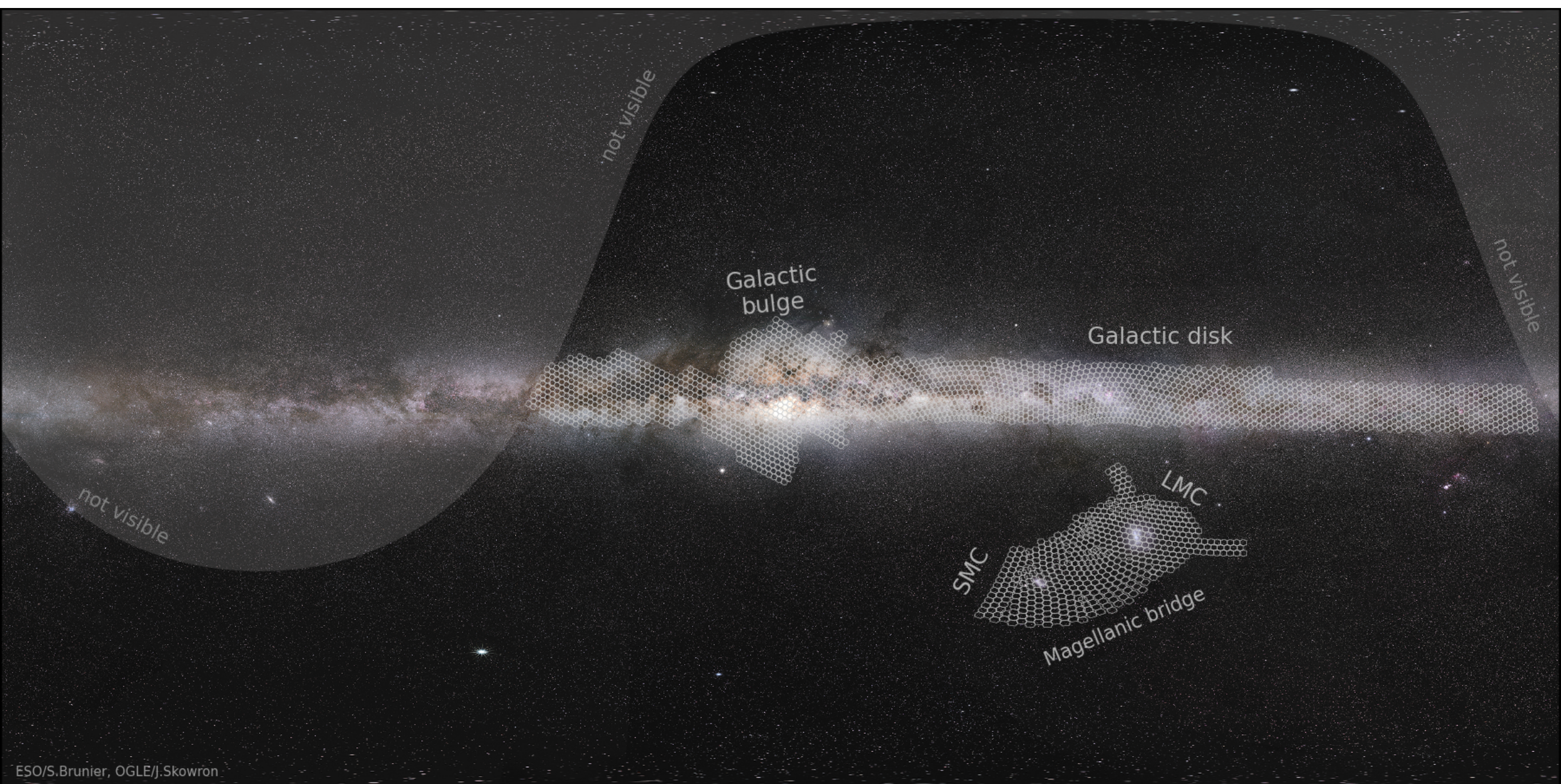


[Main page](#)

[Coverage of the Sky](#)

[Coverage of the bulge](#)

SKY COVERAGE

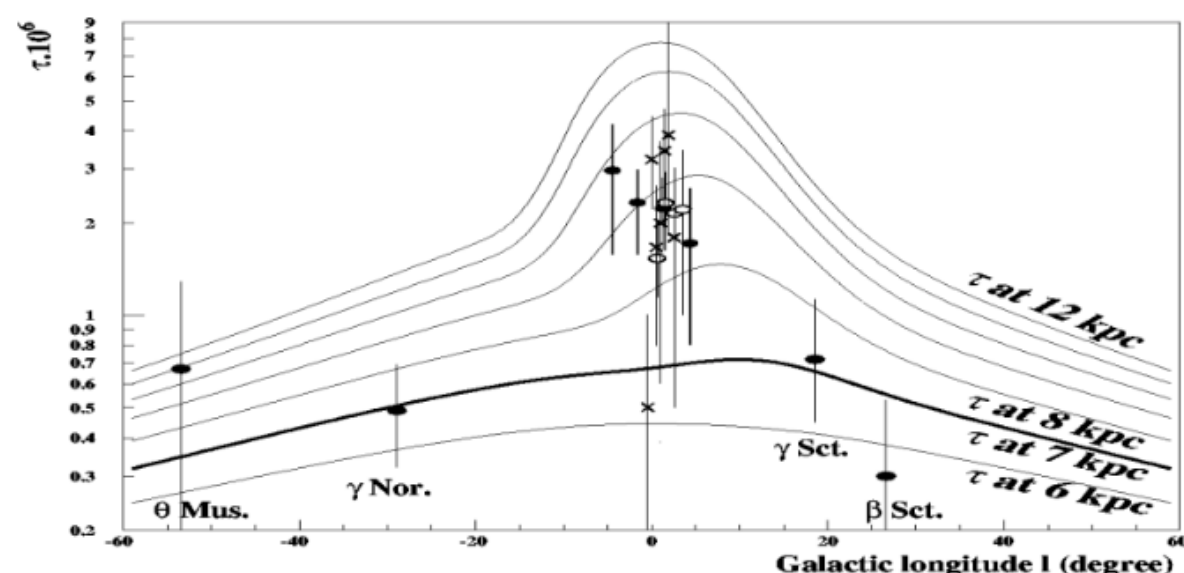
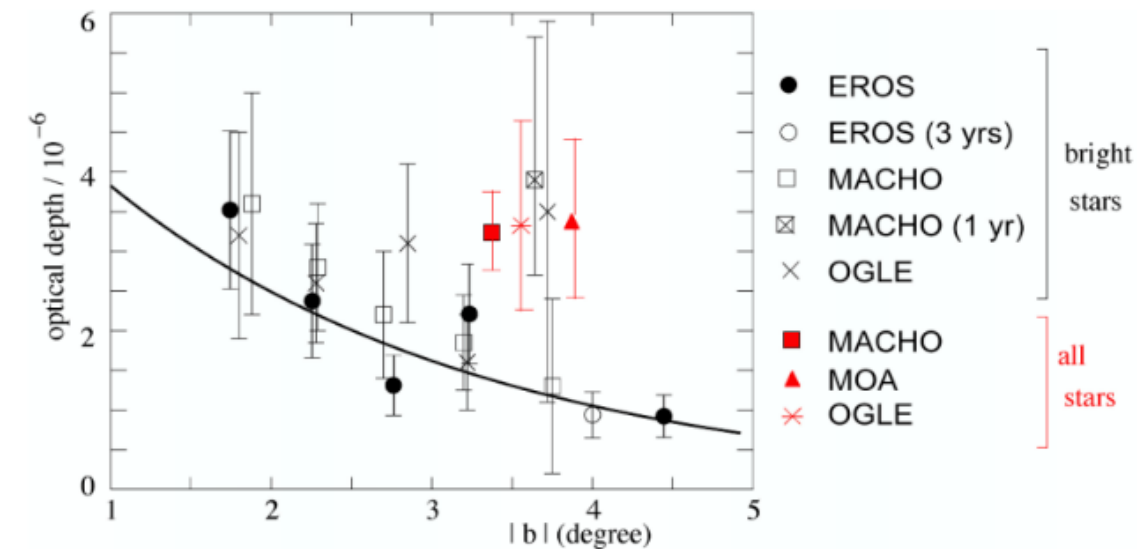


OPTICAL DEPTH AS A FUNCTION OF POSITION ON THE SKY

Unlike other probes of galactic structure, microlensing is sensitive to all stellar masses independently of distance.

The optical depth as a function of galactic coordinates gives a probe of different components of the galactic model.

The high rate and asymmetry towards the centre of the galaxy favour a galactic bar over a bulge.



| reference | sea- sons | field $deg.^2$ | stars analyzed | events for τ | l°, b° | $\langle \tau \rangle_{bulge}$ $\times 10^6$ | $\langle t_E \rangle$ corrected |
|------------|--------------|-------------------|-------------------|----------------------|--------------------|---|------------------------------------|
| OGLE [112] | 2 | 0.81 | all | 9 | $\pm 5, -3.5$ | 3.3 ± 1.2 | |
| MACHO [11] | 1 | 12. | all | 45 | $2.55, 3.64$ | $3.9^{+1.8}_{-1.2}$ | |
| MACHO [16] | 3 | 4. | all/DIA | 99 | $2.68, -3.35$ | $3.23^{+0.52}_{-0.50}$ | |
| EROS [3] | 3 | 15. | bright | 16 | $2.5, -4.0$ | 0.94 ± 0.29 | |
| MOA [104] | 1 | 18. | all/DIA | 28 | $4.2, -3.4$ | $3.36^{+1.11}_{-0.81}$ | |
| MACHO [86] | 7 | 4.5 | bright | 62 | $1.5, -2.68$ | $2.17^{+0.47}_{-0.38}$ | 21.6 ± 3 |
| OGLE [105] | 4 | 5. | bright | 32 | $1.16, -2.75$ | $2.55^{+0.57}_{-0.46}$ | 28.1 ± 4.3 |
| EROS [62] | 7 | 66. | bright | 120 | | GC map | 28.3 ± 2.8 |
| EROS [87] | 7 | 20.1 | all | 22 | | GSA map | $48. \pm 9.$ |

Moniez, 2010

LOW MASS INITIAL MASS FUNCTION

*IMF IN THE BAR/BULGE SEEKS CONSTANT
WITH THE LOCAL IMF.*

$$dN = \Phi(\log M) d\log M$$

$$\propto M^{-\alpha} dM \text{ where}$$

$$\alpha = \alpha_{bd} \text{ for } 0.01 M_\odot \leq M < 0.08 M_\odot$$

$$\alpha = \alpha_{ms} \text{ for } 0.08 M_\odot \leq M < 0.5 M_\odot = M_{break}$$

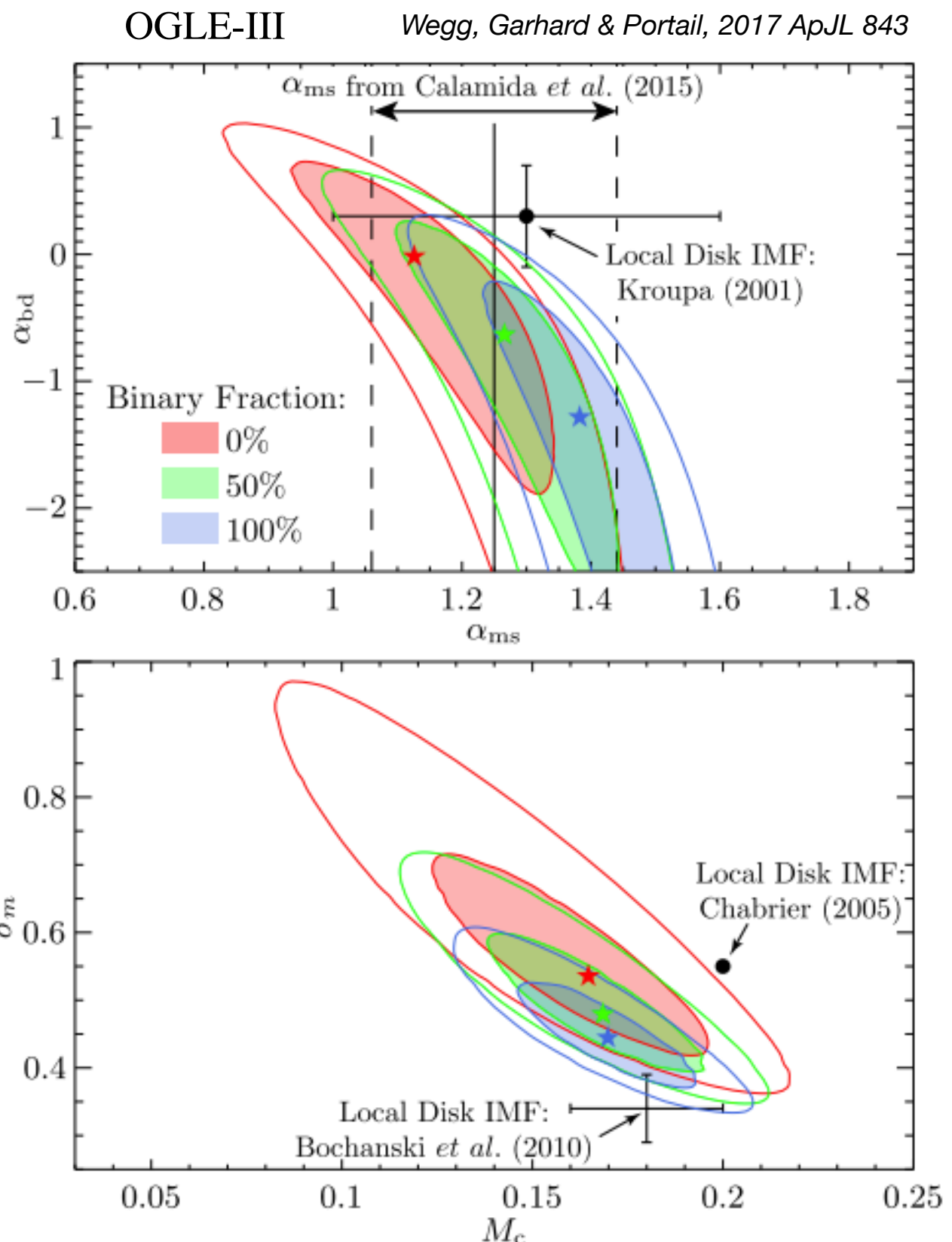
$$\alpha = 2.3 \text{ for } 0.5 M_\odot \leq M < 100 M_\odot.$$

α_{bd} brown dwarf slope

α_{ms} main sequence slope

$$\Phi(\log M) \propto \exp \left\{ \frac{-(\log M - \log M_c)^2}{2\sigma_m^2} \right\} \text{ for } M < 1.0 M_\odot$$

$$\alpha = 2.3 \text{ for } 1.0 M_\odot \leq M < 100 M_\odot.$$



LIMITS ON MACHO DARK MATTER

Event rates toward the LMC and SMC rule out realistic halo models composed of Massive Compact Halo Objects (MACHOs) between the masses of 10^{-7} and 10 solar masses.

Only about 10% of a standard halo can consist of such objects.

Previously free floating “Jupiters” ($M < 0.01 M_{\text{sun}}$ with time scales of a few hours to days) were the most plausible candidates for baryonic dark matter. They would be virtually undetectable otherwise.

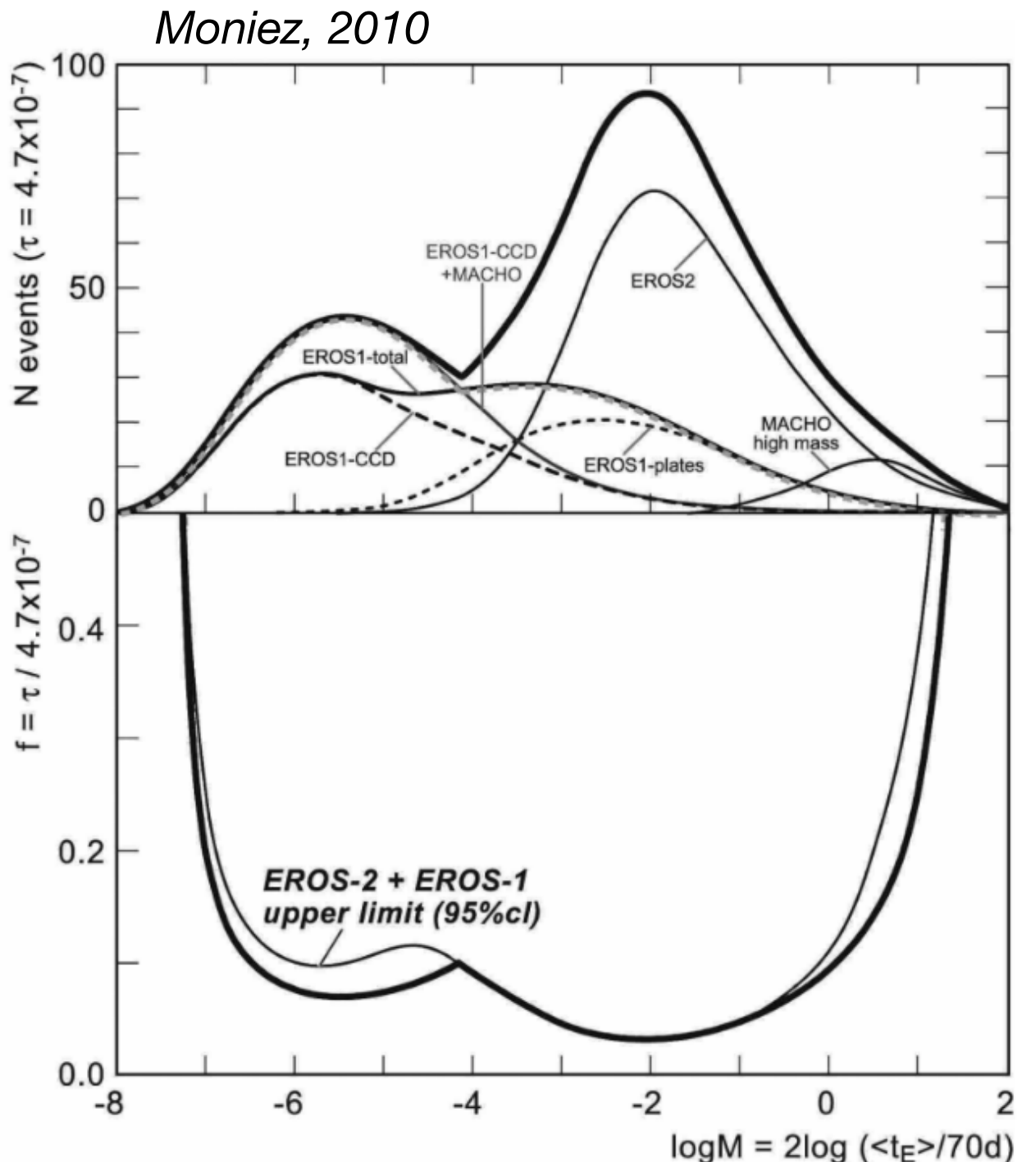
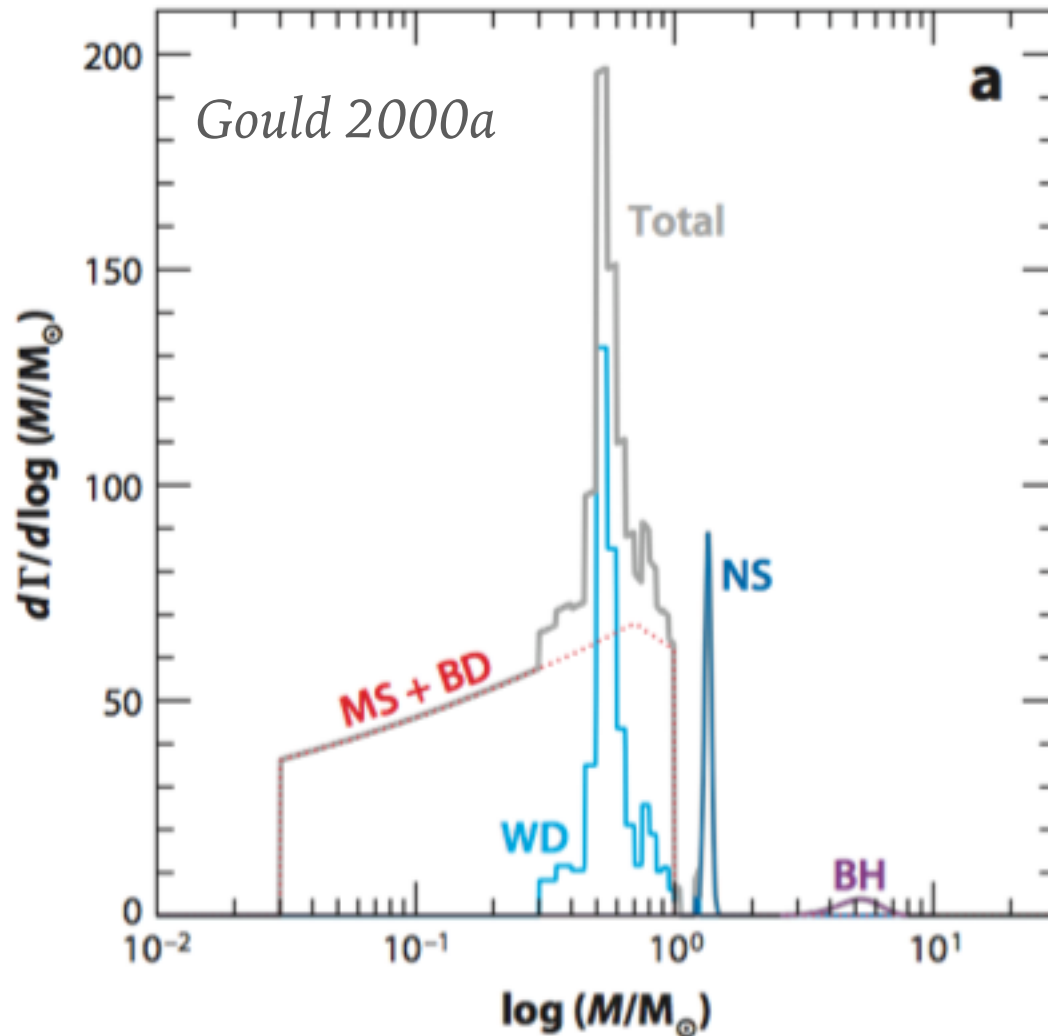


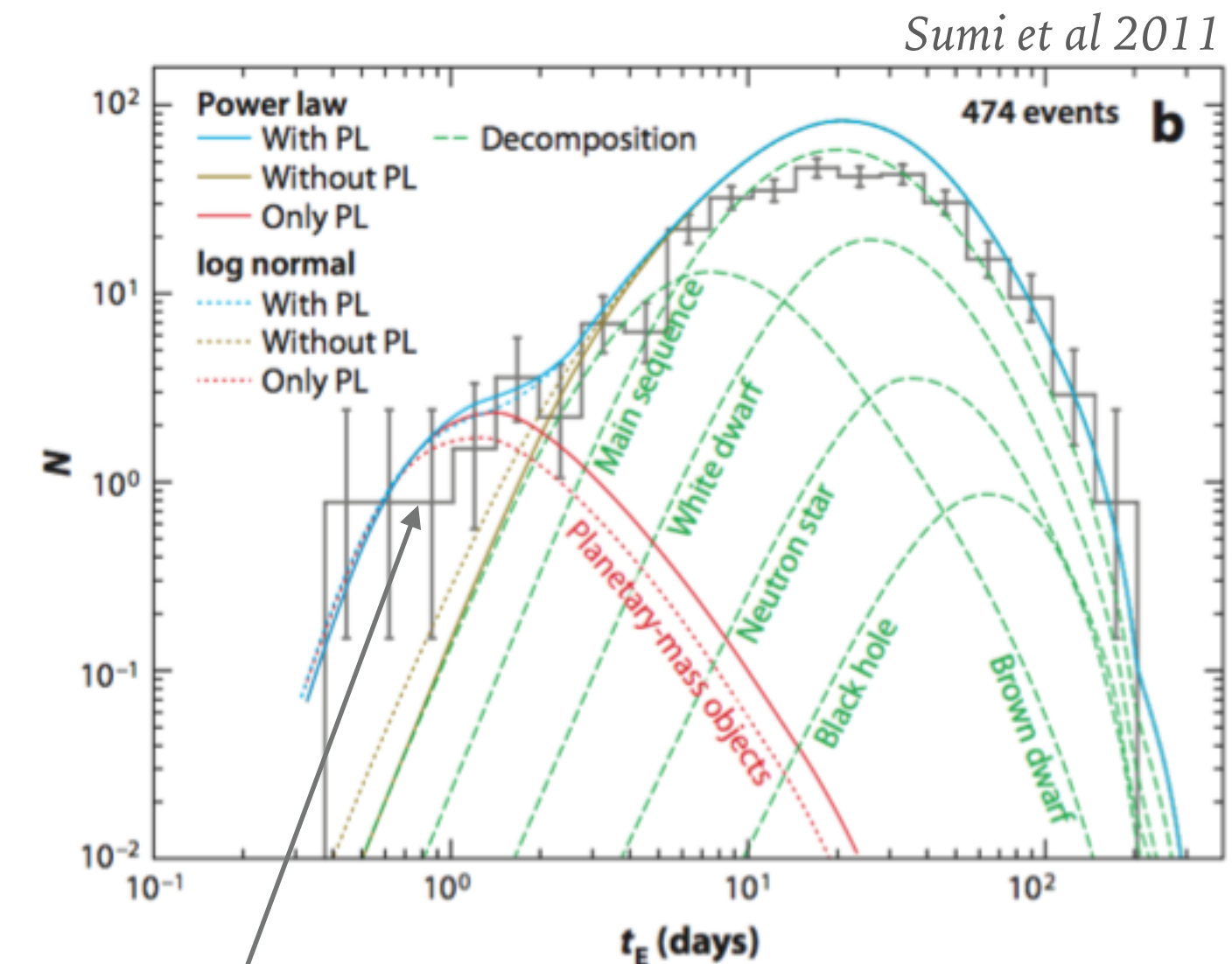
Fig. 7 The top panel shows the number of expected events towards LMC as a function of the lens mass M for the S-model. The EROS1-total line shows the sum of the expectations from the CCD-camera and from the plates (dashed lines). The MACHO-high mass line corresponds to the “zero event” high mass search. The EROS1-CCD+MACHO line (blue) is the combined result from the EROS1 CCD-camera and the MACHO 2 year analysis. The grey dashed line is the envelope of the EROS1-total and the EROS1-CCD+MACHO lines. The final combination (thick line) is the sum of EROS2, of the grey dashed line and of half of the MACHO-high mass expectations (see text). In the lower panel, the thick line shows the combined 95% CL upper limit on $f = \tau_{\text{LMC}} / 4.7 \times 10^{-7}$ based on no observed events. The thin line is the $EROS1 + EROS2$ LMC limit.

PROBING THE STELLAR POPULATIONS WITH MICROLENSING

Gaudi, 2012, *Ann. Rev. Astron. Astrophys.* 50, 411



*Theoretical estimate of
the rate of microlensing
events towards the
galactic bulge*



*Distribution of microlensing event timescales
observed by the MOA collaboration
(2006-2007)*

SOME IMPORTANT FACTS

- several collaborations have implemented the microlensing idea (proposed by B. Paczynski). These groups have monitored the galactic bulge and the Magellanic Clouds searching for microlensing events
- the relatively high rate of detections favored a barred model of the galaxy
- Towards the Magellanic Clouds, no ‘short’ events (timescales from a few hours up to 20 days) have been seen by any group. This places strong limits on ‘Jupiters’ in the dark halo: specifically, compact objects in the mass range 10^{-6} –0.05 solar masses contribute less than 10% of the dark matter around our Galaxy. This is a very important result, as these objects were previously thought to be the most plausible form of baryonic dark matter, and (for masses below 0.01 solar masses) they would have been virtually impossible to detect directly.

SOME IMPORTANT FACTS

- With the possible exception of MOA's free floating planets, generally, all the detected microlensing events are consistent with known stellar populations. Black holes can contribute up to 2% of the total mass of the halo.
- The recent detection of gravitational waves from merging BHs with intermediate masses has revived the idea of BHs as dark-matter candidates. For such lenses the time scale of the events would be large so that past microlensing surveys would not have been sensitive to them.

